Académie d'Orléans –Tours
Université François-Rabelais

FACULTE DE MEDECINE DE TOURS

Année 2011 **N°**

Thèse
pour le

DOCTORAT EN MEDECINE

Diplôme d'Etat

Par

Raphaëlle DUPREZ

Née le 16 février 1981

Présentée et soutenue publiquement le 11 avril 2011

TITRE

CARACTÉRISATION MOLÉCULAIRE DES CARCINOMES PAPILLAIRES DU SEIN

Jury

Président de Jury : Monsieur le Professeur S. GUYÉTANT
Membres du Jury : Monsieur le Professeur P. BOUGNOUX
Monsieur le Professeur J-C PAGÈS
Madame le Docteur F. ARBION
Monsieur le Docteur P. MICHENET
Madame le Docteur A. VINCENT-SALOMON

Académie d'Orléans –Tours
Université François-Rabelais

FACULTE DE MEDECINE DE TOURS

Année 2011 **N°**

Thèse
pour le

DOCTORAT EN MEDECINE

Diplôme d'Etat

Par

Raphaëlle DUPREZ

Née le 16 février 1981

Présentée et soutenue publiquement le 11 avril 2011

TITRE

CARACTÉRISATION MOLÉCULAIRE DES CARCINOMES PAPILLAIRES DU SEIN

Jury

Président de Jury : Monsieur le Professeur S. GUYÉTANT
Membres du Jury : Monsieur le Professeur P. BOUGNOUX
Monsieur le Professeur J-C PAGÈS
Madame le Docteur F. ARBION
Monsieur le Docteur P. MICHENET
Madame le Docteur A. VINCENT-SALOMON

1er Février 2011

UNIVERSITÉ FRANÇOIS RABELAIS
FACULTÉ DE MÉDECINE DE TOURS

DOYEN
Professeur Dominique PERROTIN

VICE-DOYEN
Professeur Daniel ALISON

ASSESSEURS
Professeur Christian ANDRES, Recherche
Docteur Brigitte ARBEILLE, Moyens
Professeur Christian BINET, Formation Médicale Continue
Professeur Laurent BRUNEREAU, Pédagogie
Professeur Patrice DIOT, Recherche clinique

SECRETAIRE GENERAL
Monsieur Patrick HOARAU

****

DOYENS HONORAIRES
Professeur Emile ARON (†)- *1962-1966*
Directeur de l'Ecole de Médecine - 1947-1962
Professeur Georges DESBUQUOIS (†)- *1966-1972*
Professeur André GOUAZÉ - *1972-1994*
Professeur Jean-Claude ROLLAND – *1994-2004*

PROFESSEURS EMERITES

Professeur Patrick CHOUTET
Professeur Guy GINIES
Professeur Jacques LANSAC
Professeur Olivier LE FLOCH
Professeur Chantal MAURAGE
Professeur Léandre POURCELOT
Professeur Jean-Claude ROLLAND

PROFESSEURS HONORAIRES
MM. Ph. ANTHONIOZ - A. AUDURIER - Ph. BAGROS - G. BALLON - P. BARDOS - J. BARSOTTI - A. BENATRE - Ch. BERGER - J. BRIZON - Mme M. BROCHIER - Ph. BURDIN - L. CASTELLANI - J.P. FAUCHIER - B. GRENIER - M. JAN - P. JOBARD - J.-P. LAMAGNERE - F. LAMISSE - J. LAUGIER - G. LELORD - G. LEROY - Y. LHUINTRE - M. MAILLET - Mlle C. MERCIER - E/H. METMAN - J. MOLINE - Cl. MORAINE - H. MOURAY - J.P. MUH - J. MURAT - Mme T. PLANIOL - Ph. RAYNAUD - Ch. ROSSAZZA - Ph. ROULEAU - A. SAINDELLE - J.J. SANTINI - D. SAUVAGE - M.J. THARANNE - J. THOUVENOT - B. TOUMIEUX - J. WEILL.

10 Bvd Tonnellé-B.P.3223-37032-TOURS CEDEX 1-Tél.02-47-36-60-04-FAX.02-47-36-60-99

PROFESSEURS DES UNIVERSITES - PRATICIENS HOSPITALIERS

MM.	ALISON Daniel	Radiologie et Imagerie médicale
	ANDRES Christian	Biochimie et Biologie moléculaire
	ARBEILLE Philippe	Biophysique et Médecine nucléaire
	AUPART Michel	Chirurgie thoracique et cardiovasculaire
	AUTRET Alain	Neurologie
Mme	AUTRET-LECA Elisabeth	Pharmacologie fondamentale ; Pharmacologie clinique
MM.	BABUTY Dominique	Cardiologie
Mmes	BARILLOT Isabelle	Cancérologie ; Radiothérapie
	BARTHELEMY Catherine	Physiologie
MM.	BAULIEU Jean-Louis	Biophysique et Médecine nucléaire
	BERNARD Louis	Maladies infectieuses ; maladies tropicales
	BESNARD Jean-Claude	Biophysique et Médecine nucléaire
	BEUTTER Patrice	Oto-Rhino-Laryngologie
	BINET Christian	Hématologie ; Transfusion
	BODY Gilles	Gynécologie et Obstétrique
	BONNARD Christian	Chirurgie infantile
	BONNET Pierre	Physiologie
	BOUGNOUX Philippe	Cancérologie ; Radiothérapie
	BRUNEREAU Laurent	Radiologie et Imagerie médicale
	BUCHLER Matthias	Néphrologie
	CALAIS Gilles	Cancérologie ; Radiothérapie
	CAMUS Vincent	Psychiatrie d'adultes
	CHANDENIER Jacques	Parasitologie et Mycologie
	CHANTEPIE Alain	Pédiatrie
	CHARBONNIER Bernard	Cardiologie
	COLOMBAT Philippe	Hématologie ; Transfusion
	CONSTANS Thierry	Médecine interne ; Gériatrie et Biologie du vieillissement
	CORCIA Philippe	Neurologie
	COSNAY Pierre	Cardiologie
	COTTIER Jean-Philippe	Radiologie et Imagerie médicale
	COUET Charles	Nutrition
	DANQUECHIN DORVAL Etienne	Gastroentérologie ; Hépatologie
	DE LA LANDE DE CALAN Loïc	Chirurgie digestive
	DE TOFFOL Bertrand	Neurologie
	DEQUIN Pierre-François	Thérapeutique ; médecine d'urgence
	DIOT Patrice	Pneumologie
	DU BOUEXIC de PINIEUX Gonzague	Anatomie & Cytologie pathologiques
	DUMONT Pascal	Chirurgie thoracique et cardiovasculaire
	FAUCHIER Laurent	Cardiologie
	FAVARD Luc	Chirurgie orthopédique et traumatologique
	FETISSOF Franck	Anatomie et Cytologie pathologiques
	FOUQUET Bernard	Médecine physique et de Réadaptation
	FRANCOIS Patrick	Neurochirurgie
	FUSCIARDI Jacques	Anesthésiologie et Réanimation chirurgicale ; médecine d'urgence
	GAILLARD Philippe	Psychiatrie d'Adultes
	GOGA Dominique	Chirurgie maxillo-faciale et Stomatologie
	GOUDEAU Alain	Bactériologie -Virologie ; Hygiène hospitalière
	GOUPILLE Philippe	Rhumatologie
	GRUEL Yves	Hématologie ; Transfusion
	GUILMOT Jean-Louis	Chirurgie vasculaire ; Médecine vasculaire
	GUYETANT Serge	Anatomie et Cytologie pathologiques
	HAILLOT Olivier	Urologie
	HALIMI Jean-Michel	Thérapeutique ; médecine d'urgence (Néphrologie et Immunologie clinique)
	HERAULT Olivier	Hématologie ; transfusion
	HERBRETEAU Denis	Radiologie et Imagerie médicale
Mme	HOMMET Caroline	Médecine interne, Gériatrie et Biologie du vieillissement
MM.	HUTEN Noël	Chirurgie générale
	LABARTHE François	Pédiatrie
	LAFFON Marc	Anesthésiologie et Réanimation chirurgicale ; médecine d'urgence
	LANSON Yves	Urologie
	LARDY Hubert	Chirurgie infantile
	LASFARGUES Gérard	Médecine et Santé au Travail
	LEBRANCHU Yvon	Immunologie
	LECOMTE Pierre	Endocrinologie et Maladies métaboliques

LECOMTE Thierry	Gastroentérologie ; hépatologie ; addictologie
LEMARIE Etienne	Pneumologie
LESCANNE Emmanuel	Oto-Rhino-Laryngologie
LINASSIER Claude	Cancérologie ; Radiothérapie
LORETTE Gérard	Dermato-Vénéréologie
MACHET Laurent	Dermato-Vénéréologie
MAILLOT François	Médecine Interne
MARCHAND Michel	Chirurgie thoracique et cardiovasculaire
MARRET Henri	Gynécologie et Obstétrique
NIVET Hubert	Néphrologie
PAGES Jean-Christophe	Biochimie et biologie moléculaire
PAINTAUD Gilles	Pharmacologie fondamentale, Pharmacologie clinique
PATAT Frédéric	Biophysique et Médecine nucléaire
PERROTIN Dominique	Réanimation médicale ; médecine d'urgence
PERROTIN Franck	Gynécologie et Obstétrique
PISELLA Pierre-Jean	Ophtalmologie
QUENTIN Roland	Bactériologie-Virologie ; Hygiène hospitalière
RICHARD-LENOBLE Dominique	Parasitologie et Mycologie
ROBERT Michel	Chirurgie Infantile
ROBIER Alain	Oto-Rhino-Laryngologie
ROINGEARD Philippe	Biologie cellulaire
ROSSET Philippe	Chirurgie orthopédique et traumatologique
ROYERE Dominique	Biologie et Médecine du développement et de la Reproduction
RUSCH Emmanuel	Epidémiologie, Economie de la Santé et Prévention
SALAME Ephrem	Chirurgie digestive
SALIBA Elie	Biologie et Médecine du développement et de la Reproduction
SIRINELLI Dominique	Radiologie et Imagerie médicale
THOMAS-CASTELNAU Pierre	Pédiatrie
TOUTAIN Annick	Génétique
VAILLANT Loïc	Dermato-Vénéréologie
VELUT Stéphane	Anatomie
WATIER Hervé	Immunologie.

PROFESSEURS ASSOCIES

M.	HUAS Dominique	Médecine Générale
Mme	LEHR-DRYLEWICZ Anne-Marie	Médecine Générale
MM.	POTIER Alain	Médecine Générale
	TEIXEIRA Mauro	Immunologie

PROFESSEUR détaché auprès de l'Ambassade de France à Washington pour exercer les fonctions de Conseiller pour les affaires sociales

M.	DRUCKER Jacques	Epidémiologie-Economie de la Santé et Prévention

MAITRES DE CONFERENCES DES UNIVERSITES - PRATICIENS HOSPITALIERS

Mme	ARBEILLE Brigitte	Biologie cellulaire
M.	BARON Christophe	Immunologie
Mme	BAULIEU Françoise	Biophysique et Médecine nucléaire
M.	BERTRAND Philippe	Biostatistiques, Informatique médicale et Technologies de Communication
Mme	BLANCHARD-LAUMONIER Emmanuelle	Biologie cellulaire
M	BOISSINOT Eric	Physiologie
Mmes	BONNET-BRILHAULT Frédérique	Physiologie
	BRECHOT Marie-Claude	Biochimie et Biologie moléculaire
MM.	BRILHAULT Jean	Chirurgie orthopédique et traumatologique
	DESTRIEUX Christophe	Anatomie
	DUONG Thanh Haï	Parasitologie et Mycologie
Mmes	EDER Véronique	Biophysique et Médecine nucléaire
	FOUQUET-BERGEMER Anne-Marie	Anatomie et Cytologie pathologiques
	GAUDY-GRAFFIN Catherine	Bactériologie - Virologie ; Hygiène hospitalière
M.	GIRAUDEAU Bruno	Biostatistiques, Informatique médicale et Technologies de Communication
Mme	GOUILLEUX Valérie	Immunologie
MM.	GUERIF Fabrice	Biologie et Médecine du développement et de la reproduction
	GYAN Emmanuel	Hématologie, transfusion
M.	HOARAU Cyrille	Immunologie
	HOURIOUX Christophe	Biologie cellulaire
Mme	LARTIGUE Marie-Frédérique	Bactériologie-Virologie ; Hygiène hospitalière
Mmes	LE GUELLEC Chantal	Pharmacologie fondamentale ; Pharmacologie clinique

	MACHET Marie-Christine	Anatomie et Cytologie pathologiques
MM.	MARCHAND-ADAM Sylvain	Pneumologie
	MEREGHETTI Laurent	Bactériologie-Virologie ; Hygiène hospitalière
Mme	MICHEL–ADDE Christine	Pédiatrie
M.M	MULLEMAN Denis	Rhumatologie
	PIVER Eric	Biochimie et biologie moléculaire
Mme	SAINT-MARTIN Pauline	Médecine légale et Droit de la santé
Mme	VALAT Chantal	Biophysique et Médecine nucléaire
M.	VOURC'H Patrick	Biochimie et Biologie moléculaire

MAITRES DE CONFERENCES

Mlle	BOIRON Michèle	Sciences du Médicament
Mme	ESNARD Annick	Biologie cellulaire
M.	LEMOINE Maël	Philosophie
Mlle	MONJAUZE Cécile	Sciences du langage - Orthophonie
M.	PATIENT Romuald	Biologie cellulaire

MAITRE DE CONFERENCES ASSOCIE A MI-TEMPS

M.M.	LEBEAU Jean-Pierre	Médecine Générale
	ROBERT Jean	Médecine Générale

PROFESSEUR CERTIFIE

M	DIABANGOUAYA Célestin	Anglais

CHERCHEURS C.N.R.S. - INSERM

MM.	BIGOT Yves	Directeur de Recherche CNRS – UMR CNRS 6239
	BOUAKAZ Ayache	Chargé de Recherche INSERM – UMR CNRS-INSERM 930
Mmes	BRUNEAU Nicole	Chargée de Recherche INSERM – UMR CNRS-INSERM 930
	CHALON Sylvie	Directeur de Recherche INSERM – UMR CNRS-INSERM 930
MM.	COURTY Yves	Chargé de Recherche CNRS – U 618
	GAUDRAY Patrick	Directeur de Recherche CNRS – UMR CNRS 6239
	GOUILLEUX Fabrice	Directeur de Recherche CNRS – UMR CNRS 6239
Mmes	GOMOT Marie	Chargée de Recherche INSERM – UMR CNRS-INSERM 930
	HEUZE-VOURCH Nathalie	Chargée de Recherche INSERM – U 618
MM.	LAUMONNIER Frédéric	Chargé de Recherche INSERM - UMR CNRS-INSERM 930
	LE PAPE Alain	Directeur de Recherche CNRS – U 618
Mmes	MARTINEAU Joëlle	Chargée de Recherche INSERM – UMR CNRS-INSERM 930
	POULIN Ghislaine	Chargée de Recherche CNRS – UMR CNRS-INSERM 930

CHARGES D'ENSEIGNEMENT

Pour l'Ecole d'Orthophonie

Mme	DELORE Claire	Orthophoniste
M	GOUIN Jean-Marie	Praticien Hospitalier
M.	MONDON Karl	Praticien Hospitalier
Mme	PERRIER Danièle	Orthophoniste

Pour l'Ecole d'Orthoptie

Mme	LALA Emmanuelle	Praticien Hospitalier
M.	MAJZOUB Samuel	Praticien Hospitalier

Pour l'Ethique Médicale

Mme	BIRMELE Béatrice	Praticien Hospitalier
M.	MALLET Donatien	Praticien Hospitalier.

A mon Président de thèse, Monsieur le Professeur Serge Guyétant,
Vous me faites l'honneur de présider le jury de cette thèse.
Merci d'avoir accepté de juger ce travail et de me faire bénéficier, à Tours, d'un enseignement de l'Anatomopathologie de grande qualité.

A Monsieur le Professeur Jean-Christophe Pagès,
Merci d'avoir accepté de juger ce travail, et d'apporter vos compétences et critiques en biologie moléculaire. Merci pour vos précieux conseils techniques et de rédaction.

A Monsieur le Professeur Philippe Bougnoux,
Vous avez accepté avec enthousiasme de faire partie du jury de ma thèse. Merci pour votre considération et l'intérêt que vous avez porté à mon parcours et à ce travail.

Au Docteur Flavie Arbion,
Tu me fais l'honneur de faire partie de mon jury de thèse.
Merci de m'avoir encouragée à réaliser ce projet de Recherche, et de m'enseigner la gynécopathologie avec rigueur et efficacité.

Au Docteur Patrick Michenet,
Tu as accepté avec enthousiasme de juger ce travail.
Tu m'as donné au sein de l'équipe de Sénologie d'Orléans le goût pour la pathologie mammaire et le goût d'écrire. Tu m'as donné la motivation pour réaliser mon Master Recherche à Londres. Merci pour ton perpétuel enthousiasme et ton optimisme.

A ma Directrice de thèse, le Docteur Anne Vincent-Salomon,
Tu m'as permis de réaliser ce projet de Recherche au sein de l'équipe de Pathologie Moléculaire du Breakthrough Breast Cancer Research Center à Londres. Tu as participé activement à ce projet et accepté de le critiquer.
Tu as véritablement réussi à me transmettre ta passion pour la Recherche et la pathologie mammaire. Tu es pour moi un modèle tant sur le plan professionnel que personnel.

Aux médecins anatomopathologistes de Tours,
Merci de me transmettre vos connaissances en Anatomopathologie avec rigueur et enthousiasme.
Merci également à toutes les techniciennes et l'ensemble du personnel des services d'Anatomopathologie de Trousseau et de Bretonneau.

Au Professeur Jorge Reis-Filho,
Merci de m'avoir proposé ce sujet de Recherche et énormément appris en Pathologie Moléculaire.
Merci de m'avoir donné l'immense chance de réaliser ce projet au sein de votre équipe et de m'avoir permis d'y rencontrer des personnalités passionnantes.

Au Docteur Magali Lacroix-Triki, sans qui je n'aurais pas mené à terme ce projet de Recherche.
Merci pour ton aide inestimable, ton efficacité, ton optimisme, ton humour et ton amitié.

A tous les chercheurs du Laboratoire de Pathologie Moléculaire du Breakthrough Breast Cancer Research Center, et particulièrement à Maryou Lambros et Alan MacKay, pour leur immense aide et leur participation à ce projet.

Au Docteur Gaëtan Mac Grogan, pour sa participation à ce travail.

Enfin à tous ceux qui m'ont encouragée à réaliser ce projet de Recherche à Londres, en particulier Patrick Michenet et Sarah Baccouche, ainsi qu'au Ministère de l'Enseignement Supérieur et de la Recherche, qui m'a permis financièrement de réaliser ce projet en m'accordant l'Année Recherche.

A Pierre,
Merci pour ton immense amour.
Merci pour ta patience pendant mes années d'études et mon année de Master Recherche. Merci de toujours respecter ma passion pour mon travail, et pour l'intérêt que tu y portes.

A mes parents,
C'est grâce à vous que j'ai réussi toutes ces années d'études de Médecine.
Merci pour votre amour et pour votre soutien perpétuel.

A mon frère et mes sœurs,
Vous m'avez toujours soutenue pendant mes études. Merci pour votre amour.
Merci à Pauline pour m'avoir encouragée et soutenue pendant les années difficiles de mes études.

A mes grands-parents, trop tôt disparus et qui je suis sûre sont fiers de moi.

A mes amies de Tours, fidèles depuis des années, **A tous mes amis de la Faculté de Médecine de Nice**, avec qui j'ai passé des années inoubliables.

A toute ma famille et mes amis.

Liste des abréviations

ADN Acide DésoxyriboNucléique

BAC Bacterial Artificial Chromosomes

CCI-NST carcinome canalaire infiltrant “no special type”

CCND1 cycline D1

CGH Comparative Genomic Hybridization

CISH Chromogenic in situ Hybridization

CK cytokératine

EGFR Epidermal Growth Factor Receptor

ETV6 Ets Variant 6

FISH Fluorescent in situ Hybridization

HER2 Human Epidermal Growth Factor Receptor 2

IHC immunohistochimie

LOH Loss of heterozygosity

NFIB Nuclear Factor I/B

NTRK3 Neurotrophic Tyrosine Kinase Receptor 3

OMS Organisation Mondiale de la Santé

RO récepteurs aux œstrogènes

RP récepteurs à la progestérone

TMA Tissu MicroArray

Le cancer du sein est, en France et dans les pays occidentaux, le cancer féminin le plus fréquent. Chaque année en France, plus de 50000 nouveaux cas sont diagnostiqués, et une femme sur 10 risque d'en être affectée au cours de sa vie. De ce fait, la prise en charge diagnostique et thérapeutique de ce cancer représente un enjeu majeur de Santé Publique.

La classification actuelle de l'Organisation Mondiale de la Santé (OMS) des cancers du sein est essentiellement basée sur des critères morphologiques [1]. Or, cette classification en types histologiques ne reflète pas la complexité moléculaire des cancers du sein. En outre, elle n'a qu'une faible valeur pronostique et est dépourvue de valeur prédictive [2].

En revanche, plusieurs auteurs ont démontré qu'une classification incluant à la fois des critères morphologiques et moléculaires serait plus adaptée, dans la mesure où elle intégrerait des marqueurs pronostiques et prédictifs essentiels pour la prise en charge des patientes [2].

A ce jour, seuls trois biomarqueurs prédictifs sont utilisés en routine pour la prise en charge thérapeutique des patientes ayant un cancer du sein, à savoir le statut des récepteurs aux œstrogènes (RO), des récepteurs à la progestérone (RP) et du gène *HER2* (Human Epidermal Growth Factor Receptor 2).

La classification moléculaire des cancers du sein établie par Sorlie et Perou en 2001 à partir d'études sur puces d'expressions géniques a permis d'ébaucher une taxonomie des cancers mammaires basée sur des critères moléculaires, apportant une réelle valeur pronostique par rapport à la classification actuelle (Figure 1). Sorlie et Perou décrivent cinq sous-groupes de cancers du sein : « luminal A », « luminal B », « normal breast-like », « HER2 » et « basal-like » [3, 4]. Les cancers « luminaux » expriment en immunohistochimie (IHC) les cytokératines (CK) 8 et 18, dites « luminales », ainsi que les RO. Les cancers luminaux A sont généralement de bas grade histologique et de bon pronostic. Les cancers luminaux B, souvent de plus haut grade histologique, sont associés à un moins bon pronostic que les luminaux A. Les cancers « HER2 » sont caractérisés par une amplification du gène *HER2*

associée à une surexpression de la protéine codée par ce gène. Ce sont des cancers agressifs, mais bénéficiant d'une cible thérapeutique, HER2 constituant la cible du trastuzumab, anticorps monoclonal anti-HER2. Les cancers « basal-like » sont dans la grande majorité des cas négatifs pour les RO, les RP et HER2 (dits « triple négatifs »), et expriment des gènes d'origine myoépithéliale, notamment *CK5/6*, *CK14*, *cavéolines 1* et *2* et *EGFR* (Epidermal Growth Factor Receptor). Il s'agit de tumeurs de haut grade histologique, dont l'index mitotique est souvent élevé et le pronostic défavorable [5, 6]. Enfin, les cancers « normal breast-like », très peu caractérisés, pourraient être d'origine artéfactuelle.

Cette catégorisation des cancers du sein en cinq sous-groupes apporte donc une réelle valeur pronostique, voire prédictive, en particulier dans le cadre des cancers HER2 [2].

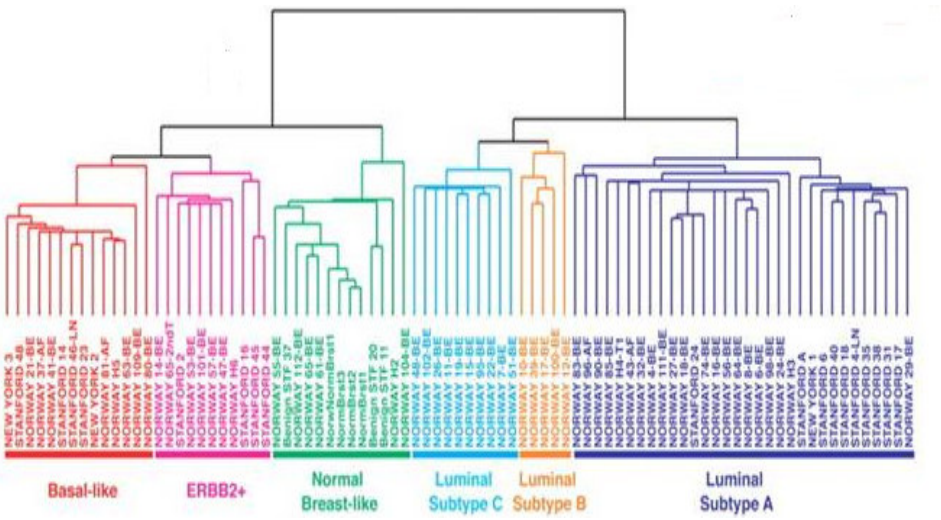

Sorlie T et al, Proc Natl Acad Sci USA 2001

Figure 1 : Mise en évidence des sous-types moléculaires de cancer du sein par clustering non supervisé après analyse des profils d'expressions géniques : luminal A, luminal B, basal-like, HER2 et normal breast-like. La mise en evidence du sous-type luminal C est plus inconstante.

Au cours de la dernière décennie, l'essor de la biologie moléculaire a permis de comprendre l'oncogenèse de nombreux cancers.

Son intérêt majeur s'est révélé lors de la découverte de gènes de fusion dans les tumeurs mésenchymateuses et hématologiques, ouvrant ainsi la voie à de nouvelles perspectives thérapeutiques ciblant ces nouveaux oncogènes [7, 8].

La biologie moléculaire des carcinomes (tumeurs malignes d'origine épithéliale) a quant à elle été bien moins étudiée. Les cancers du sein font cependant exception puisque de très nombreuses études génomiques et transcriptomiques à haute résolution ont ces dernières années tenté de décrypter leur complexité moléculaire et d'identifier de nouveaux facteurs pronostiques et de nouvelles cibles thérapeutiques [2, 9].

Le cancer du sein est cependant une maladie extrêmement hétérogène, comprenant une pléthore d'entités, aux comportements biologique et clinique très différents. Si 75% des carcinomes mammaires sont des carcinomes canalaires infiltrants dits « no special type » (CCI-NSTs), les 25% restants sont de types histologiques particuliers [1]. La classification actuelle de l'OMS décrit ainsi plus de 17 types histologiques de cancers mammaires [1, 10]. Or, la très grande majorité des études dédiées aux cancers du sein portent sur le type histologique le plus fréquent, à savoir le CCI-NST.

Les types particuliers n'ont quant à eux été que très peu étudiés. Or ces derniers, bien que rares, présentent un intérêt majeur puisqu'ils se sont avérés beaucoup plus homogènes entre eux du point de vue moléculaire que les CCI-NSTs. Ainsi, l'étude de ces types particuliers a permis de mettre en évidence d'intéressantes corrélations géno-phénotypiques [11-13].

Par exemple, les carcinomes sécrétoires du sein, type particulier extrêmement rare affectant préférentiellement les patientes d'âge jeune, sont constamment « triple négatifs » et associés à la translocation chromosomique équilibrée t(12;15), induisant le gène de fusion *ETV6-NTRK3* [14]. Le carcinome adénoïde kystique, autre type particulier de carcinome mammaire, se

caractérise par la translocation équilibrée t(6;9), plus récemment identifiée, induisant la fusion des gènes *MYB* et *NFIB* [15]. Les carcinomes lobulaires se caractérisent quant à eux par une perte de fonction de l'E-cadhérine, protéine jouant un rôle essentiel dans le maintien des jonctions adhérentes liant les cellules épithéliales entre elles, alors que certains carcinomes métaplasiques se distinguent par une amplification du gène *EGFR* [16, 17].

Contrairement aux CCI-NSTs, la plupart des types particuliers de cancers du sein ont une évolution prévisible : les carcinomes tubuleux et adénoïdes kystiques sont d'excellent pronostic ; les carcinomes médullaires, bien que de haut grade histologique, sont associés à un bon pronostic ; quant aux carcinomes métaplasiques, il s'agit de tumeurs agressives, généralement réfractaires aux chimiothérapies conventionnelles [10, 12, 18].

Par ailleurs, les analyses d'expressions géniques ont montré que chaque type particulier se rattache à l'un des phénotypes moléculaires décrits par Sorlie et Perou [10, 13]. Ainsi, les carcinomes adénoïdes kystiques, métaplasiques et médullaires sont constamment de phénotype « basal-like », alors que les carcinomes mucineux, neuroendocrines et tubuleux sont de phénotype « luminal » [13, 17-19].

De surcroît, certaines études basées sur des analyses par hybridation génomique comparative (CGH array) ont démontré que certains de ces types particuliers constituent des entités génomiquement distinctes des CCI-NSTs. Il s'agit notamment des carcinomes micro-papillaires et mucineux [13, 19, 20].

La grande homogénéité moléculaire de ces types particuliers de cancers mammaires suggère donc que ces entités constituent de bons modèles d'étude des aberrations génétiques observées dans les cancers du sein en général et pourraient permettre l'identification de nouvelles cibles thérapeutiques [10, 17, 21].

Le carcinome papillaire du sein est un type particulier rare de cancer du sein, représentant environ 1% de l'ensemble des cancers mammaires [1, 22]. Il affecte préférentiellement les

femmes post-ménopausées, et les hommes peuvent également être atteints, avec une fréquence relativement plus élevée que pour les CCI-NSTs [22].

Cette tumeur se manifeste par une masse mammaire anormale, un écoulement mamelonnaire, ou se révèle de manière fortuite à l'occasion d'un bilan radiologique de dépistage.

Le carcinome papillaire du sein est un cancer de très bon pronostic [22-25]. Cependant, sa taille peut dans certains cas imposer une mastectomie, et son exérèse incomplète être à l'origine de récidives locales.

Il s'agit d'un carcinome de bas grade histologique, présentant rarement des invasions lympho-vasculaires ou des métastases [26]. Son traitement est essentiellement chirurgical et complété par de la radio- et de l'hormonothérapie. La chimiothérapie est d'indication exceptionnelle, et, bien que le schéma thérapeutique de ce type de cancer de très bon pronostic fasse l'objet de controverses, l'évaluation du statut ganglionnaire axillaire par la technique du ganglion sentinelle est recommandée par plusieurs auteurs [22, 25].

Histologiquement, les carcinomes papillaires mammaires se caractérisent par une arborescence d'axes fibro-vasculaires, tapissés par une prolifération de cellules épithéliales malignes [1]. Si la nature papillaire de ces lésions se reconnaît assez facilement histologiquement, il existe plusieurs variantes de carcinomes papillaires et la catégorisation précise et la prise en charge de ces différentes variantes morphologiques peuvent constituer un véritable challenge pour les pathologistes, et ce même pour les pathologistes mammaires les plus expérimentés [27]. Ceci s'explique par le fait que la classification des carcinomes papillaires du sein a évolué au cours du temps, et qu'une grande partie de ces carcinomes, généralement bien limités par une épaisse capsule, ont longtemps été considérés comme des carcinomes « *in situ* » et non invasifs, *i.e.* comme des carcinomes ne franchissant pas la membrane basale épithéliale et n'envahissant donc pas le tissu conjonctif voisin [22, 23, 26, 28, 29].

La dernière édition de l'OMS distingue les « carcinomes papillaires invasifs », décrits parmi les types particuliers de cancers du sein, envahissant franchement le tissu conjonctif voisin, des carcinomes papillaires « intra-kystiques », limités par une capsule fibreuse et décrits comme une variante de carcinome canalaire *in situ*, et donc comme une lésion non invasive [1].

Cependant, Collins et al en 2006 étudient l'expression des marqueurs myoépithéliaux dans les carcinomes papillaires intra-kystiques et concluent qu'ils sont dépourvus de couche de cellules myoépithéliales en leur périphérie, témoignant d'un dépassement de la membrane basale épithéliale et de leur nature invasive. Ils proposent aussi de privilégier l'appellation « carcinomes papillaires encapsulés » et de les considérer comme une variante bien circonscrite de carcinome invasif [30].

Une troisième variante de carcinomes papillaires mammaires correspond aux carcinomes papillaires « solides », pouvant également être pris pour des carcinomes *in situ*. Ces carcinomes se caractérisent par des nodules ou plages de cellules ovoïdes ou fusiformes s'organisant autour d'axes fibro-vasculaires. Ils présentent parfois une différenciation neuroendocrine ou un contingent mucineux [27].

Ainsi, trois principales variantes de carcinomes papillaires mammaires sont actuellement décrites : 1/ les carcinomes papillaires encapsulés, ou intra-kystiques, les plus fréquents, 2/ les carcinomes papillaires solides, et 3/ les carcinomes papillaires dits « invasifs », infiltrant de façon évidente le tissu conjonctif adjacent [22].

Si de nombreuses études génomiques et transcriptomiques à haute résolution de type CGH array ou analyse par puces d'expressions géniques ont été menées sur certains types particuliers de cancers du sein [13, 19, 20, 31], aucune étude de ce type n'a été réalisée sur les carcinomes papillaires mammaires.

Pour cette raison, nous avons voulu étudier par techniques haut débit (tissu microarray et CGH array) le profil immunohistochimique et génomique d'une série de carcinomes papillaires, à la fois encapsulés, solides et invasifs.

La technique du tissu microarray (TMA) est un véritable outil d'interface entre le pathologiste et la biologie moléculaire [32, 33]. Elle consiste à prélever des carottes de nombreux tissus tumoraux différents provenant de blocs donneurs de paraffine, et de les inclure de manière orthonormée selon un plan préétabli dans un bloc de paraffine receveur (Figure 2). Ainsi, jusqu'à mille échantillons de tumeurs peuvent être inclus dans un même bloc. Les TMAs constituent un outil indispensable pour la validation à haut débit des données issues des études génomiques et transcriptomiques, en étudiant l'expression de protéines par immunohistochimie (IHC) et/ou le statut de gènes par hybridation *in situ* dans un grand nombre de tumeurs à la fois [19, 20, 34-36].

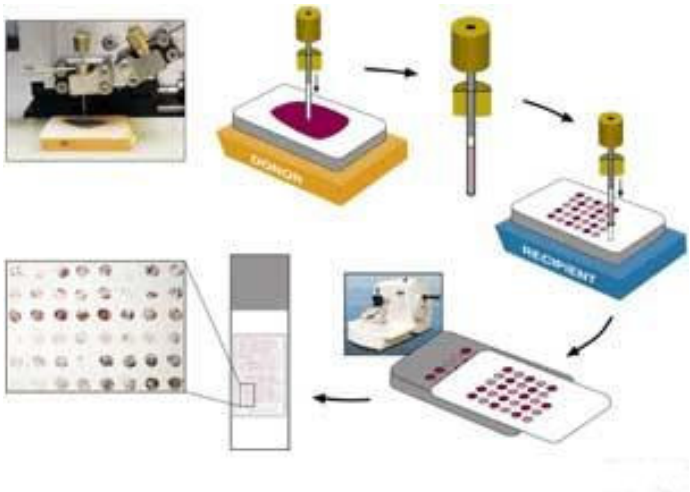

Figure 2 : Construction d'un tissu microarray (TMA) : des carottes de différents tissus tumoraux sont extraites des blocs donneurs et inclues dans un bloc receveur unique.

La technique d'hybridation génomique comparative (CGH array) permet la détection à haute résolution des variations du nombre de copies d'ADN dans un échantillon tumoral [37].

Il existe de nombreuses plateformes de CGH array, et nous avons pour cette étude utilisé la technique de CGH sur chromosomes artificiels bactériens (BAC) [35, 38-40].

Après microdissection de chaque tumeur sous stéréomicroscope afin d'obtenir un pourcentage de cellules tumorales supérieur à 90%, l'ADN est extrait. L'ADN tumoral et de l'ADN normal de référence sont marqués par deux fluorochromes différents (cyanine 5 et cyanine 3, respectivement), puis co-hybridés sur une lame de verre comprenant plusieurs milliers de BACs, couvrant l'ensemble du génome. Le ratio d'intensité fluorescente entre l'ADN tumoral et l'ADN de référence permet d'évaluer les variations du nombre de copies d'ADN, pour chaque région chromosomique, dans la tumeur étudiée (Figure 3).

Certains résultats de CGH array peuvent ensuite être validés par hybridation *in situ* et par IHC (Figure 4) [34].

Les objectifs de cette étude étaient de 1/ caractériser le profil immunohistochimique et génomique des carcinomes papillaires du sein, 2/ déterminer si les carcinomes papillaires du sein constituent ou non une entité génomique distincte des CCI-NSTs, et 3/ déterminer si les trois variantes de carcinomes papillaires correspondent ou non à la même maladie du point de vue génomique.

Pour cela, nous avons étudié une série multicentrique de 64 carcinomes papillaires du sein, à la fois encapsulés, solides et invasifs, ainsi qu'un groupe contrôle de 64 CCI-NSTs équivalents en termes de grade histologique et de statut hormonal. Nous avons étudié un panel de marqueurs immunohistochimiques sur TMAs. Nous avons ensuite analysé le profil génomique de 50 carcinomes papillaires et de 50 CCI-NSTs contrôles par CGH array. Enfin,

nous avons validé certains résultats de CGH array par hybridations fluorescente et chromogénique *in situ* (FISH et CISH).

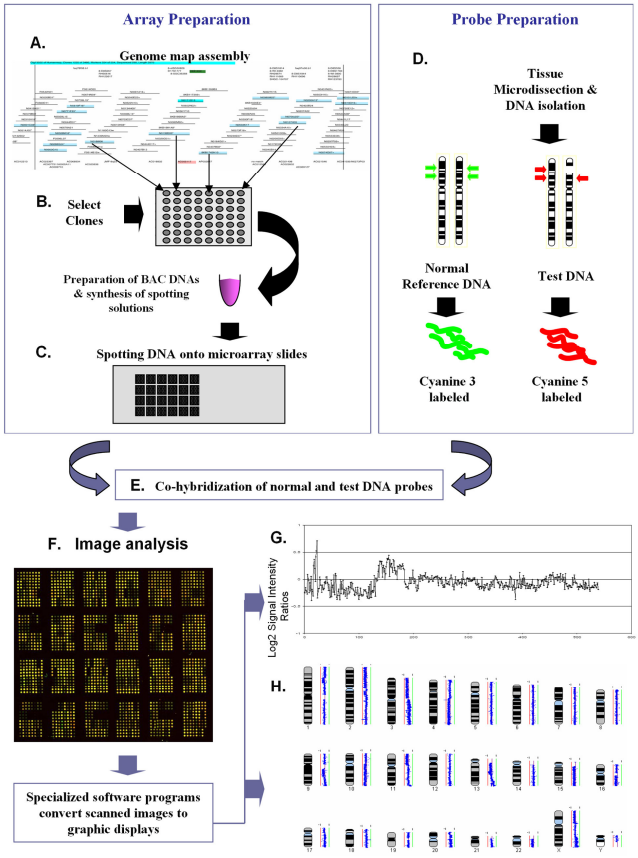

Figure 3 : Principe de l'hybridation génomique comparative : les chromosomes artificiels bactériens (BAC) sont disposés sur une lame de verre ; les ADN de référence et tumoral sont marqués par des fluorochromes, combinés, hybridés sur la lame qui est scannée puis analysée ; les ratios d'intensité fluorescente entre l'ADN tumoral et l'ADN de référence pour chaque BAC reflètent les variations du nombre de copies d'ADN dans la tumeur.

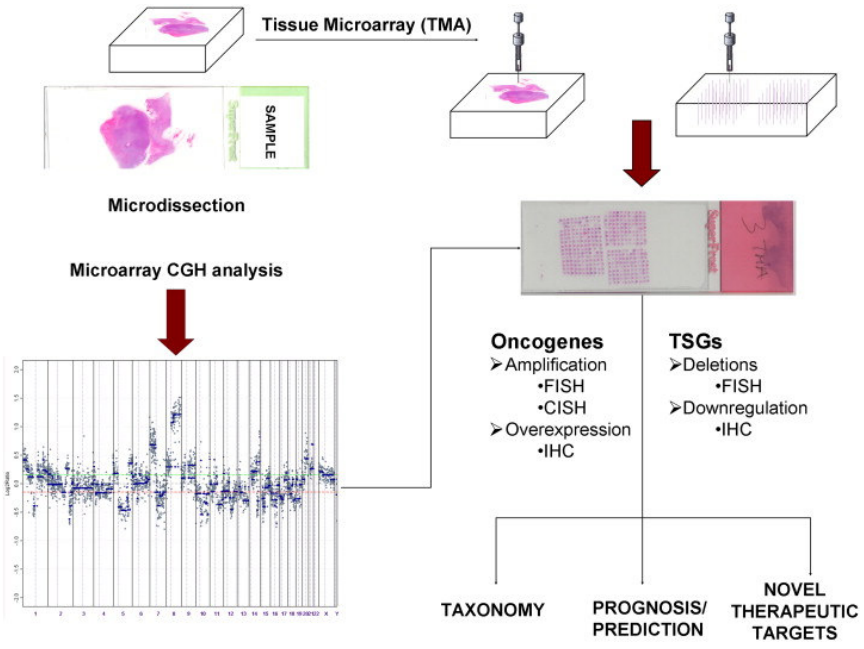

MBK Lambros et al, 2007

Figure 4 : Validation des données de CGH par FISH, CISH et IHC. CGH : hybridation génomique comparative ; FISH/CISH : hybridation *in situ* fluorescente/chromogénique ; IHC : immunohistochimie ; TSG : gène suppresseur de tumeur.

L'analyse statistique des données d'IHC a été réalisée à l'aide de la version 11.5 du logiciel SPSS (IBM®), utilisant le test du chi-deux et le test exact de Fisher. Une valeur de *p* inférieure à 0,05 était considérée comme statistiquement significative.

Le test exact de Fisher a permis la détermination des différences statistiquement significatives entre les profils génomiques des différents groupes de tumeurs.

Afin de déterminer si les carcinomes papillaires constituent une entité génomique distincte des CCI-NSTs, l'ensemble des tumeurs (cas et contrôles) a été soumis à une analyse non supervisée (clustering), méthode visant à regrouper les tumeurs en fonction de la

ressemblance de leurs profils génomiques. La proximité entre deux tumeurs a été déterminée par la distance euclidienne et les groupes ont été définis à l'aide de l'algorithme de classification hiérarchique de Wards.

Molecular characterisation of breast papillary carcinomas

Raphaëlle Duprez[1,2], Magali Lacroix-Triki[1,3], Alan MacKay[1], Maryou B Lambros[1], Rachael Natrajan[1], Eric Ward[1], Gaëtan Mac Grogan[4], Flavie Arbion[2], Patrick Michenet[5], Alan Ashworth[1] , Anne Vincent-Salomon[6], Jorge S Reis-Filho[1]

1- The Breakthrough Breast Cancer Research Centre, Institute of Cancer Research, London, SW3 6JB, UK
2- Centre Hospitalier Universitaire, 37044 Tours, France
3- Institut Claudius Regaud, 31052 Toulouse, France
4- Institut Bergonié, 33076 Bordeaux, France
5- Centre Hospitalier Régional, 45100 Orléans, France
6- Institut Curie, 75005 Paris, France

Corresponding author:

Professor Jorge S Reis-Filho

The Breakthrough Breast Cancer Research Centre

Institute of Cancer Research

237 Fulham Road

London, SW3 6JB, UK

Email: Jorge.Reis-Filho@icr.ac.uk

Abstract

Papillary carcinomas of the breast are rare tumours that are reported to have a relatively good outcome. Three main morphological subtypes are currently recognised: encapsulated, solid and frankly invasive papillary carcinomas.

The aims of this study were to characterise immunohistochemical and genomic profiles of papillary carcinomas and their subtypes, and to determine whether they are distinct from grade- and oestrogen receptor (ER)-matched invasive ductal carcinomas of no special type (IDC-NSTs) at the genomic level.

Sixty-four breast papillary carcinomas and 64 grade- and ER-matched IDC-NSTs were assessed by immunohistochemistry on tissue microarrays using antibodies against ER, progesterone receptor, HER2, Ki67, p53, Bcl2, E-cadherin, cyclin D1, cortactin, basal, myoepithelial and neuroendocrine markers. Fifty papillary carcinomas (32 encapsulated, 5 solid and 13 invasive) and 50 grade- and ER-matched IDC-NSTs were microdissected and subjected to high-resolution micro-array based comparative genomic hybridization (aCGH). Chromogenic and fluorescent *in situ* hybridizations were used to validate selected copy number aberrations detected by aCGH.

Breast papillary carcinomas were of non-high histological grade (91%), expressed ER (100%), lacked HER2 overexpression (100%) and were therefore of luminal molecular phenotype. They showed a higher expression of CCND1 than grade- and ER-matched IDC-NSTs (chi-squared test, $p = 0.002$) and a lower expression of p53 (Fisher's exact test, $p = 0.017$). Moreover, they were less frequently associated with lympho-vascular invasion and lymph node metastasis than grade- and ER-matched IDC-NSTs (Fishers' exact tests, $p = 0.024$ and 0.001, respectively). Papillary carcinomas often harboured the hallmark genetic aberration of ER positive and non-high grade IDC-NSTs (*i.e.* loss of 16q). However, when

compared with grade- and ER-matched IDC-NSTs, they harboured significantly less frequently whole arm gain of 1q and whole arms losses of 6q, 17p, 19p and 22q and more gain of 19p (multi-Fisher's exact tests $p < 0.05$).

No significant differences between the genomic profiles of encapsulated, solid and invasive variants of papillary carcinomas were observed.

Taken together, our results demonstrate that papillary breast carcinomas are preferentially non-high histological grade tumours of luminal phenotype that have genomic features largely consistent with and overlapping those of grade- and ER-matched IDC-NSTs. These findings suggest that papillary carcinomas should be considered as part of the spectrum of the non-high grade breast neoplasia family rather than as a distinct genomic entity from IDC-NSTs. Besides, it is also conceivable that papillary morphology may be underpinned by genomic aberrations other than gene copy number (*e.g.* somatic mutations or structural rearrangements) or epigenetic changes.

Keywords: papillary carcinoma, breast cancer, comparative genomic hybridization, immunohistochemistry, *in situ* hybridization

Introduction

Special types of breast cancer account for 25% of all breast cancers and the latest edition of the WHO classification of breast tumours describes 17 distinct morphological entities [1]. Previous studies have shown that those special types are more homogeneous between them than the common invasive ductal carcinomas of no special type (IDC-NSTs) at the genomic level. Therefore, they could constitute adequate models for the identification of molecular drivers in breast cancers [2-5].

Papillary carcinomas of the breast are described as one of these histological special types. Accounting for 1% of all breast cancers, they usually affect post-menopausal patients and have an overall favourable outcome [1, 6-8]. Histologically, they are characterised by arborescent fibrovascular stalks lined by a malignant epithelial proliferation [1]. Importantly, they show a lack of myoepithelial cell layer within their papillae, a feature that distinguishes them from benign intraductal papillomas [1, 9-10].

The classification of breast papillary carcinomas has changed over time and remains one of the most controversial areas in breast pathology [7]. The WHO describes 'invasive' papillary carcinomas as one of the 17 special types of breast cancer, in opposition to '*in situ*' papillary carcinomas. These '*in situ*' lesions comprise papillary ductal carcinoma *in situ* (DCIS) and encapsulated or 'intracystic' papillary carcinoma [1]. In 2006, Collins et al proposed that encapsulated papillary carcinomas should not be considered as variants of intraductal papillary carcinomas but as invasive lesions, as long as they lack a myoepithelial cell layer at their periphery [10-11]. They thus described encapsulated as well as solid papillary carcinomas among invasive lesions, in opposition to papillary DCIS, around which a remaining myoepithelial cell layer is observed.

Three main morphological subtypes of papillary carcinomas are currently recognised [8], and we have in this study categorized the tumours into these three subgroups: i) encapsulated papillary carcinomas, characterised by an often well circumscribed nodule of papillary carcinoma surrounded by a thick fibrous capsule, ii) solid papillary carcinomas, composed of nodules or sheets of ovoid to spindle-shaped cells growing in a solid pattern and that may have endocrine features and iii) invasive papillary carcinomas, characterised by a papillary carcinoma frankly invading surrounding tissue.

Few studies have been dedicated to breast papillary carcinomas but none of them has investigated the genomic profile of a large series of this particular histological entity.

Here we wanted to determine whether breast papillary carcinomas constitute a genomic entity distinct from grade- and ER-matched IDC-NSTs and whether the three morphological subtypes of papillary carcinomas described above harbour similar or distinct genomic aberrations.

The aims of this study are thus i) to characterise breast papillary carcinomas at the immunohistochemical and genomic levels, ii) to determine whether they are distinct from grade- and ER-matched IDC-NSTs and iii) to define whether encapsulated, solid and invasive papillary carcinomas constitute the same or distinct genomic entities.

To address these questions, we studied a series of 64 breast papillary carcinomas by means of immunohistochemistry, high resolution micro-array based comparative genomic hybridization (aCGH) and chromogenic and fluorescent *in situ* hybridizations (CISH/FISH).

Materials and methods

Cases

A series of 64 papillary carcinomas of the breast were retrieved from the files of The Curie Institute, Paris, France; the Royal Marsden Hospital, London, UK; the Bergonié Institute, Bordeaux, France; the Centre Hospitalier Universitaire, Tours, France; and the Centre Hospitalier Régional, Orléans, France. Patients' identification was anonymized prior to analysis and the study approved by local ethical committees.

The diagnosis of papillary carcinoma (Figure 1A) was confirmed by at least two breast pathologists (RD, MLT, ± AVS, JRF and GMG) and the tumours were categorized into one of the morphological subtypes, *i.e.* encapsulated, solid or invasive papillary carcinoma, according to the histological criteria described above. For each tumour, histological grade was assessed using Nottingham grading system [12]. The presence of associated papilloma, DCIS and IDC-NST component, as well as lympho-vascular invasion and lymph node metastasis, were also assessed.

Tissue microarrays (TMAs) were constructed from paraffin blocks with triplicate 0.6 mm tumour cores. Normal tissues were included in the TMAs as controls.

Immunohistochemistry

For each case, five immunohistochemical (IHC) stainings were performed on full sections to confirm the diagnosis of papillary carcinoma. Immunostains for myoepithelial markers p63, smooth muscle actin and cytokeratin (CK) 5/6 were performed with internal positive controls to ensure the absence of a myoepithelial cell layer within the papillary fronds of the tumour

and at its periphery [11] (Figure 1B). Neuroendocrine markers chromogranin and synaptophysin were used to determine the presence of neuroendocrine differentiation and tumours with more than 50% of the cells expressing neuroendocrine markers were excluded from the study, as those were considered as neuroendocrine carcinomas [1].

IHC profile of the included cases of papillary carcinomas was assessed on 3 µm thick TMAs sections, using a panel of antibodies against oestrogen receptor (ER), progesterone receptor (PR), HER2, Ki67, Bcl2, p53, EGFR, CK14, CK17, nestin, caveolin 1 (CAV1), caveolin 2 (CAV2), E-cadherin, cyclin D1 and cortactin. Positive and negative controls were included in each experiment. All the IHC slides were interpreted semi-quantitatively by two pathologists (RD, MLT), blinded to the results of aCGH and CISH/FISH. Antibody clones, dilutions, antigen retrieval methods, scoring systems and cut-offs used are described in Supplementary Table 1. Briefly, Allred scoring system was used for ER, PR and cyclin D1, as previously described [13-14]. Ki67 staining was considered as low if <10% of neoplastic nuclei were stained and high if >30% of neoplastic nuclei were stained [13]. The HercepTest® scoring system updated according to ASCO/CAP guidelines was used for HER2 assessment, as well as for EGFR [15-16]. For HER2, FISH was performed in case of an equivocal IHC score 2+. A cut-off of 10% was used for assessment of CK5/6, CK14, CK17, Bcl2, chromogranin and synaptophysin [17-20]. P53 was considered positive when >10% of neoplastic cells displayed moderate or strong unequivocal nuclear staining [13]. Previously described cut-offs were used for CAV1, CAV2, nestin, E-cadherin and cortactin [21-25].

Tumours were then classified into molecular subtypes described by Nielsen et al, according to their ER, HER2, CK5/6 and EGFR status [26].

The IHC profiles of the 64 papillary carcinomas were compared with those of 64 grade- and ER-matched IDC-NSTs (Table 1).

Microdissection and DNA extraction

For all 64 cases, ten 10 µm thick sections were cut from the paraffin blocks and stained with nuclear fast red. Microdissection was performed with a sterile needle under a stereomicroscope (Olympus SZ61, Tokyo, Japan) in order to ensure a percentage of tumour cells greater than 90%. DNA was then extracted using Qiagen DNeasy Blood and Tissue Kit (Hamburg, Germany). Double-strand DNA concentration was measured using the Picogreen® assay, according to the manufacturer's protocol (Invitrogen, Paisley, UK). DNA quality was assessed using four primer sets in a multiplex PCR, as previously described [27-29].

Out of 64 microdissected papillary carcinomas, 50 yielded DNA of sufficient quantity and quality for aCGH analysis.

Microarray comparative genomic hybridization

The aCGH platform used in this study was constructed at the Breakthrough Breast Cancer Research Centre and comprises 32000 bacterial artificial chromosome (BAC) clones tiled across the genome. This type of BAC array platform has been shown to be as robust as, and to have comparable resolution to, high-density oligonucleotide arrays [30-32].

DNA labelling, array hybridizations and washes were carried out as previously described [33-34]. Slides were scanned using an Axon 4000B scanner (Axon Instruments, Burlingame, CA, USA) and images were processed using Genepix Pro 6.1 image analysis software (Axon Instruments). aCGH data were pre-processed and analysed using an in-house R script in R version 2.9.0, as previously described [35-36]. After filtering polymorphic BACs, a final dataset of 31367 clones with unambiguous mapping information according to the build hg19 of the human genome (http://www.ensembl.org) was smoothed using the circular binary

segmentation (cbs) algorithm [35-36]. A categorical analysis was applied to the BACs after classifying them as representing amplification (>0.45), gain (>0.08 and ≤0.45), loss (<-0.08), or no change according to their cbs-smoothed $\log_2$ ratio values [33, 37]. Threshold values were determined and validated as previously described [33].

Categorical data were subjected to a multi-Fisher's exact test [with adjustment for multiple testing using the step-down permutation procedure maxT, providing strong control of the family-wise type I error rate (FWER)], as previously described [27-29, 34], to identify statistically significant differences between the genomic profiles of i) papillary carcinomas and grade- and ER-matched IDC-NSTs and ii) encapsulated, solid and invasive papillary carcinomas.

Hierarchical clustering analysis was performed as previously described [28-29]. Briefly, categorical aCGH states (*i.e.* gains, losses, and amplifications) were used for clustering, employing Wards clustering algorithm and Euclidean distance.

In parallel, 50 grade- and ER-matched IDC-NSTs were selected as controls for the genomic study and subjected to aCGH.

Chromogenic/fluorescent *in situ* hybridizations

Amplifications of selected genes were assessed by CISH or FISH, as a tool to validate selected amplifications revealed by aCGH [38].

CISH was performed on full sections of selected cases using the commercial digoxin-labelled probe for *CCND1* (ZytoVision, Bremerhaven, Germany). FISH was performed on full sections of selected cases using the commercial digoxin-labelled probes for *CCND1* (ZytoVision, Bremerhaven, Germany) and *HER2* (Vysis, Illinois, USA). Besides, an in-house digoxin-labelled probe for selected genes mapping to the smallest region of amplification on

7q11.23 was constructed, as previously described [39], and used for CISH and FISH. This region encompasses *EIF4H*, a gene that has been reported to play an important role in carcinogenesis through the activation of oncogenic signaling [40].

Signals were counted in the nuclei of at least 30 morphologically unequivocal neoplastic cells and gene amplification was defined as previously described [27-29]. In brief, a case was considered amplified for the selected gene/region when more than 50% of the neoplastic cells harboured more than 5 signals, gene clusters or a combination of signals and clusters.

Statistical analysis of IHC data

The SPSS statistical software package version 11.5 (SPSS Inc, an IBM Company Headquarters, Chicago, IL, USA) was used for the statistical analysis of IHC data. Correlations between categorical variables were performed using chi-square test and Fisher's exact test. All *p* values were two-tailed and 95% confidence intervals were adopted.

Results

Histological analysis

Among 64 breast papillary carcinomas, 41 were diagnosed as encapsulated, 9 as solid and 14 as invasive papillary carcinomas. Sixty-six percent (n = 42) were of histological grade I, 25% (n = 16) of grade II and 9% (n = 6) of grade III, *i.e.* 91% of the tumours were of non-high histological grade (Figure 1A and Supplementary Table 2). The mean of mitotic count was 14.6 mitoses for 10 high power fields, with a range of 1-93. Detailed histological features of the 64 papillary carcinomas are provided in Supplementary Tables 2 and 3.

In accordance with their relatively good outcome, papillary carcinomas were significantly less associated with lympho-vascular invasion and lymph node metastasis than IDC-NSTs (Fisher's exact tests, p = 0.024 and 0.001, respectively; Table 1), whereas no statistically significant differences were detected between the three variants of papillary carcinomas.

IHC analysis

IHC profile of papillary carcinomas and comparison with grade- and ER-matched IDC-NSTs are described in Table 1 and Supplementary Tables 3 and 4.

In accordance with their predominant non-high histological grade, papillary carcinomas displayed a relatively low proliferation rate, demonstrated by the low Ki67 staining (Figure 1C). All cases (n = 64) showed expression of ER and lacked HER2 overexpression. The large majority (n = 61/64) were negative for basal markers. Papillary carcinomas were therefore of luminal molecular phenotype, according to Nielsen's IHC criteria [26] (Figure 1D-H).

Of note, three cases were positive for CK5/6 and among those, one case of grade III invasive papillary carcinoma of luminal phenotype displayed positivity for most basal markers (CK5/6, EGFR, CK14 and nestin) and lacked expression of Bcl2. Although positive for ER, this case was only scored Allred 3 for this marker.

Eighty-four percent (n = 54) of the tumours showed a high expression of CCND1, and the expression of CCND1 was significantly higher in papillary carcinomas than in grade- and ER-matched IDC-NSTs (chi-squared test, p = 0.002).

On the other hand, the expression of p53 was significantly more frequently observed in IDC-NSTs than in papillary carcinomas (Fisher's exact test, p = 0.017).

When compared, the IHC profiles of the three variants of papillary carcinomas were very similar. However, it needs to be noted that whereas the three variants were positive for ER in

all cases, solid and invasive variants showed significantly less positivity for PR (Fisher's exact test, $p = 0.039$) than the encapsulated variant.

Besides, solid papillary carcinomas revealed, as expected, more neuroendocrine differentiation than the two other variants (Fisher's exact test, $p < 0.05$; Supplementary Table 3).

Genomic profiling of papillary carcinomas

Among 50 papillary carcinomas subjected to aCGH, 32 were encapsulated, 5 solid and 13 invasive papillary carcinomas.

The aCGH profile of this set of tumours revealed a relative low level of genomic changes across the genome, with a median of 12.1% of BACs showing either gains, losses or amplifications (range 3.3-33.9%, mean 14.5 ± 7.4%).

According to Hicks et al description of aCGH genomic patterns [41], 80% (n = 40/50) of papillary carcinomas displayed a 'simplex' genomic pattern, characterised by broad segments of gains or deletions, affecting entire chromosomes or chromosome arms, associated with one occasional peak of amplification. Twenty percent (n = 10/50) showed a 'firestorm' complex pattern, with at least one additional localised region of clustered, narrow peaks of amplification, with each cluster confined to a single chromosome arm. No 'sawtooth' complex pattern was observed.

Regions of recurrent gains and losses occurring in the 50 papillary carcinomas are illustrated in Supplementary Figure 1 and described in Supplementary Tables 5 and 6.

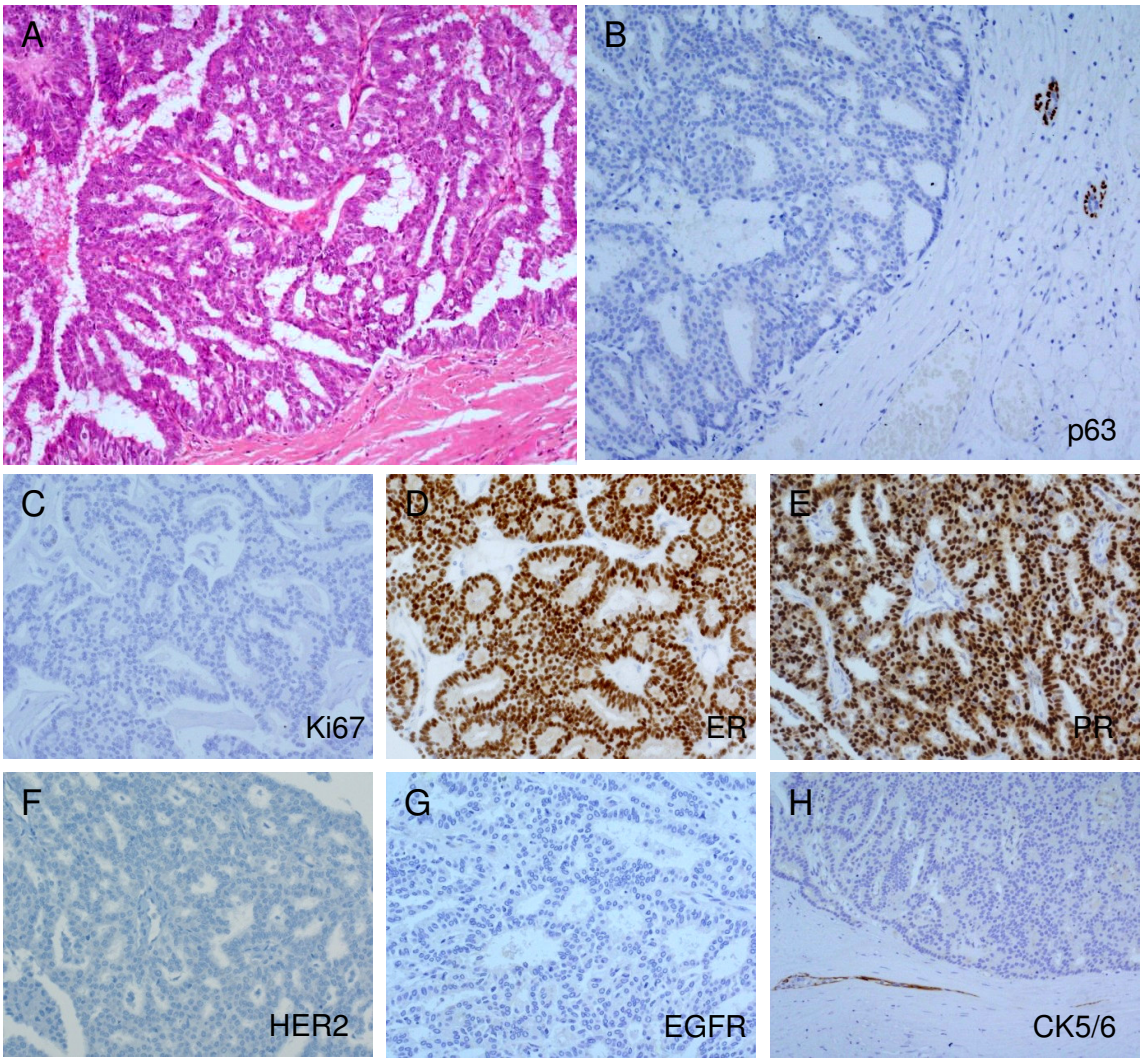

Figure 1: Histology and immunohistochemical profile of a typical papillary carcinoma of the breast.

Representative micrograph showing a typical non-high grade encapsulated papillary carcinoma (A), characterized by arborescent fibrovascular stalks lined by malignant epithelial cells. Immunohistochemical staining with myoepithelial markers showed lack of myoepithelial cell layer at the periphery of the tumour (as depicted by p63 immunostaining) (B). This papillary carcinoma exhibited a low proliferation rate, as shown by the low Ki67 nuclear staining (C). It displayed a luminal phenotype, characterized by strong expressions of ER (D) and PR (E), lack of HER2 overexpression (F) and no expression of basal markers (EGFR (G) and CK5/6 (H)). ER: oestrogen receptor; PR: progesterone receptor.

Table 1: Histopathological and immunohistochemical features of 64 papillary carcinomas and 64 grade- and ER-matched IDC-NSTs.

	N	papillary carcinomas (n=64)	IDC-NSTs (n=64)	*p* value
Histological grade	128			1**
I		42 (65.6%)	42 (65.6%)	
II		16 (25%)	16 (25%)	
III		6 (9.4%)	6 (9.4%)	
Lympho-vascular invasion	128			0.024*
present		10 (15.6%)	22 (34.4%)	
absent		54 (84.4%)	42 (65.6%)	
Lymph node metastasis	89			0.001*
present		4 (13.3%)	29 (49.2%)	
absent		26 (86.7%)	30 (50.8%)	
ER	128			NP
positive		64 (100%)	64 (100%)	
PR	128			0.492*
positive		58 (90.6%)	61 (95.3%)	
negative		6 (9.4%)	3 (4.7%)	
HER2	128			NP
negative		64 (100%)	64 (100%)	
Ki67	128			0.683**
low (<10%)		52 (81.3%)	50 (78.1%)	
intermediate (10-30%)		10 (15.6%)	13 (20.3%)	
high (>30%)		2 (3.1%)	1 (1.6%)	
p53	128			0.017*
positive		1 (1.6%)	9 (14.1%)	
negative		63 (98.4%)	55 (85.9%)	
Bcl2	125			0.109*
positive		63 (98.4%)	56 (91.8%)	
negative		1 (1.6%)	5 (8.2%)	
Cyclin D1	128			0.002**
low (Allred score 0-3)		5 (7.8%)	8 (12.5%)	
intermediate (Allred score 4-5)		5 (7.8%)	19 (29.7%)	
high (Allred score 6-8)		54 (84.4%)	37 (57.8%)	
Cortactin	128			<0.0001**
low (quick score <5)		41 (64%)	12 (18.8%)	
intermediate (quick score 5-12)		14 (21.9%)	45 (70.3%)	
high (quick score >12)		9 (14.1%)	7 (10.9%)	
E-cadherin	126			0.613**
normal		56 (90.3%)	57 (89.1%)	
reduced		6 (9.7%)	6 (9.4%)	
negative		0	1 (1.5%)	
Cytokeratin 5/6	128			0.244*
positive		3 (4.7%)	0	
negative		61 (95.3%)	64 (100%)	
Cytokeratin 14	128			>0.999*
positive		1 (1.6%)	0	
negative		63 (98.4%)	64 (100%)	

Cytokeratin 17	127			>0.999*
positive		1 (1.6%)	1 (1.6%)	
negative		62 (98.4%)	63 (98.4%)	
Basal cytokeratins	128			0.619*
positive		3 (4.7%)	1 (1.6%)	
negative		61 (95.3%)	63 (98.4%)	
EGFR	128			>0.999*
positive		1 (1.6%)	0	
negative		63 (98.4%)	64 (100%)	
Caveolin 1	127			0.496*
positive		1 (1.6%)	0	
negative		62 (98.4%)	64 (100%)	
Caveolin 2	127			0.496*
positive		1 (1.6%)	0	
negative		62 (98.4%)	64 (100%)	
Nestin	124			0.496*
positive		2 (3.2%)	0	
negative		61 (96.8%)	61 (100%)	
Any basal marker	128			0.619*
positive		3 (4.7%)	1 (1.6%)	
negative		61 (95.3%)	63 (98.4%)	
Molecular phenotype[#]	128			NP
luminal		64 (100%)	64 (100%)	

* Fisher's exact test; ** Chi-squared test; [#] molecular phenotype classification according to Nielsen et al [26]; ER: oestrogen receptor; IDC-NSTs: invasive ductal carcinomas of no special type; NP: not performed (no statistics computed as the value is constant); PR: progesterone receptor.

Recurrent amplifications observed in 2 cases or more are listed in Table 2.

After exclusion of regions mapping to known copy number polymorphisms (according to http://projects.tcag.ca/variation/), the most recurrent amplification, observed in 12% of the cases (n = 6), mapped to 11q13, encompassing *CCND1* and *CTTN*.

Comparison of genomic profiles of papillary carcinomas and grade- and ER-matched IDC-NSTs

Genomic profiles of all 50 papillary carcinomas were compared with those of 50 grade- and ER-matched IDC-NSTs (Figure 2).

This comparison indicated that papillary carcinomas displayed genomic aberrations that are largely consistent with those of grade- and ER-matched IDC-NSTs. Indeed, they very often exhibited loss of 16q, a genomic hallmark of non-high grade and ER positive IDC-NSTs [42-43].

However, IDC-NSTs displayed more genomic changes across the genome than papillary carcinomas, with a median of 14.6% of BACs showing either gains, losses or amplifications (range 6.8-53%, mean 20 ± 12.6%) in IDC-NSTs (Student's *t*-Test, $p = 0.009$).

Moreover, a few significant differences in the genomic profiles of the two subgroups of tumours were observed, papillary carcinomas displaying significantly less whole arm gain of 1q and whole arms losses of 6q, 17p, 19p and 22q and more gain of 19p than IDC-NSTs (multi-Fisher's exact test $p < 0.05$; Figure 2A, Table 3 and Supplementary Tables 7 and 8).

In subgroup analysis according to grade, gain of 1q and losses of 6q, 17p and 22q were still significant in grade I tumours. Gains of 1q and 19p and losses of 6q, 17p and 22q were also significant in grade II tumours (multi-Fisher's exact test $p < 0.05$) (Supplementary Figure 2A-B). However, these differences were not reported when comparing grade III tumours (Supplementary Figure 2C). Of note, this might be due to the limited number of grade III tumours included in the study ($n = 5$).

Table 2: Recurrent (in 2 or more cases) genomic amplifications observed in 50 papillary carcinomas.

Chromosome	Cytobands	Start (Mb)	End (Mb)	Number of BACs	Number of cases	Genes	mi-RNAs	aCGH CNVs
7	q11.22-q11.23	70,5	75,52	72	2	WBSCR17, CALN1, TYW1B, POM121, NSUN5C, TRIM74, STAG3L3, NSUN5, TRIM50, FKBP6, FZD9, BAZ1B, BCL7B, TBL2, MLXIPL, VPS37D, DNAJC30, WBSCR22, STX1A, ABHD11, CLDN3, CLDN4, WBSCR27, WBSCR28, ELN, LIMK1, EIF4H, LAT2, RFC2, CLIP2, GTF2IRD1, GTF2I, STAG3L2, NCF1, GTF2IRD2, PMS2L5, WBSCR16, GTF2IRD2B, NCF1C, GATSL1, STAG3L1, TRIM73, NSUN5B, POM121C, PMS2L3, HIP1, CCL26, CCL24, RHBDD2	hsa-mir-590	V_4541_LC9597_Wong et al. (2007), V_4542_LC9602_Wong et al. (2007), V_4543_LC9606_Wong et al. (2007), V_4544_LC9609_Wong et al. (2007), V_4545_LC9609_Wong et al. (2007) [60]
8	p11.22	38,43	38,77	5	2	TACC1, PLEKHA2*		V_4589_LC10531_Wong et al. (2007)
8	p11.21	40,04	41,86	19	2	ZMAT4, SFRP1, GOLGA7, GINS4, AGPAT6, NKX6-3, ANK1, MYST3*	hsa-mir-486	
8	q21.2	86,43	86,58	9	5	REXO1L1*		V_4601_LC10727_Wong et al. (2007)
11	q13.1-q13.2	65,86	66,46	5	2	PACS1, KLC2, RAB1B, CNIH2, YIF1A, TMEM151A, CD248, RIN1, BRMS1, SLC29A2, NPAS4, MRPL11, PELI3, BBS1, ZDHHC24, CTSF, CCDC87, CCS, RBM4, RBM4B, SPTBN2		V_4754_LC13285_Wong et al. (2007)
11	q13.3-q13.4	68,75	71,26	29	6	MRGPRF, TPCN2, MYEOV, CCND1, ORAOV1, FGF19, FGF4, FGF3, ANO1, FADD, PPFIA1, CTTN, SHANK2, DHCR7, NADSYN1, KRTAP5-10	hsa-mir-548k	V_4755_LC13316_Wong et al. (2007), V_4756_LC13329_Wong et al. (2007)
16	p13.3	1,15	1,41	3	2	CACNA1H, TPSG1, TPSB2, TPSAB1, TPSD1, PRSS29P, UBE2I, BAIAP3, C16orf42, GNPTG*		V_4779_LC16593_Wong et al. (2007), V_4915_LC16593_Wong et al. (2007)
18	q21.1	44,3	44,59	7	9	ST8SIA5, PIAS2, KATNAL2, TCEB3CL2, TCEB3CL, TCEB3C, TCEB3B*		
20	q11.23	34,43	36,28	24	2	PHF20, SCAND1, C20orf152, EPB41L1, C20orf4, DLGAP4, MYL9, TGIF2, C20orf24, SLA2, NDRG3, DSN1, C20orf117, C20orf118, SAMHD1, RBL1, C20orf132, RPN2, GHRH, MANBAL, SRC, BLCAP, NNAT		V_5136_LC19617_Wong et al. (2007)
20	q13.2	52,71	53,24	8	2	CYP24A1, PFDN4, DOK5*		

20	q13.31-q13.32	56,23	56,72	4	2	PMEPA1*		
20	q13.33	59,36	61,43	21	2	CDH4, TAF4, LSM14B, PSMA7, SS18L1, GTPBP5, HRH3, OSBPL2, ADRM1, LAMA5, RPS21, CABLES2, C20orf151, GATA5, C20orf166, SLCO4A1, C20orf90, NTSR1*	hsa-mir-1257, hsa-mir-1-1, hsa-mir-133a-2	V_5144_LC19966_Wong et al. (2007), V_5145_LC19985_Wong et al. (2007), V_5146_LC19985_Wong et al. (2007), V_5147_LC19985_Wong et al. (2007), V_5148_LC19985_Wong et al. (2007)

Mb: megabase pair; BACs: bacterial artificial chromosomes; aCGH: array comparative genomic hybridization; CNV: copy number variation; * Regions reported to map to copy number polymorphism according to http://projects.tcag.ca/variation/.

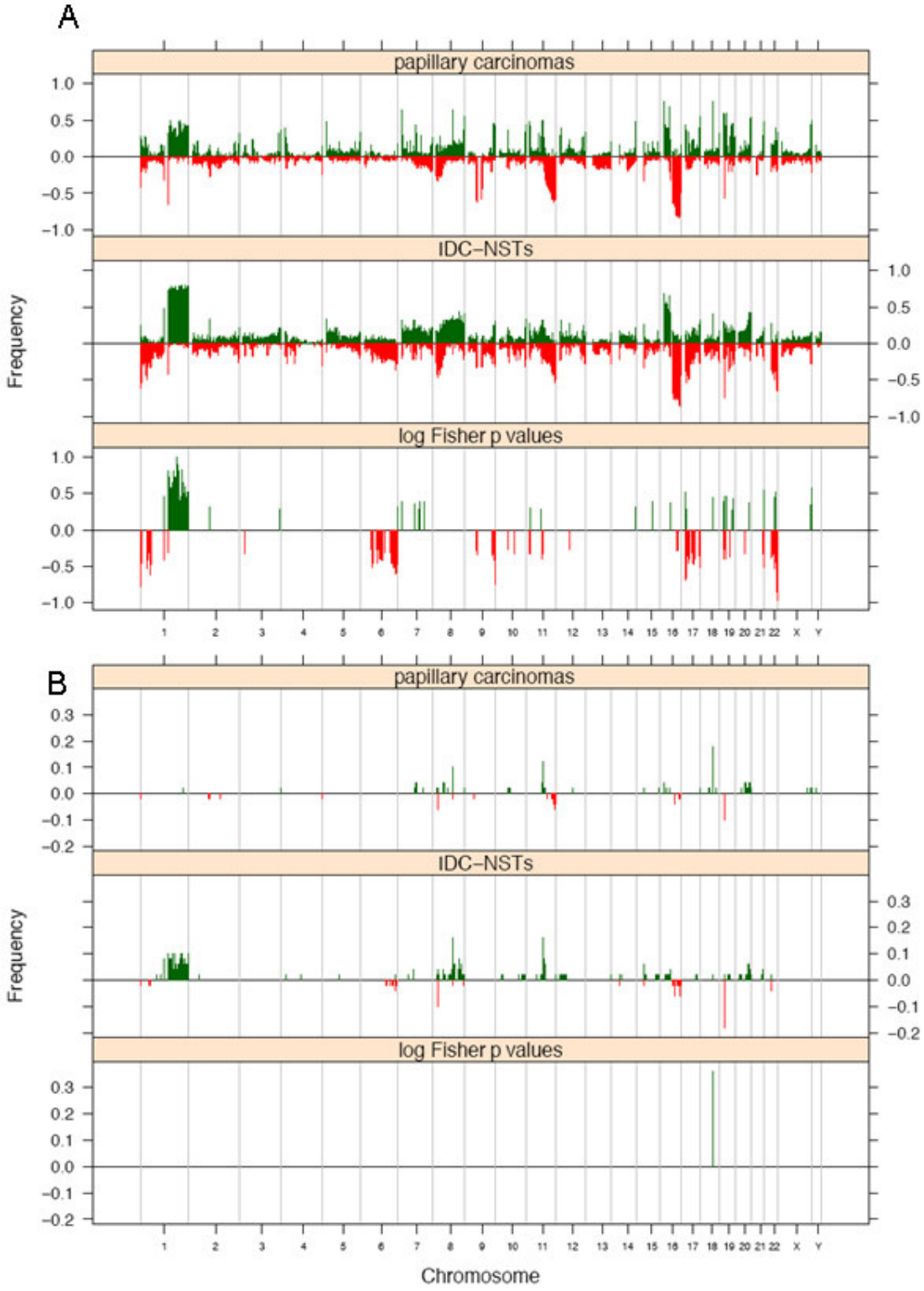

Figure 2: Multi Fisher's exact test comparing genomic copy number aberrations observed in papillary carcinomas and in grade- and ER-matched IDC-NSTs.
Frequency plots of chromosomal gains and losses (A) and amplifications and deletions (B) observed in 50 papillary carcinomas and 50 grade- and ER-matched IDC-NSTs. The proportion of tumours in which each bacterial artificial chromosome (BAC) clone is gained (green bars) or lost (red bars) is plotted (Y axis) for each BAC clone according to its genomic location (X axis). Inverse Log_{10} values of the Fisher's exact test *p* values are plotted according to genomic location (X axis). ER: oestrogen receptor; IDC-NSTs: invasive ductal carcinomas of no special type.

When considering only non-high grade tumours, gain of whole arm of 1q was much more frequent in IDC-NSTs (78%) than in papillary carcinomas (40%). However, 29% of papillary carcinomas displayed gain of partial arm of 1q, versus 13% in IDC-NSTs (Fisher's exact test, $p = 0.001$). On the other hand, losses of 16q were equally seen in papillary carcinomas and IDC-NSTs. As a result, another genomic hallmark of non-high grade breast tumours, *i.e.* concurrent gain of 1q and loss of 16q [44-46], was observed in only 35% of non-high grade papillary carcinomas, versus in 62% of non-high grade IDC-NSTs (Fisher's exact test, $p = 0.02$). The same tendency was observed when considering all histological grades.

When considering all tumours together, losses of whole arms of 6q, 17p, 19p and 22q were more prevalent in IDC-NSTs than in papillary carcinomas, whereas losses of partial arms of these chromosomes were more frequently observed in papillary carcinomas than in IDC-NSTs. The same tendency was observed when considering only non-high grade tumours (Table 3).

Unsupervised hierarchical analysis comprising all papillary carcinomas and IDC-NSTs revealed that papillary carcinomas did not cluster separately from IDC-NSTs (two-tailed Fisher's exact test, $p = 0.254$; Figure 3A). When considering only non-high grade tumours, this analysis led to the same observation (two-tailed Fisher's exact test, $p = 0.083$; Figure 3B).

After exclusion of regions mapping to known copy number polymorphisms, no significant difference between amplifications and deletions observed in papillary carcinomas and grade- and ER-matched IDC-NSTs was detected (Figure 2B).

Table 3: Comparison of the most frequent chromosomal aberrations observed in papillary carcinomas and grade- and ER-matched IDC-NSTs.

		grade I/II papillary carcinomas (n=45)	grade I/II IDC-NSTs (n=45)	all papillary carcinomas (n=50)	all IDC-NSTs (n=50)
Chr 1q	Partial gain	13 (29%)	6 (13%)	15 (30%)	7 (14%)
	Whole arm gain (1q+)	18 (40%)	35 (78%)	19 (38%)	37 (74%)
	No change	14 (31%)	4 (9%)	16 (32%)	6 (12%)
1q+ *p* value*		***0.001***		***0.001***	
Chr 16q	Partial loss	6 (13%)	7 (15%)	9 (18%)	9 (18%)
	Whole arm loss (16q-)	37 (82%)	36 (80%)	39 (78%)	39 (78%)
	No change	2 (4%)	2 (4%)	2 (4%)	2 (4%)
16q- *p* value*		***1***		***1***	
1q+ 16q-**		16 (35%)	28 (62%)	16 (32%)	30 (60%)
1q+ 16q- *p* value*		***0.02***		***0.009***	
Chr 6q	Partial loss	19 (42.2%)	10 (22.2%)	20 (40%)	13 (26%)
	Whole arm loss (6q-)	0	9 (20%)	0	9 (18%)
	No change	26 (57.8%)	26 (57.8%)	30 (60%)	28 (56%)
6q- *p* value*		***0.001***		***0.003***	
Chr 17p	Partial loss	27 (60%)	15 (33.3%)	29 (58%)	15 (30%)
	Whole arm loss (17p-)	2 (4.4%)	12 (26.7%)	4 (8%)	16 (32%)
	No change	16 (35.6%)	18 (40%)	17 (34%)	19 (38%)
17p- *p* value*		***0.004***		***0.002***	
Chr 19p	Partial gain	15 (33.3%)	14 (31.1%)	18 (36%)	17 (34%)
	Whole arm gain (19p+)	19 (42.2%)	9 (20%)	20 (40%)	9 (18%)
	No change	11 (24.4%)	22 (48.9%)	12 (24%)	24 (48%)
19p+ *p* value*		***0.029***		***0.018***	
Chr 19p	Partial loss	34 (75.6%)	22 (48.9%)	38 (76%)	25 (50%)
	Whole arm loss (19p-)	0	7 (15.6%)	0	7 (14%)
	No change	11 (24.4%)	16 (35.5%)	12 (24%)	18 (36%)
19p- *p* value*		***0.003***		***0.003***	
Chr 22q	Partial loss	24 (53.3%)	16 (35.6%)	28 (56%)	16 (32%)
	Whole arm loss (22q-)	6 (13.3%)	15 (33.3%)	6 (12%)	17 (34%)
	No change	15 (33.3%)	14 (31.1%)	16 (32%)	17 (34%)
22q- *p* value*		***0.063***		***0.013***	

* Fisher's exact test; ** concurrent whole arm gain of 1q and whole arm loss of 16q; Chr: chromosome; ER: oestrogen receptor; IDC-NSTs: invasive ductal carcinomas of no special type.

Comparison of genomic profiles of encapsulated, solid and invasive papillary carcinomas

When compared, the genomic profiles of the three variants of papillary carcinomas were quite similar (Figure 4).

Loss of 16q was significantly more prevalent in encapsulated papillary carcinomas than in both solid and invasive variants (multi-Fisher's exact test $p < 0.05$; Supplementary Table 10 and Figure 4E). However, it needs to be noted that the frequency of non-high grade tumours among encapsulated papillary carcinomas was higher (100%) than among the two other subtypes (80% and 69% in solid and invasive papillary carcinomas, respectively) (Supplementary Figure 3).

Unsupervised hierarchical analysis of all 50 papillary carcinomas revealed that the three morphological variants do not cluster separately (Supplementary Figure 3).

Moreover, after exclusion of regions mapping to known copy number polymorphisms, no difference in amplifications and deletions observed in the three morphological subtypes was revealed (data not shown).

CISH/FISH validation of selected genetic amplifications

Two cases of grade I (one encapsulated and one solid papillary carcinomas) and two cases of grade II and III invasive papillary carcinomas were scored as IHC equivocal (2+) for HER2. Amplification of *HER2* however was not revealed by FISH, and aCGH did not either detect *HER2* amplification in these four cases.

CCND1 amplification was detected by aCGH in 6 cases (4 cases of non-high grade encapsulated papillary carcinomas and 2 cases of non-high grade invasive papillary carcinomas) and confirmed in all by CISH and FISH (one case shown in Supplementary

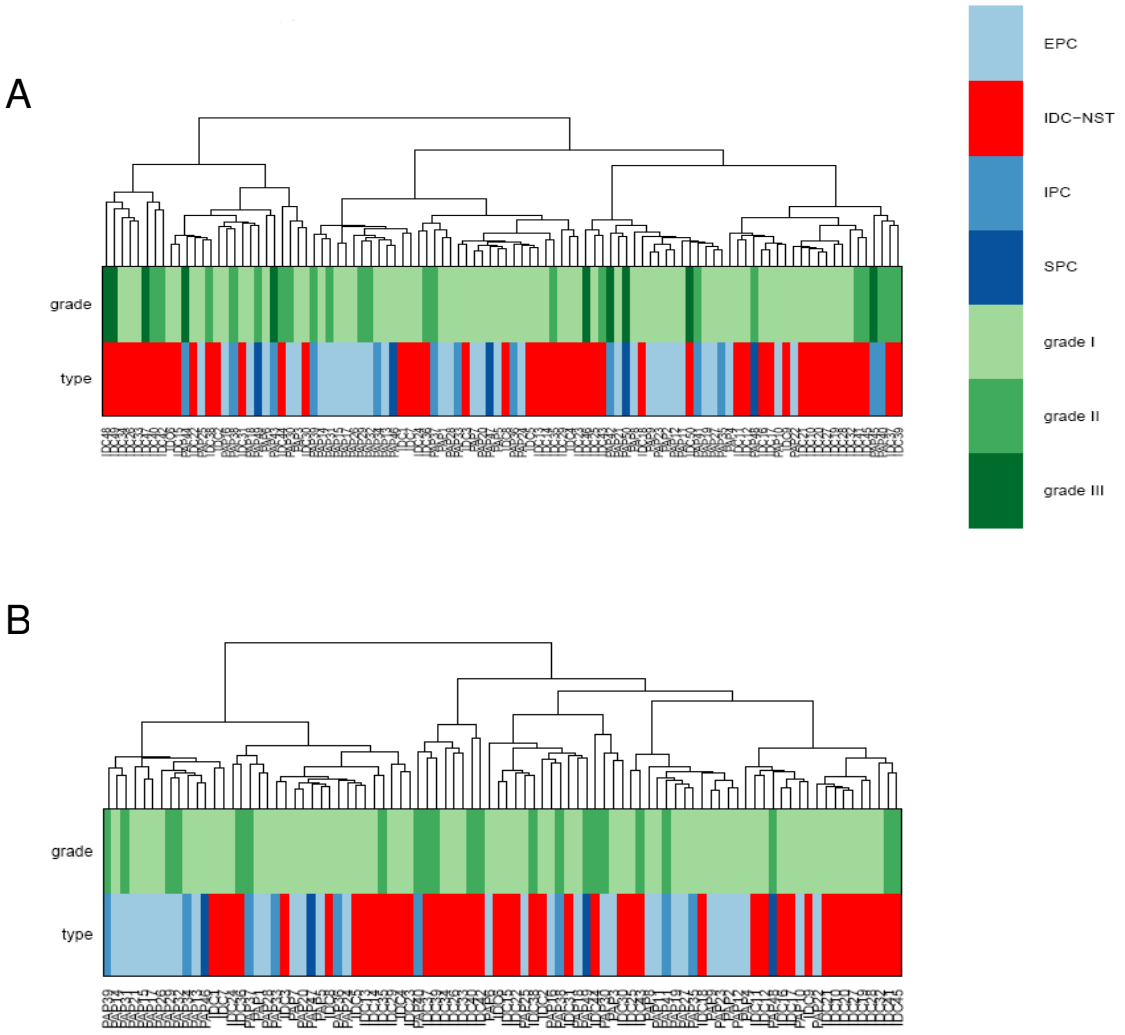

Figure 3: Hierarchical clustering analyses of papillary carcinomas and grade- and ER-matched IDC-NSTs. Dendograms of 50 papillary carcinomas and 50 grade- and ER-matched IDC-NSTs (A) and 45 non-high grade papillary carcinomas and 45 non-high grade IDC-NSTs (B). Hierarchical clustering analyses were performed with aCGH categorical states (*i.e.* gains, losses and amplifications) and employed Euclidean distance and the Wards algorithm. When considering all tumours together (A) or only non-high grade tumours (B), the two groups of tumours did not cluster separately (two-tailed Fisher's exact tests, $p = 0.254$ and 0.083, respectively). ER: oestrogen receptor; IDC-NSTs: invasive ductal carcinomas of no special type; aCGH: array comparative genomic hybridization.

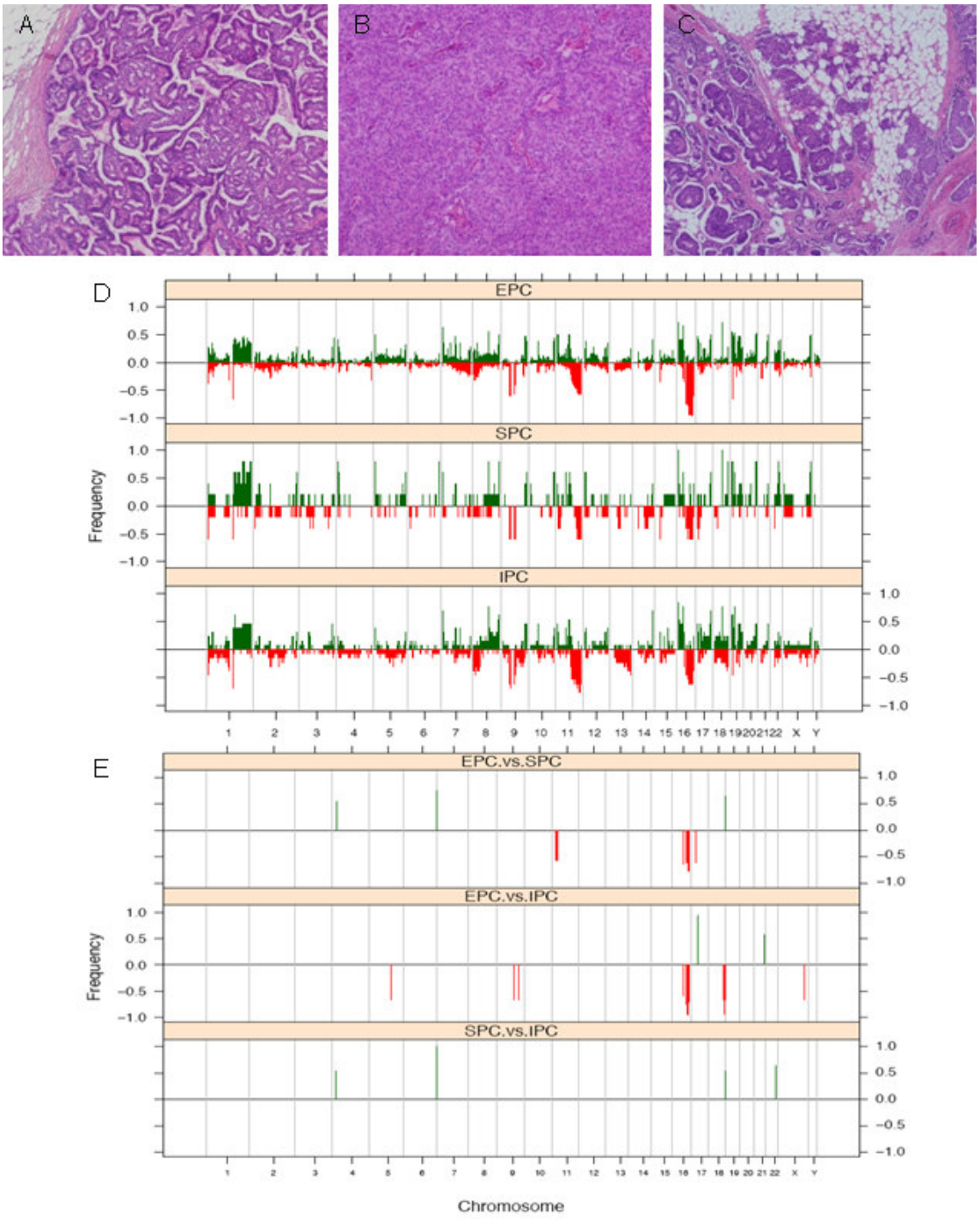

Figure 4: Comparative genomic profiling of encapsulated, solid and invasive papillary carcinomas. Representative micrographs showing the three currently recognised subtypes of breast papillary carcinomas: an encapsulated papillary carcinoma (EPC) (A), characterized by a well circumscribed nodule of papillary carcinoma surrounded by a thick fibrous capsule; a solid papillary carcinoma (SPC) (B), composed of nodules of ovoid to spindle-shaped cells growing in a solid pattern; and a frankly invasive papillary carcinoma (IPC) (C), literally 'invading' surrounding fat tissue. Frequency plots of chromosomal gains and losses in EPC, SPC and IPC (D). Multi Fisher's exact comparisons of gains and losses observed in EPC, SPC and IPC (E). The proportion of tumours in which each bacterial artificial chromosome (BAC) clone is gained (green bars) or lost (red bars) is plotted (Y axis) for each BAC clone according to its genomic location (X axis). Inverse Log_{10} values of the Fisher's exact test *p* values are plotted according to genomic location (X axis).

Figure 4A-B). Besides, all these cases showed high expression of CCND1, with 5 of them displaying the maximum Allred score (Supplementary Figure 4C).

Amplification at 7q11.23 was observed in 2 cases (one non-high grade encapsulated and one high grade invasive papillary carcinomas) and confirmed by CISH and FISH using the in-house probe mapping to this genomic region (one case shown in Supplementary Figure 4D-E).

Discussion

Very few studies have been dedicated to breast papillary carcinomas, and a large majority of the literature devoted to this subtype of breast cancer is comprised of mere individual case reports [8]. Several authors have used polymorphic DNA microsatellite markers and PCR methods to investigate loss of heterozygosity (LOH) in papillary lesions of the breast [47-49], and a recurrent LOH at 16q23 was thus described in papillary carcinomas [47].

However, microarray-based comparative genomic hybridization, extensively used in the past decade for the study of breast cancer and its subtypes [27-29, 31] and enabling rapid and high resolution analysis of global genomic copy number changes in tumours, has not yet been applied to papillary breast carcinomas.

Here we provide the genomic analysis of a large series of papillary carcinomas of the breast, using microarray-based high-throughput technologies.

Our results show that breast papillary carcinomas are preferentially non-high grade tumours and display a luminal phenotype.

In accordance with their relatively good outcome [6-8], they were significantly less associated with lympho-vascular invasion and lymph node metastasis than grade- and ER-matched IDC-NSTs.

The high expression of CCND1 (84% of Allred score 6-8) seen in papillary carcinomas is in accordance with the literature, showing a correlation between strong CCND1 expression and good prognostic parameters, including non-high histological grade and ER positivity [50]. However, 11q13 amplification mapping to *CCND1*, observed in 12% of the cases, was surprisingly not much more frequent in papillary carcinomas than previously described in all breast cancers [13, 50-51].

The genomic analysis of our series of papillary carcinomas indicates that they exhibit genomic features largely consistent with those of grade- and ER-matched IDC-NSTs.

Indeed, up to 90% of papillary carcinomas subjected to aCGH were of histological grade I or II, and among those, 82% harboured the genomic hallmark of non-high grade breast carcinomas, *i.e.* whole arm loss of chromosome 16 [42-43].

In our series, this chromosomal aberration was observed in 80% of non-high grade IDC-NSTs. In other series, loss of 16q was described in up to 85% of grade I IDC-NSTs [45, 52-53].

However, a few genomic changes were significantly less prevalent in papillary carcinomas than in IDC-NSTs (*i.e.* whole arm gain of 1q, whole arms losses of 6q, 17p, 19p and 22q), whereas gain of 19p was more frequent in papillary carcinomas than in IDC-NSTs. Whereas whole arm gain of 1q was observed in up to 78% of non-high grade IDC-NSTs, this genomic aberration was reported in only 40% of non-high grade papillary carcinomas. Therefore, the concurrent 1q+/16q-, another hallmark of grade I IDC-NSTs and classic lobular carcinomas [44-46, 54-55], was observed in 35% of non-high grade papillary carcinomas, whereas reaching 62% in non-high grade IDC-NSTs controls.

It should be noted, however, that partial gain of 1q was seen in up to 29% of non-high grade papillary carcinomas, versus 13% in non-high grade IDC-NSTs. The same observation applies to losses of 6q, 17p, 19p and 22q. Indeed, whole arms losses of 6q, 17p, 19p and 22q

were significantly more prevalent in IDC-NSTs, whereas partial losses of these chromosome arms were seen significantly more frequently in papillary carcinomas.

These findings provide evidence to suggest that the genomic aberrations harboured by these two types of tumours largely overlap and that papillary carcinomas may evolve through the same genetic pathways as non-high grade IDC-NSTs.

Interestingly, it is reported that when circumscribed papillary carcinomas start invading surrounding tissue and become frankly 'invasive', they tend to lose their characteristic papillary morphology and assume the pattern of IDC-NSTs [1].

These genomic and histological observations lead one to believe that papillary carcinomas and IDC-NSTs are likely to be part of the same spectrum of breast lesions and that papillary carcinomas might acquire additional genomic copy number aberrations consistent with those of IDC-NSTs when 'invading'. Therefore, papillary carcinomas should be considered more as part of the spectrum of the non-high grade breast neoplasia family [46] than as a distinct genomic entity.

Moreover, unsupervised hierarchical analysis comprising all papillary carcinomas and grade- and ER-matched IDC-NSTs failed to reveal any statistically significant difference between the two groups of tumours.

Hence, array CGH data being unable to fully elucidate the morphological differences between papillary carcinomas and grade- and ER-matched IDC-NSTs, it cannot be excluded that the morphological differences between these two groups of tumours are underpinned by genomic aberrations other than genomic copy number changes (*i.e.* structural rearrangements such as balanced translocations or somatic mutations) or by epigenetic alterations.

With the advent of next generation technologies, *i.e.* massively parallel sequencing, enabling the simultaneous identification of somatic mutations and (un)balanced rearrangements, those questions are very likely to be answered in a near future [56-59].

Here we were able to demonstrate that the three morphological subtypes of papillary carcinomas of the breast harbour very similar genomic aberrations. Additionally, no significant difference in terms of lympho-vascular invasion and lymph node metastasis was detected between them.

It needs to be noted however that whereas the three subtypes expressed ER in all cases, the solid and invasive variants were interestingly significantly less positive for PR than the encapsulated variant.

Nevertheless, taken together these observations provide evidence that encapsulated, solid and invasive papillary carcinomas are likely to constitute the same disease rather than distinct genomic entities.

Furthermore, their morphological differences might not be underpinned by mere genomic copy number changes. Here again, further next generation analyses will be required in order to understand the genomic, transcriptomic and/or epigenetic phenomenon(s) lying behind those morphological differences [56].

Besides, it needs to be noted that due to the limited number of cases of solid and invasive papillary carcinomas, these findings require to be corroborated by further larger series including these variants of papillary carcinoma.

Conclusion

Papillary carcinomas of the breast are preferentially non-high grade tumours that display a luminal phenotype. Their genomic aberrations largely overlap with those of grade- and ER-matched IDC-NSTs, providing evidence to suggest that these tumours may be part of the same spectrum of lesions rather than distinct genomic entities.

Besides, we have here shown that encapsulated, solid and invasive papillary carcinomas harbour very similar copy number aberrations, and that consequently, are likely to constitute the same disease.

These findings suggest that the morphological differences between these tumours may not be entirely driven by copy number changes. Therefore, it is conceivable that papillary features and their variants may be underpinned by genomic aberrations other than gene copy number or by epigenetic changes.

Further high-throughput and next generation studies will be required to understand if such aberrations can exhaustively elucidate the morphological differences between papillary carcinomas and IDC-NSTs and between the three morphological subtypes of papillary carcinoma.

Competing interests

The authors declare that they have no competing interests.

Authors' contributions

RD, MLT and AM conceived, carried out experiments and analysed data. MBL and JRF conceived experiments and analysed data. EW carried out experiments. RN, GMG, FA, PM, AA and AVS analysed data. All authors were involved in writing the article and had final approval of the submitted version.

Acknowledgements

This study was funded by Breakthrough Breast Cancer. Raphaëlle Duprez is funded by a grant from the French Higher Education and Research Department. Tumour samples were retrieved from the files of The Curie Institute (Paris, France), the Royal Marsden Hospital (London, UK), the Bergonié Institute (Bordeaux, France) and University Hospital Centers of Tours and Orléans (France).

References

1. Tavassoli FA, Devilee P (eds). *Tumours of the Breast. International Agency for Research of Cancer (IARC)*: Lyon, 2003.
2. Weigelt B, Geyer FC, and Reis-Filho JS. *Histological types of breast cancer: how special are they?* Mol Oncol 2010; 4(3): 192-208.
3. Reis-Filho JS and Lakhani SR. *Breast cancer special types: why bother?* J Pathol 2008; 216(4): 394-8.
4. Weigelt B and Reis-Filho JS. *Histological and molecular types of breast cancer: is there a unifying taxonomy?* Nat Rev Clin Oncol 2009; 6(12): 718-30.
5. Weigelt B, Horlings HM, Kreike B, et al. *Refinement of breast cancer classification by molecular characterization of histological special types.* J Pathol 2008; 216(2): 141-50.
6. Solorzano CC, Middleton LP, Hunt KK, et al. *Treatment and outcome of patients with intracystic papillary carcinoma of the breast.* Am J Surg 2002; 184(4): 364-8.
7. Grabowski J, Salzstein SL, Sadler GR, et al. *Intracystic papillary carcinoma: a review of 917 cases.* Cancer 2008; 113(5): 916-20.
8. Pal SK, Lau SK, Kruper L, et al. *Papillary carcinoma of the breast: an overview.* Breast Cancer Res Treat 2010; 122(3): 637-45.
9. Hill CB and Yeh IT. *Myoepithelial cell staining patterns of papillary breast lesions: from intraductal papillomas to invasive papillary carcinomas.* Am J Clin Pathol 2005; 123(1): 36-44.
10. Collins LC and Schnitt SJ. *Papillary lesions of the breast: selected diagnostic and management issues.* Histopathology 2008; 52(1): 20-9.
11. Collins LC, Carlo VP, Hwang H, et al. *Intracystic papillary carcinomas of the breast: a reevaluation using a panel of myoepithelial cell markers.* Am J Surg Pathol 2006; 30(8): 1002-7.
12. Elston CW and Ellis IO. *Pathological prognostic factors in breast cancer. I. The value of histological grade in breast cancer: experience from a large study with long-term follow-up.* Histopathology 1991; 19: 403-410.
13. Reis-Filho JS, Savage K, Lambros MB, et al. *Cyclin D1 protein overexpression and CCND1 amplification in breast carcinomas: an immunohistochemical and chromogenic in situ hybridisation analysis.* Mod Pathol 2006; 19(7): 999-1009.
14. Harvey JM, Clark GM, Osborne CK, et al. *Estrogen receptor status by immunohistochemistry is superior to the ligand-binding assay for predicting response to adjuvant endocrine therapy in breast cancer.* J Clin Oncol 1999; 17(5): 1474-81.
15. Wolff AC, Hammond ME, Schwartz JN, et al. *American Society of Clinical Oncology/College of American Pathologists guideline recommendations for human epidermal growth factor receptor 2 testing in breast cancer.* J Clin Oncol 2007; 25(1): 118-45.
16. Reis-Filho JS, Pinheiro C, Lambros MB, et al. *EGFR amplification and lack of activating mutations in metaplastic breast carcinomas.* J Pathol 2006; 209(4): 445-53.
17. Callagy GM, Pharoah PD, Pinder SE, et al. *Bcl-2 is a prognostic marker in breast cancer independently of the Nottingham Prognostic Index.* Clin Cancer Res 2006; 12(8): 2468-75.
18. Dawson SJ, Makretsov N, Blows FM, et al. *BCL2 in breast cancer: a favourable prognostic marker across molecular subtypes and independent of adjuvant therapy received.* Br J Cancer 2010; 103(5): 668-75.

19. Abdel-Fatah TM, Powe DG, Ball G, et al. *Proposal for a modified grading system based on mitotic index and Bcl2 provides objective determination of clinical outcome for patients with breast cancer.* J Pathol 2010; 222(4): 388-99.
20. Tan DS, Marchio C, Jones RL, et al. *Triple negative breast cancer: molecular profiling and prognostic impact in adjuvant anthracycline-treated patients.* Breast Cancer Res Treat 2008; 111(1): 27-44.
21. Savage K, Lambros MB, Robertson D, et al. *Caveolin 1 is overexpressed and amplified in a subset of basal-like and metaplastic breast carcinomas: a morphologic, ultrastructural, immunohistochemical, and in situ hybridization analysis.* Clin Cancer Res 2007; 13(1): 90-101.
22. Savage K, Leung S, Todd SK, et al. *Distribution and significance of caveolin 2 expression in normal breast and invasive breast cancer: an immunofluorescence and immunohistochemical analysis.* Breast Cancer Res Treat 2008; 110(2): 245-56.
23. Parry S, Savage K, Marchio C, et al. *Nestin is expressed in basal-like and triple negative breast cancers.* J Clin Pathol 2008; 61(9): 1045-50.
24. Mahler-Araujo B, Savage K, Parry S, et al. *Reduction of E-cadherin expression is associated with non-lobular breast carcinomas of basal-like and triple negative phenotype.* J Clin Pathol 2008; 61(5): 615-20.
25. Dedes KJ, Lopez-Garcia MA, Geyer FC, et al. *Cortactin gene amplification and expression in breast cancer: a chromogenic in situ hybridisation and immunohistochemical study.* Breast Cancer Res Treat 2010; 124(3): 653-66.
26. Nielsen TO, Hsu FD, Jensen K, et al. *Immunohistochemical and clinical characterization of the basal-like subtype of invasive breast carcinoma.* Clin Cancer Res 2004; 10(16): 5367-74.
27. Marchio C, Iravani M, Natrajan R, et al. *Genomic and immunophenotypical characterization of pure micropapillary carcinomas of the breast.* J Pathol 2008; 215(4): 398-410.
28. Lacroix-Triki M, Suarez PH, MacKay A, et al. *Mucinous carcinoma of the breast is genomically distinct from invasive ductal carcinomas of no special type.* J Pathol 2010; 222(3): 282-98.
29. Marchio C, Iravani M, Natrajan R, et al. *Mixed micropapillary-ductal carcinomas of the breast: a genomic and immunohistochemical analysis of morphologically distinct components.* J Pathol 2009; 218(3): 301-15.
30. Coe BP, Ylstra B, Carvalho B, et al. *Resolving the resolution of array CGH.* Genomics 2007; 89(5): 647-53.
31. Tan DS, Lambros MB, Natrajan R, et al. *Getting it right: designing microarray (and not 'microawry') comparative genomic hybridization studies for cancer research.* Lab Invest 2007; 87(8): 737-54.
32. Gunnarsson R, Staaf J, Jansson M, et al. *Screening for copy-number alterations and loss of heterozygosity in chronic lymphocytic leukemia--a comparative study of four differently designed, high resolution microarray platforms.* Genes Chromosomes Cancer 2008; 47(8): 697-711.
33. Natrajan R, Lambros MB, Rodriguez-Pinilla SM, et al. *Tiling path genomic profiling of grade 3 invasive ductal breast cancers.* Clin Cancer Res 2009; 15(8): 2711-22.
34. Marchio C, Natrajan R, Shiu KK, et al. *The genomic profile of HER2-amplified breast cancers: the influence of ER status.* J Pathol 2008; 216(4): 399-407.
35. Mackay A, Tamber N, Fenwick K, et al. *A high-resolution integrated analysis of genetic and expression profiles of breast cancer cell lines.* Breast Cancer Res Treat 2009; 118(3): 481-98.

36. Natrajan R, Weigelt B, Mackay A, et al. *An integrative genomic and transcriptomic analysis reveals molecular pathways and networks regulated by copy number aberrations in basal-like, HER2 and luminal cancers.* Breast Cancer Res Treat 2010; 121(3): 575-89.
37. Reis-Filho JS, Drury S, Lambros MB, et al. *ESR1 gene amplification in breast cancer: a common phenomenon?* Nat Genet 2008; 40(7): 809-10; author reply 810-2.
38. Lambros MB, Natrajan R, and Reis-Filho JS. *Chromogenic and fluorescent in situ hybridization in breast cancer.* Hum Pathol 2007; 38(8): 1105-22.
39. Lambros MB, Simpson PT, Jones C, et al. *Unlocking pathology archives for molecular genetic studies: a reliable method to generate probes for chromogenic and fluorescent in situ hybridization.* Lab Invest 2006; 86(4): 398-408.
40. Wu D, Matsushita K, Matsubara H, et al. *An alternative splicing isoform of eukaryotic initiation factor 4H promotes tumorigenesis in vivo and is a potential therapeutic target for human cancer.* Int J Cancer 2011; 128(5): 1018-30.
41. Hicks J, Krasnitz A, Lakshmi B, et al. *Novel patterns of genome rearrangement and their association with survival in breast cancer.* Genome Res 2006; 16(12): 1465-79.
42. Roylance R, Gorman P, Papior T, et al. *A comprehensive study of chromosome 16q in invasive ductal and lobular breast carcinoma using array CGH.* Oncogene 2006; 25(49): 6544-53.
43. Natrajan R, Lambros MB, Geyer FC, et al. *Loss of 16q in high grade breast cancer is associated with estrogen receptor status: Evidence for progression in tumors with a luminal phenotype?* Genes Chromosomes Cancer 2009; 48(4): 351-65.
44. Loo LW, Grove DI, Williams EM, et al. *Array comparative genomic hybridization analysis of genomic alterations in breast cancer subtypes.* Cancer Res 2004; 64(23): 8541-9.
45. Simpson PT, Reis-Filho JS, Gale T, et al. *Molecular evolution of breast cancer.* J Pathol 2005; 205(2): 248-54.
46. Abdel-Fatah TM, Powe DG, Hodi Z, et al. *Morphologic and molecular evolutionary pathways of low nuclear grade invasive breast cancers and their putative precursor lesions: further evidence to support the concept of low nuclear grade breast neoplasia family.* Am J Surg Pathol 2008; 32(4): 513-23.
47. Di Cristofano C, Mrad K, Zavaglia K, et al. *Papillary lesions of the breast: a molecular progression?* Breast Cancer Res Treat 2005; 90(1): 71-6.
48. Lininger RA, Park WS, Man YG, et al. *LOH at 16p13 is a novel chromosomal alteration detected in benign and malignant microdissected papillary neoplasms of the breast.* Hum Pathol 1998; 29(10): 1113-8.
49. Tsuda H, Uei Y, Fukutomi T, et al. *Different incidence of loss of heterozygosity on chromosome 16q between intraductal papilloma and intracystic papillary carcinoma of the breast.* Jpn J Cancer Res 1994; 85(10): 992-6.
50. Elsheikh S, Green AR, Aleskandarany MA, et al. *CCND1 amplification and cyclin D1 expression in breast cancer and their relation with proteomic subgroups and patient outcome.* Breast Cancer Res Treat 2008; 109(2): 325-35.
51. Ormandy CJ, Musgrove EA, Hui R, et al. *Cyclin D1, EMS1 and 11q13 amplification in breast cancer.* Breast Cancer Res Treat 2003; 78(3): 323-35.
52. Buerger H, Otterbach F, Simon R, et al. *Comparative genomic hybridization of ductal carcinoma in situ of the breast-evidence of multiple genetic pathways.* J Pathol 1999; 187(4): 396-402.
53. Roylance R, Gorman P, Harris W, et al. *Comparative genomic hybridization of breast tumors stratified by histological grade reveals new insights into the biological progression of breast cancer.* Cancer Res 1999; 59(7): 1433-6.

54. Reis-Filho JS, Simpson PT, Turner NC, et al. *FGFR1 emerges as a potential therapeutic target for lobular breast carcinomas.* Clin Cancer Res 2006; 12(22): 6652-62.
55. Bertucci F, Orsetti B, Nègre V, et al. *Lobular and ductal carcinomas of the breast have distinct genomic and expression profiles.* Oncogene 2008; 27(40): 5359-72.
56. Reis-Filho JS. *Next-generation sequencing.* Breast Cancer Res 2009; 11 Suppl 3: S12.
57. Campbell PJ, Stephens PJ, Pleasance ED, et al. *Identification of somatically acquired rearrangements in cancer using genome-wide massively parallel paired-end sequencing.* Nat Genet 2008; 40(6): 722-9.
58. Persson M, Andren Y, Mark J, et al. *Recurrent fusion of MYB and NFIB transcription factor genes in carcinomas of the breast and head and neck.* Proc Natl Acad Sci U S A 2009; 106(44): 18740-4.
59. Shah SP, Morin RD, Khattra J, et al. *Mutational evolution in a lobular breast tumour profiled at single nucleotide resolution.* Nature 2009; 461(7265): 809-13.
60. Wong KK, deLeeuw RJ, Dosanjh NS, et al. *A comprehensive analysis of common copy-number variations in the human genome.* Am J Hum Genet 2007; 80(1): 91-104.

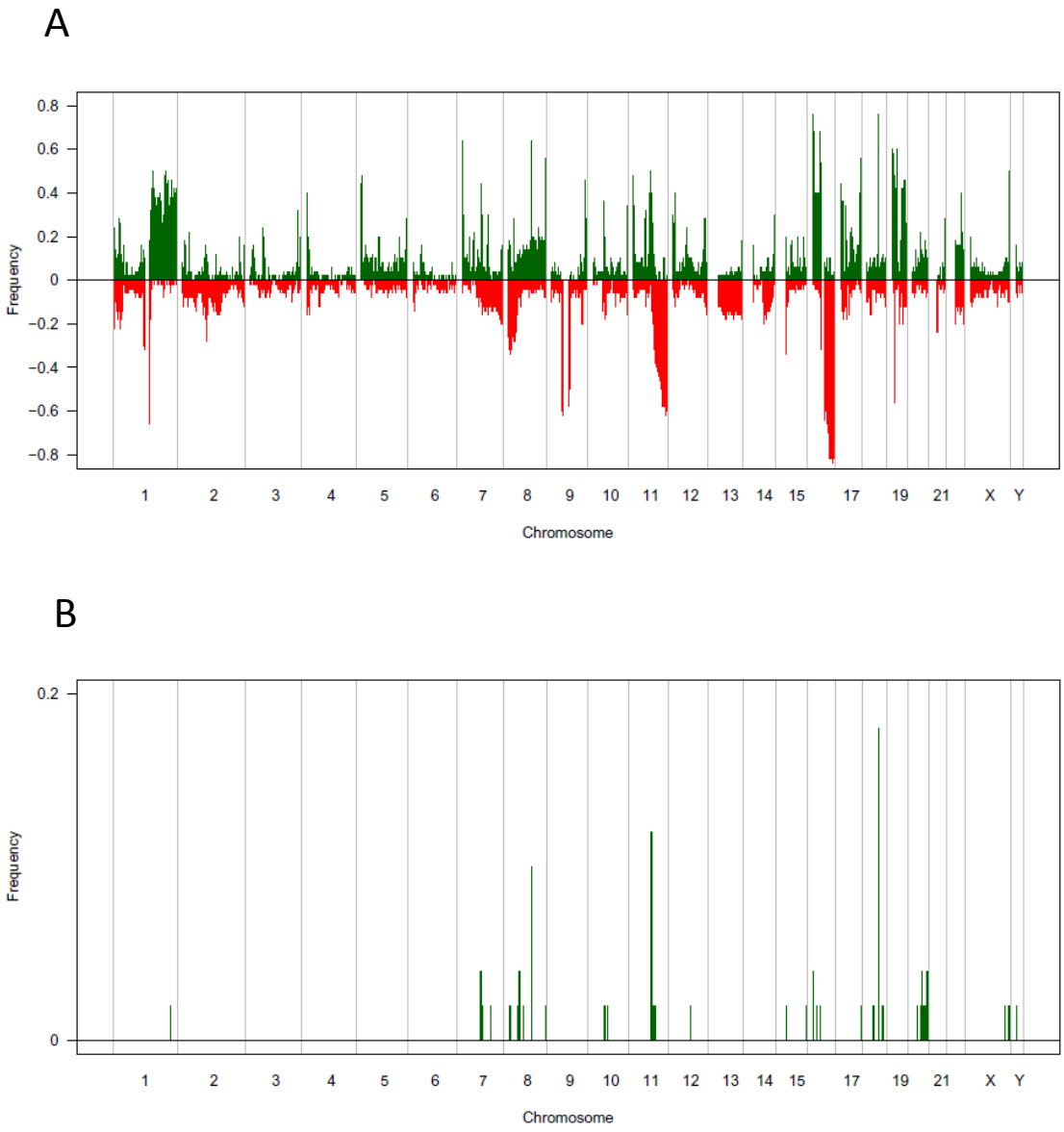

Supplementary Figure 1: Frequency plots of chromosomal gains, losses and amplifications observed in 50 papillary carcinomas.
Frequency plots of chromosomal gains, losses (A) and amplifications (B) observed in 50 papillary carcinomas. The proportion of tumours in which each bacterial artificial chromosome (BAC) clone is gained (green bars) or lost (red bars) is plotted (Y axis) for each BAC clone according to its genomic location (X axis).

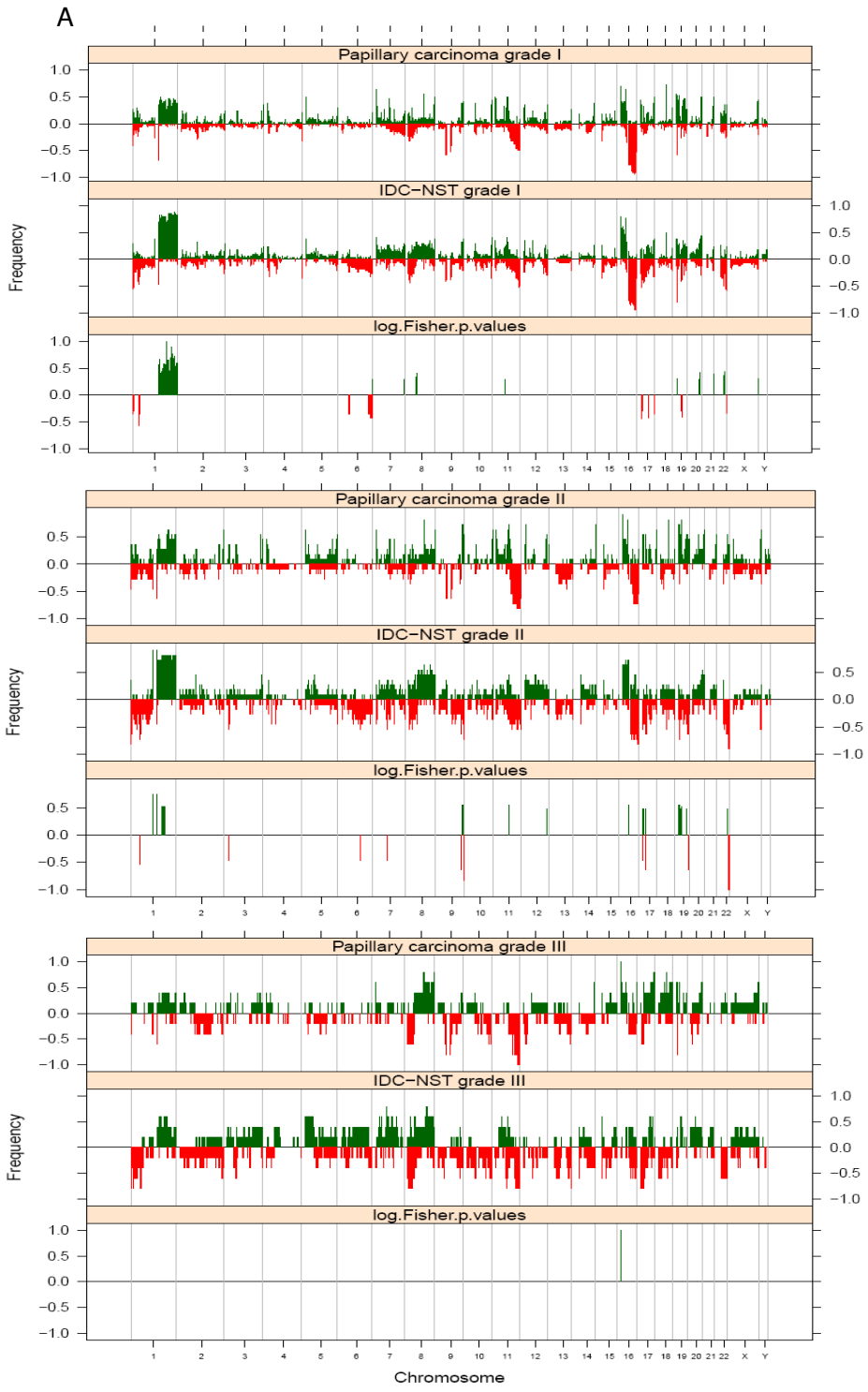

Supplementary Figure 2: Multi Fisher's exact test comparing genomic copy number aberrations observed in papillary carcinomas and in grade- and ER-matched IDC-NSTs according to histological grade. Frequency plots of chromosomal gains and losses observed in 34 grade I papillary carcinomas and 34 grade I IDC-NSTs (A), 11 grade II papillary carcinomas and 11 grade II IDC-NSTs (B) and 5 grade III papillary carcinomas and 5 grade III IDC-NSTs (C). The proportion of tumours in which each bacterial artificial chromosome (BAC) clone is gained (green bars) or lost (red bars) is plotted (Y axis) for each BAC clone according to its genomic location (X axis). Inverse Log_{10} values of the Fisher's exact test *p* values are plotted according to genomic location (X axis). IDC-NSTs: invasive ductal carcinomas of no special type.

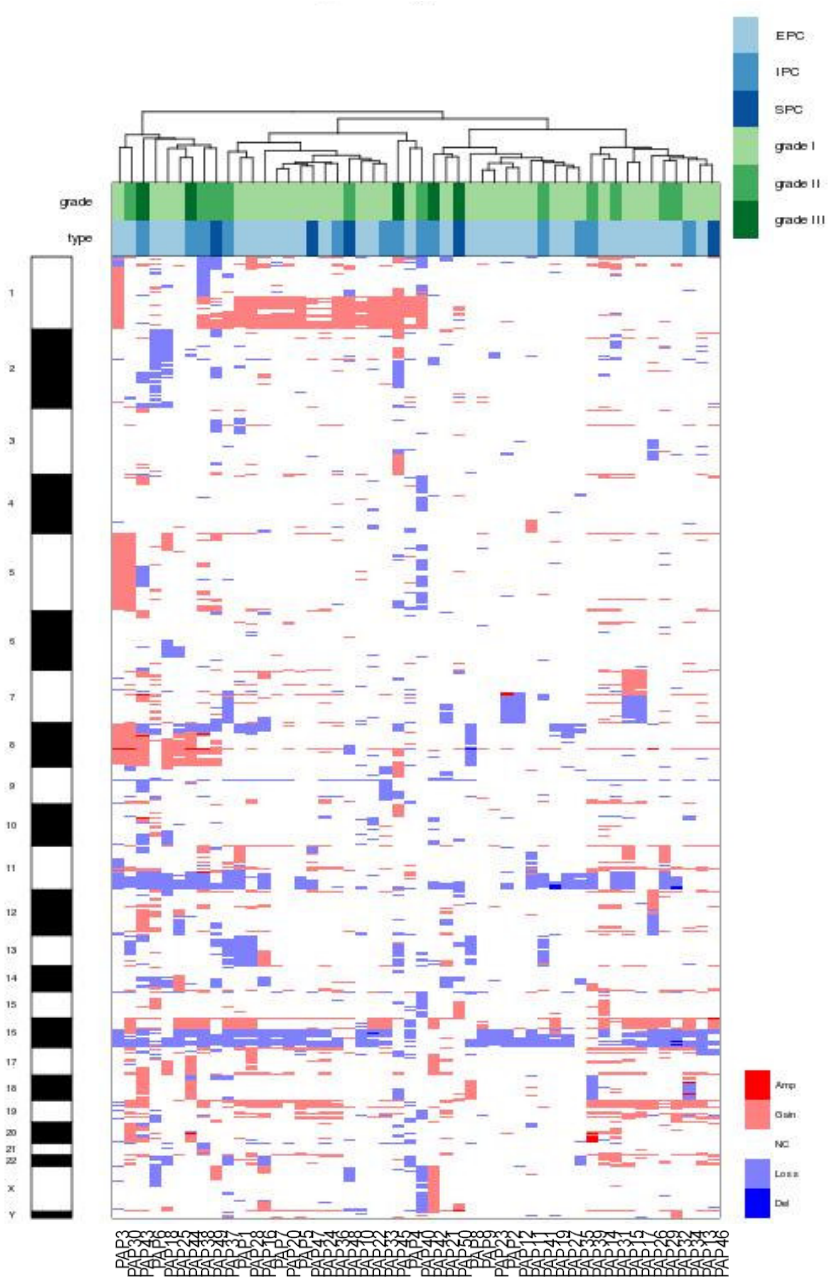

Supplementary Figure 3: Hierarchical clustering analysis of encapsulated, solid and invasive papillary carcinomas. Dendogram and heat map of 32 encapsulated papillary carcinomas, 5 solid papillary carcinomas and 13 invasive papillary carcinomas. Hierarchical clustering analysis was performed with aCGH categorical states (*i.e.* gains, losses and amplifications) and employed Euclidean distance and the Wards algorithm. The three variants of papillary carcinoma did not cluster separately.

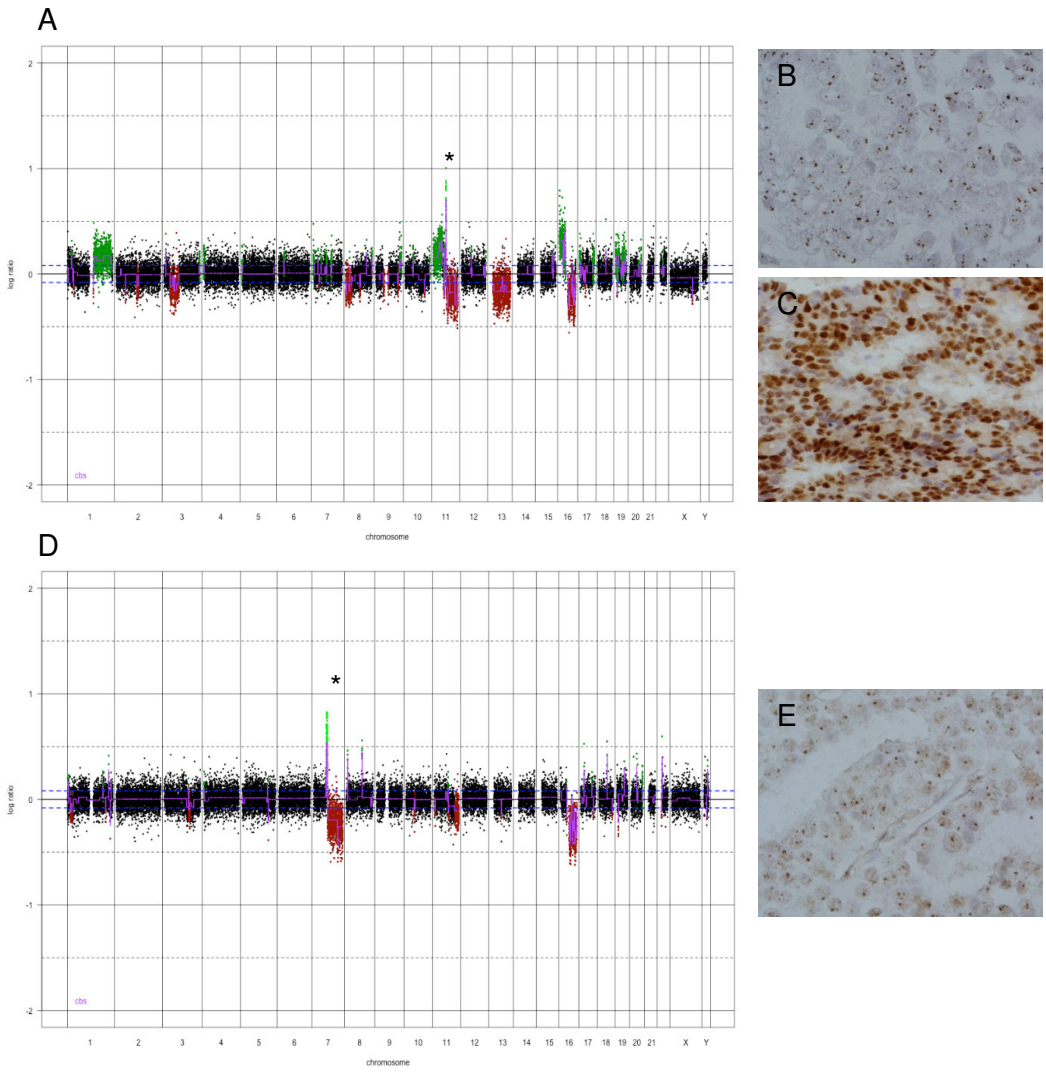

Supplementary Figure 4: Amplifications of *CCND1* and at 7q11.23 in two encapsulated non-high grade ER positive papillary carcinomas.
Representative genome plot of a typical non-high grade ER positive papillary carcinoma (A), displaying a genomic amplification located at 11q13, encompassing *CCND1* (highlighted by *). *CCND1* amplification was confirmed by CISH (B), and IHC analysis showed high expression of CCND1, with an Allred score of 8 (C). Representative genome plot of a non-high grade ER positive papillary carcinoma (D), displaying a genomic amplification located at 7q11.23 (highlighted by *). This amplification was confirmed by CISH (E). In (A) and (D), circular binary segmentation (cbs)-smoothed Log_2 ratios are plotted on the Y axis against each bacterial artificial chromosome (BAC) clone according to genomic location on the X axis. BACs categorised as displaying genomic gains or amplification are plotted in green and those categorised as genomic losses in red. ER: oestrogen receptor; CISH: chromogenic *in situ* hybridisation; IHC: immunohistochemistry.

Supplementary Table 1: Summary of the antibodies, clones, dilutions, antigen retrieval methods, scoring systems and cut-offs used

Marker	Clone	Dilution	Antigen retrieval	Company	Scoring system	Cut off
ER	6F11	1:150	Menarini PTM citrate pH 9.0	DAKO, Glostrup, Denmark	Allred scoring system	Positive: > 2
PR	Pgr 636	1:200	2 min, PC citrate pH 6.0	DAKO, Glostrup, Denmark	Allred scoring system	Positive: > 2
KI67	MIB1	1:300	2 min, PC citrate pH 6.0	DAKO, Glostrup, Denmark	% nuclei stained	< 10%: Low 10-30%: Intermediate > 30%: High
HER2 (HercepTest™)	Polyclo-nal K520411-2	RTU	41 min, water bath, Dako antigen retrieval solution, pH 6.0	DAKO, Glostrup, Denmark	Score 0, 1+, 2+, 3+ following the HercepTest® kit scoring system updated according to ASCO/CAP guidelines	Score 0/1+: Negative Score 2+: Equivocal Score 3+: Positive
EGFR	31G7	1:50	10 min, 0.1% pronase	Zymed, San Francisco, CA, USA	HercepTest® scoring system with a 10% stained cells cut-off	Positive ≥ 2
Cytokeratin 5/6	D5/16B4	1:600	18 min, MW, citrate pH 6.0	Chemicon, Temecula, CA, USA	Any (weak or strong) cytoplasmic and/or membranous staining in ≥10% of neoplastic cells	≥ 10%
Cytokeratin 14	LL002	1:50	18 min, MW, citrate pH 6.0	Biogenex	Any (weak or strong) cytoplasmic and/or membranous staining in ≥10% of neoplastic cells	≥ 10%
Cytokeratin 17	E3	1:100	18 min, MW, citrate pH 6.0	DAKO, Glostrup, Denmark	Any (weak or strong) cytoplasmic and/or membranous staining in ≥10% of neoplastic cells	≥ 10%
CAV1	2297	1:150	18 min, MW, Dako antigen retrieval solution pH 6.0	Transduction Labs, Lexington, KY, USA	% of membranous staining with or without cytoplasmic staining + intensity as compared to normal endothelial cells	Positive ≥ 4
CAV2	65	1:100	30 min, water bath 98°C	BD Transduction Labs	% of membranous staining with or without cytoplasmic staining + intensity as compared to normal endothelial cells	Positive ≥ 4

Nestin	2C1 3B9	1:400	30 min, PTM citrate pH 6.0	Covance, Emeryville, California, USA	% of cytoplasmic staining distributed in score 0: <1%, 1+: 1-9%, 2+: ≥ 10%	Positive ≥ 1
E-cadherin	HECD-1	1:200	2 min, PC citrate pH 6.0	Zymed, San Francisco, CA, USA	% stained cells (membranous staining): 0-10%=score 0, 10-25%=score 1, 25-50%=score 2, 50-75%=score 3, >75%=score 4	<2: negative, 2: reduced, ≥3: normal
Bcl2	124	1:20	2 min, PC citrate pH 6.0	DAKO, Glostrup, Denmark	Any (weak or strong) cytoplasmic staining in ≥10% of neoplastic cells	≥ 10%
Cyclin D1	SP4	1:50	2 min PC, EDTA pH8.0	Neomarkers, Suffolk, UK	Allred scoring system	0-3: Negative 4-5: Low 6-8: High
Cortactin	30	1 :1000	18 min, MW citrate pH 6.0	BD Transduction Labs	Quick score system	<5: low 5-12: intermediate >12: high
p53	D0-7	1:200	2 min, PC citrate pH 6.0	DAKO, Glostrup, Denmark	% cells displaying unequivocal nuclear staining	> 10% (moderate or strong staining)
Chromogranin	DAK-A3	1:150	30 min, PTM citrate pH 6.0	DAKO, Glostrup, Denmark	Any (weak or strong) cytoplasmic staining in ≥10% of neoplastic cells	≥ 10%
Synaptophysin	SY38	1:50	30 min, PTM citrate pH 6.0	DAKO, Glostrup, Denmark	Any (weak or strong) cytoplasmic staining in ≥10% of neoplastic cells	≥ 10%
p63	4A4	1:200	18 min, MW citrate pH 6.0	Insight, Santa Cruz, CA, USA	Any nuclear staining	Any nuclear staining
SMA	1A4	1:300	none	DAKO, Glostrup, Denmark	Any cytoplasmic staining	Any cytoplasmic staining

ER: oestrogen receptor; PR: progesterone receptor; EGFR: Epidermal Growth Factor Receptor; CAV: caveolin; MW: microwave oven; PC: pressure cooker; PTM: pre-treatment module; RTU: ready to use; ASCO/CAP: American Society of Clinical Oncology/College of American Pathologists; SMA: smooth muscle actin.

	papillary carcinomas (n=64)
Histological subtype	
encapsulated	41 (64.1%)
solid	9 (14.1%)
invasive	14 (21.9%)
Tumour size	
mean	26 mm
range	7-90 mm
Histological grade[#]	
I	42 (65.6%)
II	16 (25%)
III	6 (9.4%)
Mitosis score[#]	
1	45 (70.3%)
2	11 (17.2%)
3	8 (12.5%)
Mitotic count (per 10 HPF)	
mean	14.6
median	11
range	1-93
Ductal carcinoma *in situ* component	
present	41 (64.1%)
absent	23 (35.9%)
Associated IDC-NST	
present	9 (14.1%)
absent	55 (85.9%)
Lympho-vascular invasion	
present	10 (15.6%)
absent	54 (84.4%)
Lymph node metastasis	
present	4 (13.3%)
absent	26 (86.7%)
NA	34
Associated papilloma	
present	4 (6.5%)
absent	58 (93.5%)
NA	2

Supplementary Table 2: Histopathological features of 64 papillary carcinomas.
[#] Histological grade was assessed according to Nottingham grading system; HPF: high-power field; IDC-NST: invasive ductal carcinoma of no special type; NA: not available.

	N	encapsulated papillary carcinomas (n=41)	solid papillary carcinomas (n=9)	invasive papillary carcinomas (n=14)	*p* value
Histological grade	64				1**
I		35 (85.4%)	2 (22.2%)	5 (35.7%)	
II		6 (14.6%)	5 (55.6%)	5 (35.7%)	
III		0	2 (22.2%)	4 (28.6%)	
Lympho-vascular invasion	64				0.176*
present		6 (14.6%)	0	4 (28.6%)	
absent		35 (85.4%)	9 (100%)	10 (71.4%)	
Lymph node metastasis	30				0.548*
present		3 (17.6%)	0	1 (14.3%)	
absent		14 (82.4%)	6 (100%)	6 (85.7%)	
ER	64				NP
positive		41 (100%)	9 (100%)	14 (100%)	
PR	64				0.039*
positive		40 (97.6%)	7 (77.8%)	11 (78.6%)	
negative		1 (2.4%)	2 (22.2%)	3 (21.4%)	
HER2	64				NP
negative		41 (100%)	9 (100%)	14 (100%)	
Ki67	64				0.700**
low (<10%)		35 (85.4%)	7 (77.8%)	10 (71.4%)	
intermediate (10-30%)		5 (12.2%)	2 (22.2%)	3 (21.4%)	
high (>30%)		1 (2.4%)	0	1 (7.1%)	
p53	64				0.752*
positive		1 (2.4%)	0	0	
negative		40 (97.6%)	9 (100%)	14 (100%)	
Bcl2	64				0.163*
positive		41 (100%)	9 (100%)	13 (92.9%)	
negative		0	0	1 (7.1%)	
Cyclin D1	64				0.098**
low (Allred score 0-3)		2 (4.9%)	0	3 (21.4%)	
intermediate (Allred score 4-5)		2 (4.9%)	2 (22.2%)	1 (7.1%)	
high (Allred score 6-8)		37 (92.2%)	7 (77.8%)	10 (71.4%)	
Cortactin	64				0.376**
low (quick score <5)		23 (56.1%)	7 (77.8%)	11 (78.6%)	
intermediate (quick score 5-12)		10 (24.4%)	2 (22.2%)	2 (14.3%)	
high (quick score >12)		8 (19.5%)	0	1 (7.1%)	
E-cadherin	62				0.516**
normal		35 (87.5%)	8 (100%)	13 (92.9%)	
reduced		5 (12.5%)	0	1 (7.1%)	
negative		0	0	0	
Cytokeratin 5/6	64				0.150*
positive		1 (2.4%)	0	2 (14.3%)	
negative		40 (97.6%)	9 (100%)	12 (85.7%)	
Cytokeratin 14	64				0.163*
positive		0	0	1 (7.1%)	
negative		41 (100%)	9 (100%)	13 (92.9%)	
Cytokeratin 17	63				0.169*
positive		0	0	1 (7.1%)	
negative		40 (100%)	9 (100%)	13 (92.9%)	
EGFR	64				0.163*
positive		0	0	1 (7.1%)	

negative		41 (100%)	9 (100%)	13 (92.9%)	
Caveolin 1	63				0.169*
positive		0	0	1 (7.1%)	
negative		40 (100%)	9 (100%)	13 (92.9%)	
Caveolin 2	63				0.169*
positive		0	0	1 (7.1%)	
negative		40 (100%)	9 (100%)	13 (92.9%)	
Nestin	63				0.027*
positive		0	0	2 (14.3%)	
negative		40 (100%)	9 (100%)	12 (85.7%)	
Any basal marker	64				0.150*
positive		1 (2.4%)	0	2 (14.3%)	
negative		40 (97.6%)	9 (100%)	12 (85.7%)	
chromogranin	64				0.045*
positive		0	1 (11.1%)	0	
negative		41 (100%)	8 (88.9%)	14 (100%)	
synaptophysin	64				0.002*
positive		0	2 (22.2%)	0	
negative		41 (100%)	7 (77.8%)	14 (100%)	
Molecular phenotype[#]	64				NP
luminal		41 (100%)	9 (100%)	14 (100%)	

Supplementary Table 3: Histopathological and immunohistochemical features of 41 encapsulated, 9 solid and 14 invasive papillary carcinomas. * Fisher's exact test; ** Chi-squared test; [#] molecular phenotype classification according to Nielsen et al [26]; ER: oestrogen receptor; NP: not performed (no statistics computed as the value is constant); PR: progesterone receptor.

	papillary carcinomas (n=50)		papillary carcinomas (n=50)
Histological type		**E-cadherin**	
EPC	32 (64%)	normal	46 (93.9%)
SPC	5 (10%)	reduced	3 (6.1%)
IPC	13 (26%)	NA	1
Histological grade		**Cytokeratin 5/6**	
I	34 (68%)	positive	3 (6%)
II	11 (22%)	negative	47 (94%)
III	5 (10%)	**Cytokeratin 14**	
Lympho-vascular invasion		positive	1 (2%)
present	9 (18%)	negative	49 (98%)
absent	41 (82%)	**Cytokeratin 17**	
Lymph node metastasis		positive	1 (2%)
present	2 (9.1%)	negative	48 (98%)
absent	20 (90.9%)	NA	1
NA	28	**EGFR**	
ER		positive	1 (2%)
positive	50 (100%)	negative	49 (98%)
PR		**Caveolin 1**	
positive	45 (90%)	positive	1 (2%)
negative	5 (10%)	negative	48 (98%)
HER2		NA	1
negative	50 (100%)	**Caveolin 2**	
Ki67		positive	1 (2%)
low (<10%)	39 (78%)	negative	48 (98%)
intermediate (10-30%)	9 (18%)	NA	1
high (>30%)	2 (4%)	**Nestin**	
p53		positive	2 (4.1%)
negative	50 (100%)	negative	47 (95.9%)
Bcl2		NA	1
positive	49 (98%)	**Any basal marker**	
negative	1 (2%)	positive	3 (6%)
Cyclin D1		negative	47 (94%)
low (Allred score 0-3)	4 (8%)	**chromogranin**	
intermediate (Allred score 4-5)	4 (8%)	positive	1 (2%)
high (Allred score 6-8)	42 (84%)	negative	49 (98%)
Cortactin		**synaptophysin**	
low (quick score <5)	30 (60%)	positive	1 (2%)
intermediate (quick score 5-12)	11 (22%)	negative	49 (98%)
high (quick score >12)	9 (18%)	**Molecular phenotype[#]**	
		luminal	50 (100%)

Supplementary Table 4: Histopathological and immunohistochemical features of 50 papillary carcinomas subjected to aCGH.

EPC: encapsulated papillary carcinoma; SPC: solid papillary carcinoma; IPC: invasive papillary carcinoma; ER: oestrogen receptor; PR: progesterone receptor; [#] molecular phenotype classification according to Nielsen et al; aCGH: array comparative genomic hybridization.

Supplementary Table 5: Most frequent (in five or more cases) chromosomal gains observed in 50 papillary carcinomas.

Chromosome	Cytobands	Start (Mb)	End (Mb)	Number of BACs	Papillary carcinomas (n=50)	Genes	mi-RNAs	aCGH CNVs
1	p36.33-p36.32	1.37	4.21	30	14	VWA1, ATAD3C, ATAD3B, ATAD3A, C1orf70, SSU72, MIB2, MMP23B, CDC2L2, SLC35E2, NADK, GNB1, CALML6, TMEM52, C1orf222, KIAA1751, GABRD, PRKCZ, C1orf86, SKI, MORN1, RER1, PEX10, PLCH2, PANK4, HES5, TNFRSF14, C1orf93, MMEL1, TTC34, ACTRT2, PRDM16, ARHGEF16, MEGF6, TPRG1L, WDR8, TP73, CCDC27, LRRC47, KIAA0562, DFFB, C1orf174	hsa-mir-551a	V_0002_LC0028_Iafrate et al. (2004), V_2042_LC0028_Locke et al. (2006), V_4192_LC0040_Wong et al. (2007), V_4193_LC0040_Wong et al. (2007), V_4194_LC0040_Wong et al. (2007), V_4195_LC0040_Wong et al. (2007), V_4196_LC0040_Wong et al. (2007), V_4197_LC0040_Wong et al. (2007)
1	p36.31-p36.23	6.12	8.89	28	12	KCNAB2, CHD5, RPL22, RNF207, ICMT, HES3, GPR153, ACOT7, HES2, ESPN, TNFRSF25, PLEKHG5, NOL9, TAS1R1, ZBTB48, KLHL21, PHF13, THAP3, DNAJC11, CAMTA1, VAMP3, PER3, UTS2, TNFRSF9, PARK7, ERRFI1, SLC45A1, RERE		V_0003_LC0126_Iafrate et al. (2004), V_4200_LC0104_Wong et al. (2007), V_4201_LC0106_Wong et al. (2007), V_4202_LC0106_Wong et al. (2007), V_4203_LC0113_Wong et al. (2007), V_4204_LC0118_Wong et al. (2007)
1	p36.23-p36.22	8.94	12.28	36	7	ENO1, CA6, SLC2A7, SLC2A5, GPR157, H6PD, SPSB1, SLC25A33, TMEM201, PIK3CD, C1orf200, CLSTN1, CTNNBIP1, LZIC, NMNAT1, RBP7, UBE4B, KIF1B, PGD, APITD1, DFFA, PEX14, CASZ1, C1orf127, TARDBP, MASP2, SRM, EXOSC10, FRAP1, ANGPTL7, UBIAD1, PTCHD2, FBXO2, FBXO44, FBXO6, MAD2L2, C1orf187, AGTRAP, C1orf167, MTHFR, CLCN6, NPPA, NPPB, KIAA2013, PLOD1, MFN2, MIIP, TNFRSF8, TNFRSF1B	hsa-mir-34a	V_0676_LC0150_Sharp et al. (2005), V_4205_LC0141_Wong et al. (2007)
1	p36.13	16.58	17.4	6	6	FBXO42, C1orf144, SPATA21, NECAP2, NBPF1, MSTP9, CROCC, MFAP2, ATP13A2, SDHB, PADI2		V_0005_LC0177_Iafrate et al. (2004), V_0679_LC0177_Sharp et al. (2005), V_2044_LC0177_Locke et al. (2006), V_4207_LC0177_Wong et al. (2007), V_4208_LC0177_Wong et al. (2007)…
1	p36.12-p36.11	23.37	24.52	15	14	KDM1, LUZP1, HTR1D, HNRNPR, ZNF436, C1orf213, TCEA3, ASAP3, E2F2, ID3, MDS2, RPL11, TCEB3, C1orf128, LYPLA2, GALE, HMGCL, FUCA1, CNR2, PNRC2, FUSIP1, MYOM3, IL22RA1, IL28RA		
1	p36.11-p35.3	25.97	29.58	45	13	MAN1C1, SEPN1, FAM54B, C1orf135, PAQR7, STMN1, PAFAH2, EXTL1, SLC30A2, TRIM63, PDIK1L, GRRP1, ZNF593, CNKSR1, CATSPER4, CCDC21, SH3BGRL3, UBXN11, CD52, AIM1L, ZNF683, LIN28, DHDDS, HMGN2, RPS6KA1, ARID1A, PIGV, ZDHHC18, SFN, GPN2, GPATCH3, NUDC, NR0B2, C1orf172, FAM46B, SLC9A1, WDTC1, TMEM222, SYTL1, MAP3K6, FCN3, CD164L2, GPR3, WASF2, AHDC1, FGR, IFI6, FAM76A, STX12, PPP1R8, C1orf38, RPA2, SMPDL3B, XKR8, EYA3, PTAFR, DNAJC8, ATPIF1, SESN2, MED18, PHACTR4, SNHG3, TRNAU1AP, SNHG12, RAB42, TAF12, GMEB1, YTHDF2, OPRD1, EPB41, SFRS4, MECR, PTPRU	hsa-mir-1976	V_4218_LC0253_Wong et al. (2007)
1	p35.2-p35.1	31.29	33.77	27	6	SDC3, PUM1, NKAIN1, SNRNP40, ZCCHC17, FABP3, SERINC2, TINAGL1, HCRTR1, PEF1, COL16A1, BAI2, SPOCD1, PTP4A2, KHDRBS1, TMEM39B, KPNA6, TXLNA, CCDC28B, IQCC, DCDC2B, C1orf91, EIF3I, FAM167B, LCK, HDAC1, MARCKSL1, TSSK3, BSDC1, ZBTB8B, ZBTB8A, ZBTB8OS, RBBP4, SYNC, KIAA1522, YARS, S100PBP, FNDC5, HPCA, TMEM54, RNF19B, AK2, ADC, TRIM62, ZNF362, A3GALT2		
1	p34.3-p34.2	39.97	40.57	8	8	BMP8A, PABPC4, HEYL, NT5C1A, HPCAL4, PPIE, BMP8B, OXCT2, TRIT1, MYCL1, MFSD2, CAP1, PPT1		V_4219_LC0315_Wong et al. (2007)
1	p13.3	108.41	110.94	23	8	VAV3, SLC25A24, NBPF4, NBPF5, NBPF6, FAM102B, C1orf59, PRPF38B, FNDC7, STXBP3, C1orf62, GPSM2, CLCC1, WDR47, RPL17P36, TAF13, TMEM167B, C1orf194, KIAA1324, SARS, CELSR2, PSRC1, MYBPHL, SORT1, PSMA5, SYPL2, ATXN7L2, CYB561D1, AMIGO1, GPR61, GNAI3, GNAT2, AMPD2, GSTM4, GSTM2, GSTM1, GSTM5, GSTM3, EPS8L3, CSF1, AHCYL1, FAM40A, ALX3, UBL4B, SLC6A17, KCNC4, RBM15, SLC16A4	hsa-mir-197	V_2049_LC0673_Locke et al. (2006), V_4241_LC0680_Wong et al. (2007)
1	p12-p11.2	120.45	121.35	5	7	NOTCH2, FAM72B, FCGR1B		V_4246_LC0743_Wong et al. (2007)
1	q21.1-q44	143.51	248.88	1081	25	PPIAL4G, FAM72D, SRGAP2P2, PPIAL4B, NBPF9, PDE4DIP, SEC22B, NOTCH2NL, HFE2, TXNIP, POLR3GL, ANKRD34A, LIX1L, RBM8A, GNRHR2, PEX11B, ITGA10, ANKRD35, PIAS3, NUDT17, POLR3C, RNF115, CD160, PDZK1, GPR89A, GPR89C, NBPF8, NBPF8, NBPF12, PRKAB2, FMO5, CHD1L, BCL9, ACP6, GJA5, GJA8, GPR89B, NBPF11, FAM108A2, PPIAL4A, NBPF14, NBPF10, NBPF16, FCGR1C, HIST2H3PS2, FAM72C, PPIAL4C, FAM91A2, FCGR1A, HIST2H2BF, HIST2H3D, HIST2H4A, HIST2H3C, HIST2H2AA3, HIST2H2AA4, HIST2H3A, HIST2H4B, HIST2H2BE, BOLA1, HIST2H2AC, HIST2H2AB, SV2A, SF3B4, MTMR11, OTUD7B, VPS45, PLEKHO1, ANP32E, CA14, APH1A, C1orf54, C1orf51, MRPS21, PRPF3, RPRD2, TARS2, ECM1, ADAMTSL4, C1orf138, MCL1, ENSA, GOLPH3L, HORMAD1, CTSS, CTSK, ARNT, SETDB1, LASS2, ANXA9, FAM63A, PRUNE, BNIPL, C1orf56, CDC42SE1, MLLT11, GABPB2, SEMA6C, TNFAIP8L2, LYSMD1, SCNM1, TMOD4, VPS72, PIP5K1A, PSMD4, ZNF687, PI4KB, RFX5, SELENBP1, PSMB4, POGZ, CGN, TUFT1, SNX27, TNRC4, MRPL9, OAZ3, TDRKH, LINGO4, RORC, THEM5, THEM4, S100A10, S100A11, TCHHL1, TCHH, RPTN, HRNR, FLG, FLG2, CRNN, LCE5A, CRCT1, LCE3E, LCE3D, LCE3B, LCE3A, LCE2D, LCE2C, LCE2B, LCE2A, LCE4A, C1orf68, KPRP, LCE1E, LCE1D, LCE1C, LCE1B, LCE1A, LCE6A, SMCP, IVL, SPRR4, SPRR1A, SPRR3, SPRR1B, SPRR2D, SPRR2B, SPRR2A, SPRR2E, SPRR2F, SPRR2G, LELP1, PRR9, LOR, PGLYRP3, PGLYRP4, S100A9, S100A12, S100A8, S100A7A, S100A7L2, S100A7, S100A6, S100A5, S100A4, S100A3, S100A2, S100A16, S100A14, S100A13, S100A1, C1orf77, SNAPIN, ILF2, NPR1, INTS3, C1orf193, SLC27A3, GATAD2B, DENND4B, CRTC2, SLC39A1, CREB3L4, JTB, RAB13, RPS27, NUP210L, TPM3, C1orf189, C1orf43, UBAP2L, HAX1, AQP10, ATP8B2, IL6R, SHE, TDRD10, UBE2Q1, CHRNB2, ADAR, KCNN3, PMVK, PBXIP1, PYGO2, SHC1, CKS1B, FLAD1, LENEP, ZBTB7B, DCST2, DCST1, ADAM15, EFNA4, EFNA1, RAG1AP1, DPM3, KRTCAP2, TRIM46, MUC1, THBS3, MTX1, GBAP, GBA, C1orf2, SCAMP3, CLK2, HCN3, PKLR, FDPS, RUSC1, ASH1L, MSTO1, YY1AP1, DAP3, GON4L, SYT11, RIT1, KIAA0907, RXFP4, ARHGEF2, SSR2, UBQLN4, ROBLD3, RAB25, LMNA, SEMA4A, SLC25A44, PMF1, PAQR6, SMG5, C1orf85, TMEM79, CCT3, C1orf182, RHBG, C1orf61, MEF2D, IQGAP3, TTC24, APOA1BP, GPATCH4, HAPLN2, BCAN, NES, CRABP2, ISG20L2, C1orf66, MRPL24, HDGF, PRCC, SH2D2A, NTRK1, INSRR, PEAR1, C1orf92, ARHGEF11, ETV3, FCRL5, FCRL4, FCRL3, FCRL2, FCRL1, CD5L, KIRREL, CD1D, CD1A, CD1C, CD1B, CD1E…	hsa-mir-554, hsa-mir-190b, hsa-mir-92b, hsa-mir-555, hsa-mir-9-1, hsa-mir-765, hsa-mir-556, hsa-mir-921, hsa-mir-1255b-2, hsa-mir-557, hsa-mir-1295, hsa-mir-214, hsa-mir-199a-2, hsa-mir-488, hsa-mir-1278, hsa-mir-181b-1, hsa-mir-181a-1, hsa-mir-1231, hsa-mir-135b, hsa-mir-29c, hsa-mir-29b-2, hsa-mir-205, hsa-mir-215, hsa-mir-194-1, hsa-mir-320b-2, hsa-mir-1182, hsa-mir-1537	V_0014_LC0941_Iafrate et al. (2004), V_0015_LC0954_Iafrate et al. (2004), V_0016_LC1285_Iafrate et al. (2004), V_0017_LC1401_Iafrate et al. (2004), V_0685_LC0752_Sharp et al. (2005), V_0686_LC1055_Sharp et al. (2005), V_0687_LC1055_Sharp et al. (2005), V_2050_LC0752_Locke et al. (2006), V_2051_LC0752_Locke et al. (2006), V_2052_LC0752_Locke et al. (2006), V_2053_LC1052_Locke et al. (2006), V_2054_LC1055_Locke et al. (2006), V_2055_LC1055_Locke et al. (2006), V_2056_LC1401_Locke et al. (2006), V_2091_LC1120_Locke et al. (2006), V_4249_LC0752_Wong et al. (2007), V_4250_LC0752_Wong et al. (2007), V_4251_LC0752_Wong et al. (2007), V_4252_LC0752_Wong et al. (2007), V_4253_LC0752_Wong et al. (2007), V_4254_LC0752_Wong et al. (2007), V_4255_LC0752_Wong et al. (2007), V_4256_LC0752_Wong et al. (2007), V_4257_LC0831_Wong et al. (2007), V_4258_LC0863_Wong et al. (2007), V_4259_LC0863_Wong et al. (2007), V_4260_LC0878_Wong et al. (2007), V_4261_LC0907_Wong et al. (2007), V_4262_LC0938_Wong et al. (2007), V_4263_LC0946_Wong et al. (2007), V_4264_LC0975_Wong et al. (2007), V_4265_LC0992_Wong et al. (2007), V_4266_LC1019_Wong et al. (2007), V_4267_LC1097_Wong et al. (2007), V_4268_LC1117_Wong et al. (2007), V_4269_LC1125_Wong et al. (2007), V_4270_LC1176_Wong et al. (2007), V_4271_LC1296_Wong et al. (2007), V_4272_LC1302_Wong et al. (2007)
2	p25.1	9.47	11.68	26	9	ASAP2, ITGB1BP1, CPSF3, IAH1, ADAM17, YWHAQ, TAF1B, GRHL1, KLF11, CYS1, RRM2, C2orf48, HPCAL1,		

						ODC1, NOL10, ATP6V1C2, PDIA6, KCNF1, C2orf50, PQLC3, ROCK2, E2F6		
2	p23.3-p23.2	24.05	28	39	11	ATAD2B, UBXN2A, C2orf44, FKBP1B, TP53I3, PFN4, C2orf84, ITSN2, NCOA1, C2orf79, CENPO, ADCY3, DNAJC27, EFR3B, POMC, DNMT3A, DTNB, ASXL2, KIF3C, RAB10, FAM59B, HADHA, HADHB, GPR113, C2orf39, OTOF, C2orf70, CIB4, KCNK3, C2orf18, CENPA, DPYSL5, MAPRE3, TMEM214, AGBL5, EMILIN1, KHK, CGREF1, ABHD1, PREB, C2orf53, TCF23, SLC5A6, C2orf28, CAD, SLC30A3, DNAJC5G, TRIM54, UCN, MPV17, GTF3C2, EIF2B4, SNX17, ZNF513, PPM1G, NRBP1, KRTCAP3, IFT172, FNDC4, GCKR, C2orf16, GPN1, CCDC121, SUPT7L, SLC4A1AP, MRPL33	hsa-mir-1301	
2	p11.2	85.61	86.2	5	5	ELMOD3, CAPG, SH2D6, MAT2A, GGCX, VAMP8, VAMP5, RNF181, TMEM150, C2orf68, USP39, SFTPB, GNLY, ATOH8, ST3GAL5		
2	p11.1-q11.1	90.23	91.94	12	8			
2	q21.1-q21.2	132	132.58	8	6	PLEKHB2, POTEE, C2orf14, FAM128A, TUBA3D, CCDC74A, C2orf27A, C2orf27B		V_0025_LC2234_Iafrate et al. (2004), V_4307_LC2234_Wong et al. (2007)
2	q35	218.9	220.68	20	10	RUFY4, IL8RB, IL8RA, ARPC2, AAMP, PNKD, TMBIM1, C2orf62, SLC11A1, CTDSP1, VIL1, USP37, ROCD1, PLCD4, ZNF142, BCS1L, RNF25, STK36, TTLL4, CYP27A1, PRKAG3, WNT6, WNT10A, CDK5R2, FEV, CRYBA2, CCDC108, IHH, NHEJ1, SLC23A3, C2orf24, FAM134A, ZFAND2B, ATG9A, ABCB6, ANKZF1, GLB1L, STK16, TUBA4A, TUBA4B, DNAJB2, PTPRN, DNPEP, DES, SPEG, GMPPA, ACCN4, CHPF, TMEM198, OBSL1, INHA, STK11IP, SLC4A3	hsa-mir-26b, hsa-mir-375, hsa-mir-153-1	V_0030_LC2686_Iafrate et al. (2004)
2	q37.3	240.9	243.07	24	16	NDUFA10, OR6B2, PRR21, OR6B3, MYEOV2, OTOS, GPC1, ANKMY1, DUSP28, RNPEPL1, CAPN10, GPR35, AQP12B, AQP12A, KIF1A, AGXT, C2orf54, SNED1, MTERFD2, PASK, PPP1R7, ANO7, HDLBP, Sep-02, FARP2, STK25, BOK, THAP4, ATG4B, DTYMK, ING5, D2HGDH, GAL3ST2, NEU4, PDCD1, C2orf85	hsa-mir-149	V_0032_LC2814_Iafrate et al. (2004), V_0694_LC2814_Sharp et al. (2005), V_4331_LC2814_Wong et al. (2007)
3	p25.3	9.47	10.54	11	7	SETD5, LHFPL4, MTMR14, CPNE9, BRPF1, OGG1, CAMK1, TADA3L, TTLL3, RPUSD3, CIDEC, JAGN1, IL17RE, IL17RC, CRELD1, PRRT3, TMEM111, FANCD2, VHL, IRAK2, TATDN2, GHRL, SEC13, ATP2B2	hsa-mir-885	
3	p25.2-p25.1	12.47	15.02	23	8	PPARG, TSEN2, MKRN2, RAF1, TMEM40, CAND2, RPL32, IQSEC1, NUP210, HDAC11, FBLN2, WNT7A, TPRXL, CHCHD4, TMEM43, XPC, LSM3, SLC6A6, GRIP2, C3orf19, C3orf20, FGD5, NR2C2		
3	p21.31-p21.1	46.56	53.31	76	12	LRRC2, LUZPP1, TDGF1, ALS2CL, TMIE, MYL3, PTH1R, CCDC12, NBEAL2, SETD2, KIF9, KLHL18, PTPN23, SCAP, C3orf75, CSPG5, SMARCC1, DHX30, MAP4, CDC25A, CAMP, ZNF589, NME6, SPINK8, FBXW12, PLXNB1, CCDC51, CCDC72, ATRIP, TREX1, SHISA5, PFKFB4, UCN2, COL7A1, UQCRC1, TMEM89, SLC26A6, CELSR3, NCKIPSD, IP6K2, PRKAR2A, SLC25A20, C3orf71, ARIH2, P4HTM, WDR6, DALRD3, NDUFAF3, IMPDH2, QRICH1, QARS, USP19, LAMB2, CCDC71, KLHDC8B, CCDC36, C3orf62, USP4, GPX1, RHOA, TCTA, AMT, NICN1, DAG1, BSN, APEH, MST1, RNF123, AMIGO3, GMPPB, IP6K1, CDH29, C3orf54, UBA7, TRAIP, CAMKV, MST1R, MON1A, RBM6, RBM5, SEMA3F, GNAT1, GNAI2, SEMA3B, C3orf45, IFRD2, NAT6, HYAL1, HYAL2, TUSC2, RASSF1, ZMYND10, TUSC4, CYB561D2, TMEM115, CACNA2D2, C3orf18, HEMK1, CISH, MAPKAPK3, DOCK3, ARMET, RBM15B, VPRBP, RAD54L2, TEX264, GRM2, IQCF6, IQCF3, IQCF2, IQCF5, IQCF1, RRP9, PARP3, GPR62, PCBP4, ABHD14B, ACY1, RPL29, DUSP7, C3orf74, WDR51A, ALAS1, TWF2, PPM1M, WDR82, GLYCTK, DNAH1, BAP1, PHF7, SEMA3G, TNNC1, NISCH, STAB1, NT5DC2, PBRM1, GNL3, GLT8D1, SPCS1, NEK4, ITIH1, ITIH3, ITIH4, TMEM110, SFMBT1, RFT1, PRKCD, TKT	hsa-mir-1226, hsa-mir-425, hsa-mir-191, hsa-mir-566, hsa-let-7g, hsa-mir-135a-1	V_4334_LC3163_Wong et al. (2007), V_4335_LC3182_Wong et al. (2007), V_4336_LC3182_Wong et al. (2007), V_4337_LC3192_Wong et al. (2007), V_4338_LC3192_Wong et al. (2007), V_4339_LC3195_Wong et al. (2007)
3	q27.1-q27.2	182.73	184.53	17	16	MCCC1, LAMP3, MCF2L2, B3GNT5, KLHL6, KLHL24, YEATS2, MAP6D1, PARL, ABCC5, HTR3D, HTR3C, HTR3E, EIF2B5, DVL3, AP2M1, ABCF3, VWA5B2, ALG3, ECE2, CAMK2N2, PSMD2, EIF4G1, FAM131A, CLCN2, POLR2H, THPO, CHRD, EPHB3, MAGEF1	hsa-mir-1224	
3	q29	193.65	197.79	44	18	HES1, CPN2, LRRC15, GP5, ATP13A3, TMEM44, LSG1, FAM43A, C3orf21, ACAP2, PPP1R2, APOD, MUC20, MUC4, TNK2, TFRC, ZDHHC19, PCYT1A, TCTEX1D2, TM4SF19, UBXN7, RNF168, C3orf43, WDR53, FBXO45, PIGX, LRRC33, C3orf34, PAK2, SENP5, NCBP2, PIGZ, MFI2, DLG1, BDH1, KIAA0226, FYTTD1, LRCH3, IQCG, RPL35A, LMLN	hsa-mir-570, hsa-mir-922	V_0042_LC4028_Iafrate et al. (2004), V_0696_LC4028_Sharp et al. (2005), V_0697_LC4028_Sharp et al. (2005), V_2062_LC4004_Locke et al. (2006), V_2063_LC4020_Locke et al. (2006), V_2064_LC4028_Locke et al. (2006), V_2065_LC4028_Locke et al. (2006), V_4366_LC4028_Wong et al. (2007), V_4367_LC4028_Wong et al. (2007), V_4368_LC4048_Wong et al. (2007)
4	p16.3	0.02	3.42	51	20	ZNF595, ZNF732, ZNF141, ZNF721, PIGG, PDE6B, ATP5I, MYL5, MFSD7, PCGF3, CPLX1, GAK, TMEM175, DGKQ, SLC26A1, IDUA, FGFRL1, RNF212, TMED11P, SPON2, CTBP1, C4orf42, MAEA, KIAA1530, CRIPAK, NKX1-1, FAM53A, SLBP, TMEM129, TACC3, FGFR3, LETM1, WHSC1, WHSC2, NAT8L, POLN, HAUS3, MXD4, ZFYVE28, RNF4, C4orf8, TNIP2, SH3BP2, ADD1, MFSD10, NOP14, GRK4, HTT, C4orf44, RGS12	hsa-mir-571, hsa-mir-943	V_2066_LC4068_Locke et al. (2006), V_4371_LC4159_Wong et al. (2007)
4	p16.2-p16.1	5.88	9.68	44	10	CRMP1, C4orf50, JAKMIP1, WFS1, PPP2R2C, MAN2B2, MRFAP1, S100P, MRFAP1L1, CNO, KIAA0232, TBC1D14, CCDC96, GRPEL1, SORCS2, PSAPL1, AFAP1, ABLIM2, SH3TC1, HTRA3, ACOX3, C4orf23, GPR78, CPZ, HMX1, FAM90A2P, USP17, DEFB131	hsa-mir-95, hsa-mir-548i-2	V_0698_LC4236_Sharp et al. (2005), V_0699_LC4236_Sharp et al. (2005), V_2067_LC4192_Locke et al. (2006), V_2068_LC4236_Locke et al. (2006), V_2069_LC4236_Locke et al. (2006), V_2070_LC4236_Locke et al. (2006), V_4373_LC4228_Wong et al. (2007), V_4374_LC4228_Wong et al. (2007), V_4375_LC4231_Wong et al. (2007), V_4376_LC4234_Wong et al. (2007), V_4377_LC4236_Wong et al. (2007), V_4378_LC4236_Wong et al. (2007)
5	p15.33-p15.32	0.02	5.19	62	24	PLEKHG4B, CCDC127, SDHA, PDCD6, C5orf55, EXOC3, SLC9A3, CEP72, TPPP, ZDHHC11, ZDHHC11B, BRD9, TRIP13, NKD2, SLC12A7, SLC6A19, SLC6A18, TERT, CLPTM1L, SLC6A3, LPCAT1, MRPL36, NDUFS6, IRX4, IRX2, C5orf38, IRX1, ADAMTS16		V_0704_LC6379_Sharp et al. (2005), V_0705_LC6379_Sharp et al. (2005), V_0706_LC6379_Sharp et al. (2005), V_0707_LC6379_Sharp et al. (2005), V_2077_LC6379_Locke et al. (2006), V_2078_LC6379_Locke et al. (2006), V_2079_LC6379_Locke et al. (2006), V_2080_LC6379_Locke et al. (2006), V_2081_LC6379_Locke et al. (2006), V_4228_LC6379_Wong et al. (2007), V_4427_LC6379_Wong et al. (2007)…
5	p15.2	12.54	12.9	4	5			
5	p15.1	16.57	17.5	24	8	FAM134B, MYO10, BASP1		V_0061_LC6634_Iafrate et al. (2004), V_4431_LC6634_Wong et al. (2007)
5	p14.3	19.32	19.81	4	5	CDH18		V_4433_LC6655_Wong et al. (2007)
5	p14.3	20.08	21.03	16	6			V_0708_LC6659_Sharp et al. (2005), V_4434_LC6659_Wong et al. (2007)
5	p14.1	26.61	27.13	6	5	CDH9		
5	p13.2	36.9	37.44	4	5	NIPBL, C5orf42, NUP155, WDR70		
5	p13.1-p12	41.83	43.99	19	6	OXCT1, C5orf51, FBXO4, GHR, SEPP1, C5orf39, ZNF131, HMGCS1, CCL28, C5orf28, C5orf34, PAIP1, NNT		V_4441_LC6869_Wong et al. (2007)
5	q11.2	55.16	56.11	17	5	IL31RA, IL6ST, ANKRD55		
5	q13.2	68.41	71.56	29	10	SLC30A5, CCNB1, CENPH, MRPS36, CDK7, CCDC125, TAF9, RAD17, MARVELD2, OCLN, GTF2H2B, SERF1B, SMN2, GUSBP1, SERF1A, SMN1, NAIP, GTF2H2, BDP1, MCCC2, CARTPT, MAP1B, MRPS27		V_0064_LC7017_Iafrate et al. (2004), V_0710_LC7017_Sharp et al. (2005), V_0711_LC7017_Sharp et al. (2005), V_2088_LC7017_Locke et al. (2006), V_2089_LC7017_Locke et al. (2006), V_4447_LC7017_Wong et al. (2007), V_4448_LC7017_Wong et al. (2007), V_4449_LC7017_Wong et al. (2007), V_4450_LC7017_Wong et al. (2007), V_4451_LC7017_Wong et al. (2007), V_4452_LC7017_Wong et al. (2007), V_4453_LC7022_Wong et al. (2007)

5	q23.3-q31.1	130.28	130.87	6	6	HINT1, LYRM7, CDC42SE2, RAPGEF6		
5	q31.2	138.29	139.12	7	5	SIL1, MATR3, PAIP2, SLC23A1, DNAJC18, ECSCR, TMEM173, UBE2D2, CXXC5		
5	q32-q33.1	148.59	150.27	17	10	ABLIM3, AFAP1L1, GRPEL2, PCYOX1L, IL17B, PPARGC1B, PDE6A, SLC26A2, TIGD6, HMGXB3, CSF1R, PDGFRB, CDX1, SLC6A7, CAMK2A, ARSI, TCOF1, CD74, RPS14, NDST1, SYNPO, MYOZ3, RBM22, DCTN4, IRGM	hsa-mir-143, hsa-mir-145, hsa-mir-378	
5	q33.1	151.97	152.31	3	5			
5	q33.3-q34	159.26	159.9	8	5	ADRA1B, TTC1, PWWP2A, FABP6, CCNJL, C1QTNF2, C5orf54, SLU7, PTTG1		
5	q35.1-q35.2	171.37	173.41	29	7	FBXW11, STK10, EFCAB9, UBTD2, SH3PXD2B, NEURL1B, DUSP1, ERGIC1, RPL26L1, ATP6V0E1, C5orf41, BNIP1, NKX2-5, STC2, BOD1, CPEB4		
5	q35.2-q35.3	175.55	180.68	66	17	C5orf25, KIAA1191, ARL10, NOP16, HIGD2A, CLTB, FAF2, RNF44, PCDH24, GPRIN1, SNCB, EIF4E1B, TSPAN17, UNC5A, HK3, UIMC1, ZNF346, FGFR4, NSD1, RAB24, PRELID1, MXD3, LMAN2, RGS14, SLC34A1, PFN3, F12, GRK6, PRR7, DBN1, PDLIM7, DOK3, DDX41, TMED9, B4GALT7, FAM153A, PROP1, FAM153C, RMND5B, NHP2, HNRNPAB, AGXT2L2, COL23A1, CLK4, ZNF354A, ZNF354B, ZFP2, ZNF454, GRM6, ZNF354C, ADAMTS2, RUFY1, HNRNPH1, CBY3, CANX, MAML1, LTC4S, MGAT4B, SQSTM1, C5orf45, TBC1D9B, RNF130, RASGEF1C, RPS8P7, MAPK9, GFPT2, CNOT6, SCGB3A1, FLT4, OR2Y1, MGAT1, ZFP62, BTNL8, BTNL3, BTNL9, OR2V1, OR2V2, TRIM7, TRIM41, GNB2L1	hsa-mir-1271, hsa-mir-1229, hsa-mir-340	V_0068_LC7886_Iafrate et al. (2004), V_2093_LC7886_Locke et al. (2006), V_2094_LC7886_Locke et al. (2006), V_4481_LC7886_Wong et al. (2007), V_4482_LC7886_Wong et al. (2007), V_0372_LC7886_Bejjani et al. (2005)
6	p21.33-p21.32	30.63	32.19	18	6	TUBBP1, VARS2, DPCR1, MUC21, CDSN, POU5F1, HLA-C, LTB, APOM, LY6G6C, LSM2, HSPA1A, EHMT2, C4B, TNXB, ATF6B, PRRT1, RNF5, GPSM3	hsa-mir-1236	V_4492_LC8203_Wong et al. (2007)
6	p21.32-p21.31	33.16	34.78	18	8	RPS18P12, DAXX, SYNGAP1, ZBTB9, BAK1, GGNBP1, C6orf227, ITPR3, C6orf125, IP6K3, LEMD2, MLN, GRM4, HMGA1, C6orf1, NUDT3, RPS10, PACSIN1, SPDEF, C6orf106, SNRPC, UHRF1BP1	hsa-mir-219-1, hsa-mir-1275	
6	q27	170.33	171.01	8	9	DLL1, FAM120B, PSMB1, TBP, PDCD2		
7	p22.3-p22.1	0.01	7.12	68	32	FAM20C, PDGFA, PRKAR1B, HEATR2, UNC84A, ADAP1, CYP2W1, C7orf50, GPR146, GPER, ZFAND2A, UNCX, MICALL2, INTS1, MAFK, TMEM184A, PSMG3, MAD1L1, FTSJ2, NUDT1, SNX8, EIF3B, CHST12, LFNG, C7orf27, IQCE, TTYH3, AMZ1, GNA12, CARD11, SDK1, FOXK1, RADIL, PAPOLB, MMD2, RNF216L, RBAK, WIPI2, SLC29A4, TNRC18, FBXL18, ACTB, FSCN1, RNF216, OCM, C7orf28A, RSPH10B, PMS2, AIMP2, EIF2AK1, ANKRD61, USP42, CYTH3, C7orf70, RAC1, DAGLB, KDELR2, GRID2IP, ZDHHC4, C7orf26, ZNF12, RSPH10B2, C7orf28B	hsa-mir-339, hsa-mir-589	V_0093_LC9158_Iafrate et al. (2004), V_4519_LC9158_Wong et al. (2007), V_4520_LC9158_Wong et al. (2007), V_4521_LC9158_Wong et al. (2007), V_4522_LC9158_Wong et al. (2007), V_4523_LC9158_Wong et al. (2007), V_4524_LC9249_Wong et al. (2007)
7	p21.3-p21.1	11.6	20.52	100	6	THSD7A, TMEM106B, VWDE, SCIN, ARL4A, ETV1, DGKB, TMEM195, MEOX2, SOSTDC1, ANKMY2, BZW2, TSPAN13, AGR2, AGR3, AHR, SNX13, PRPS1L1, HDAC9, TWIST1, FERD3L, TWISTNB, TMEM196, MACC1, ITGB8	hsa-mir-1302-6	V_0094_LC9325_Iafrate et al. (2004), V_0096_LC9323_Iafrate et al. (2004), V_0097_LC9326_Iafrate et al. (2004), V_0099_LC9326_Iafrate et al. (2004), V_0100_LC9326_Iafrate et al. (2004), V_0101_LC9327_Iafrate et al. (2004), V_0102_LC9326_Iafrate et al. (2004), V_0103_LC9328_Iafrate et al. (2004), V_4526_LC9320_Wong et al. (2007)
7	p15.3	20.9	21.19	3	5			
7	p15.2	26.79	27.39	6	10	SKAP2, HOXA1, HOXA2, HOXA3, HOXA4, HOXA5, HOXA6, HOXA7, HOXA9, HOXA10, HOXA11, HOXA13, EVX1	hsa-mir-196b	
7	p13	43.76	45.26	22	11	C7orf44, BLVRA, MRPS24, UBE2D4, POLR2J4, SPDYE1, DBNL, PGAM2, POLM, AEBP1, POLD2, MYL7, GCK, YKT6, CAMK2B, NUDCD3, NPC1L1, DDX56, TMED4, OGDH, ZMIZ2, PPIA, H2AFV, PURB, MYO1G, C7orf40, CCM2, NACAD, TBRG4, RAMP3		V_4531_LC9464_Wong et al. (2007), V_4532_LC9464_Wong et al. (2007), V_4533_LC9471_Wong et al. (2007)
7	q11.1-q11.21	61.06	62.16	7	7			V_0104_LC9545_Iafrate et al. (2004), V_0721_LC9545_Sharp et al. (2005), V_2100_LC9545_Locke et al. (2006), V_4538_LC9545_Wong et al. (2007), V_4539_LC9545_Wong et al. (2007), V_4540_LC9545_Wong et al. (2007), V_0375_LC9545_Bejjani et al. (2005)
7	q11.23	72.21	76.12	55	22	TYW1B, POM121, NSUN5C, TRIM74, STAG3L3, NSUN5, TRIM50, FKBP6, FZD9, BAZ1B, BCL7B, TBL2, MLXIPL, VPS37D, DNAJC30, WBSCR22, STX1A, ABHD11, CLDN3, CLDN4, WBSCR27, WBSCR28, ELN, LIMK1, EIF4H, LAT2, RFC2, CLIP2, GTF2IRD1, GTF2I, STAG3L2, NCF1, GTF2IRD2, PMS2L5, WBSCR16, GTF2IRD2B, NCF1C, GATSL1, STAG3L1, TRIM73, NSUN5B, POM121C, PMS2L3, HIP1, CCL26, CCL24, RHBDD2, POR, TMEM120A, STYXL1, MDH2, HSPB1, YWHAG, SRCRB4D, ZP3, UPK3B	hsa-mir-590	V_4541_LC9597_Wong et al. (2007), V_4542_LC9602_Wong et al. (2007), V_4543_LC9606_Wong et al. (2007), V_4544_LC9609_Wong et al. (2007), V_4545_LC9609_Wong et al. (2007)
7	q21.3-q22.1	97.74	102.22	52	15	LMTK2, BHLHA15, TECPR1, BRI3, BAIAP2L1, NPTX2, TMEM130, TRRAP, SMURF1, KPNA7, ARPC1B, PDAP1, BUD31, PTCD1, CPSF4, ZNF789, ZNF394, ZKSCAN5, C7orf38, ZNF655, ZNF498, CYP3A5, CYP3A7, CYP3A5P1, CYP3A4, CYP3A43, TRIM4, GJC3, AZGP1, AZGP1P1, ZKSCAN1, ZSCAN21, ZNF3, COPS6, MCM7, AP4M1, TAF6, CNPY4, MBLAC1, C7orf59, C7orf43, GAL3ST4, GPC2, STAG3, GATS, PVRIG, PMS2L1, PILRB, PILRA, ZCWPW1, MEPCE, C7orf47, C7orf61, TSC22D4, C7orf51, AGFG2, LRCH4, FBXO24, PCOLCE, MOSPD3, TFR2, ACTL6B, GNB2, GIGYF1, POP7, EPO, ZAN, EPHB4, SLC12A9, TRIP6, SRRT, UFSP1, ACHE, MUC3B, MUC3A, MUC12, MUC17, TRIM56, SERPINE1, AP1S1, VGF, C7orf52, MOGAT3, PLOD3, ZNHIT1, CLDN15, FIS1, RABL5, EMID2, MYL10, CUX1, SH2B2, PRKRIP1, ORAI2, ALKBH4, LRWD1, POLR2J, RASA4B, POLR2J3, SPDYE2	hsa-mir-25, hsa-mir-93, hsa-mir-106b, hsa-mir-548o	V_0107_LC9766_Iafrate et al. (2004), V_0724_LC9769_Sharp et al. (2005), V_2104_LC9753_Locke et al. (2006), V_2105_LC9769_Locke et al. (2006), V_2106_LC9769_Locke et al. (2006), V_4547_LC9750_Wong et al. (2007), V_4548_LC9750_Wong et al. (2007), V_4549_LC9755_Wong et al. (2007), V_4550_LC9756_Wong et al. (2007), V_4551_LC9756_Wong et al. (2007), V_4552_LC9762_Wong et al. (2007), V_4553_LC9769_Wong et al. (2007)
7	q36.1	150.48	151.44	8	7	TMEM176B, TMEM176A, ABP1, KCNH2, NOS3, ATG9B, ABCB8, ACCN3, CDK5, SLC4A2, FASTK, TMUB1, AGAP3, GBX1, ASB10, ABCF2, SMARCD3, NUB1, WDR86, CRYGN, RHEB, PRKAG2	hsa-mir-671	V_4574_LC10061_Wong et al. (2007)
7	q36.3	156.61	159.12	34	13	LMBR1, NOM1, MNX1, UBE3C, DNAJB6, PTPRN2, NCAPG2, FAM62B, WDR60, VIPR2	hsa-mir-153-2, hsa-mir-595	
8	p23.3	0.05	2.14	25	9	OR4F21, ZNF596, FAM87A, FBXO25, C8orf42, ERICH1, C8orf68, CLN8, ARHGEF10, KBTBD11, MYOM2	hsa-mir-596	V_0731_LC10225_Sharp et al. (2005), V_2112_LC10225_Locke et al. (2006), V_2113_LC10225_Locke et al. (2006), V_4276_LC10225_Wong et al. (2007), V_4575_LC10225_Wong et al. (2007), V_4576_LC10225_Wong et al. (2007)
8	p23.1	6.92	8.04	6	8	FAM90A3, FAM90A13, FAM90A5, FAM90A20, DEFB108P2, DEFB103A, SPAG11B, DEFB104B, DEFB106B, DEFB105B, DEFB107B, FAM90A23, FAM90A22, FAM90A15, FAM90A10, FAM90A8, FAM90A16, FAM90A9, DEFB107A, DEFB105A, DEFB106A, DEFB104A, SPAG11A, DEFB103B, DEFB4, DEFB108P1, FAM66E, FAM90A11, FAM90A12	hsa-mir-548i-3	V_0733_LC10380_Sharp et al. (2005), V_0734_LC10380_Sharp et al. (2005), V_0735_LC10380_Sharp et al. (2005), V_0736_LC10380_Sharp et al. (2005), V_0737_LC10380_Sharp et al. (2005), V_0738_LC10380_Sharp et al. (2005), V_0739_LC10380_Sharp et al. (2005), V_2114_LC10380_Locke et al. (2006), V_2115_LC10380_Locke et al. (2006), V_2116_LC10380_Locke et al. (2006), V_2117_LC10380_Locke et al. (2006), V_2118_LC10380_Locke et al. (2006), V_2119_LC10380_Locke et al. (2006), V_4577_LC10380_Wong et al. (2007), V_4578_LC10380_Wong et al. (2007), V_4579_LC10380_Wong et al. (2007), V_4580_LC10380_Wong et al. (2007)

8	p21.3	21.65	23.18	22	14	DOK2, XPO7, NPM2, FGF17, EPB49, FAM160B2, NUDT18, HR, REEP4, LGI3, SFTPC, BMP1, PHYHIP, POLR3D, PIWIL2, SLC39A14, PPP3CC, SORBS3, PDLIM2, KIAA1967, BIN3, EGR3, RHOBTB2, TNFRSF10B, TNFRSF10C, TNFRSF10D, TNFRSF10A, CHMP7, LOXL2	hsa-mir-320a	V_4586_LC10461_Wong et al. (2007)
8	p12-p11.1	34.65	43.47	99	7	UNC5D, KCNU1, ZNF703, ERLIN2, PROSC, GPR124, BRF2, RAB11FIP1, GOT1L1, ADRB3, EIF4EBP1, ASH2L, STAR, LSM1, BAG4, DDHD2, PPAPDC1B, WHSC1L1, LETM2, FGFR1, C8orf86, TACC1, PLEKHA2, HTRA4, TM2D2, ADAM9, ADAM32, ADAM5P, ADAM3A, ADAM18, ADAM2, IDO1, C8orf4, ZMAT4, SFRP1, GOLGA7, GINS4, AGPAT6, NKX6-3, ANK1, MYST3, AP3M2, PLAT, IKBKB, POLB, DKK4, VDAC3, SLC20A2, C8orf40, CHRNB3, CHRNA6, THAP1, RNF170, HOOK3, FNTA, POTEA	hsa-mir-486	V_4589_LC10531_Wong et al. (2007)
8	q11.1-q24.3	47.78	146.24	969	32	KIAA0146, CEBPD, PRKDC, MCM4, UBE2V2, EFCAB1, SNAI2, C8orf22, SNTG1, PXDNL, PCMTD1, ST18, FAM150A, RB1CC1, NPBWR1, OPRK1, ATP6V1H, RGS20, TCEA1, LYPLA1, MRPL15, SOX17, RP1, XKR4, TMEM68, TGS1, LYN, RPS20, MOS, PLAG1, CHCHD7, SDR16C5, SDR16C6, PENK, IMPAD1, C8orf71, FAM110B, UBXN2B, CYP7A1, SDCBP, NSMAF, TOX, CA8, RAB2A, RLBP1L1, ASPH, NKAIN3, GGH, TTPA, YTHDF3, IFITM8P, BHLHE22, CYP7B1, ARMC1, MTFR1, PDE7A, DNAJC5B, TRIM55, CRH, RRS1, ADHFE1, C8orf46, MYBL1, VCPIP1, C8orf44, SGK3, PTTG3, C8orf45, TCF24, LRRC67, COPS5, CSPP1, ARFGEF1, CPA6, PREX2, C8orf34, RPS15AP25, SULF1, SLCO5A1, PRDM14, NCOA2, TRAM1, LACTB2, XKR9, EYA1, MSC, TRPA1, KCNB2, TERF1, C8orf84, RPL7, RDH10, STAU2, UBE2W, TCEB1, TMEM70, LY96, JPH1, GDAP1, PI15, CRISPLD1, HNF4G, ZFHX4, PXMP3, PKIA, FAM164A, IL7, STMN2, HEY1, MRPS28, TPD52, ZBTB10, ZNF704, PAG1, FABP5, PMP2, FABP9, FABP4, FABP12, IMPA1, SLC10A5, ZFAND1, CHMP4C, SNX16, HNRNPA1P4, RALYL, LRRCC1, E2F5, CA13, CA1, CA3, CA2, REXO1L1, PSKH2, ATP6V0D2, SLC7A13, WWP1, FAM82B, CPNE3, CNGB3, CNBD1, WDR21C, MMP16, RIPK2, OSGIN2, NBN, DECR1, CALB1, TMEM64, TMEM55A, OTUD6B, LRRC69, SLC26A7, RUNX1T1, C8orf83, FAM92A1, RBM12B, C8orf39, TMEM67, PPM2C, CDH17, GEM, RAD54B, KIAA1429, DPY19L4, INTS8, CCNE2, C8orf38, TP53INP1, PLEKHF2, C8orf37, GDF6, UQCRB, MTERFD1, PTDSS1, SDC2, TSPYL5, MTDH, LAPTM4B, MATN2, RPL30, C8orf47, HRSP12, POP1, NIPAL2…	hsa-mir-124-2, hsa-mir-599, hsa-mir-875, hsa-mir-1273, hsa-mir-548a-3, hsa-mir-2053, hsa-mir-548d-1, hsa-mir-1204, hsa-mir-1205, hsa-mir-1207, hsa-mir-1208, hsa-mir-30b, hsa-mir-30d, hsa-mir-151, hsa-mir-937, hsa-mir-661, hsa-mir-939, hsa-mir-1234	V_0119_LC10711_Iafrate et al. (2004), V_0121_LC10727_Iafrate et al. (2004), V_0123_LC10906_Iafrate et al. (2004), V_0124_LC10922_Iafrate et al. (2004), V_2126_LC10727_Locke et al. (2006), V_4591_LC10578_Wong et al. (2007), V_4592_LC10583_Wong et al. (2007), V_4593_LC10587_Wong et al. (2007), V_4594_LC10611_Wong et al. (2007), V_4595_LC10619_Wong et al. (2007), V_4596_LC10633_Wong et al. (2007), V_4597_LC10634_Wong et al. (2007), V_4598_LC10640_Wong et al. (2007), V_4599_LC10697_Wong et al. (2007), V_4600_LC10722_Wong et al. (2007), V_4601_LC10727_Wong et al. (2007), V_4602_LC10727_Wong et al. (2007), V_4603_LC10727_Wong et al. (2007), V_4604_LC10727_Wong et al. (2007), V_4605_LC10727_Wong et al. (2007), V_4606_LC10731_Wong et al. (2007), V_4607_LC10749_Wong et al. (2007), V_4608_LC10811_Wong et al. (2007), V_4609_LC10877_Wong et al. (2007), V_4610_LC10912_Wong et al. (2007), V_4611_LC10941_Wong et al. (2007), V_4612_LC10994_Wong et al. (2007), V_4613_LC11006_Wong et al. (2007), V_4614_LC11012_Wong et al. (2007), V_4791_LC10979_Wong et al. (2007)
9	q31.3	114	114.41	6	6	OR2K2, KIAA0368, ZNF483, PTGR1, C9orf29, DNAJC25		
9	q33.3	127.94	128.27	3	5	PPP6C, RABEPK, HSPA5, GAPVD1, MAPKAP1		
9	q33.3-q34.3	129.48	141.06	129	23	ZBTB43, ZBTB34, RALGPS1, ANGPTL2, GARNL3, SLC2A8, ZNF79, RPL12, LRSAM1, FAM129B, STXBP1, TTC16, C9orf117, TOR2A, SH2D3C, CDK9, FPGS, ENG, AK1, ST6GALNAC6, ST6GALNAC4, PIP5KL1, DPM2, FAM102A, NAIF1, SLC25A25, PTGES2, LCN2, C9orf16, CIZ1, DNM1, GOLGA2, C9orf119, TRUB2, COQ4, SLC27A4, TMSL4, URM1, CERCAM, ODF2, GLE1, SPTAN1, WDR34, SET, PKN3, ZDHHC12, ZER1, TBC1D13, ENDOG, C9orf114, CCBL1, LRRC8A, PHYHD1, DOLK, NUP188, SH3GLB2, FAM73B, DOLPP1, CRAT, PPP2R4, IER5L, METTL11A, C9orf50, ASB6, PRRX2, PTGES, TOR1B, TOR1A, C9orf78, USP20, FNBP1, GPR107, FREQ, HMCN2, ASS1, FUBP3, PRDM12, EXOSC2, ABL1, QRFP, FIBCD1, LAMC3, AIF1L, NUP214, FAM78A, PPAPDC3, BAT2L, POMT1, UCK1, RAPGEF1, MED27, NTNG2, SETX, TTF1, C9orf171, BARHL1, DDX31, GTF3C4, C9orf98, C9orf9, TSC1, GFI1B, GTF3C5, CEL, RALGDS, GBGT1, OBP2B, ABO, SURF6, MED22, RPL7A, SURF1, SURF2, SURF4, C9orf96, REXO4, ADAMTS13, C9orf7, SLC2A6, ADAMTSL2, FAM163B, DBH, SARDH, VAV2, BRD3, WDR5, RXRA, COL5A1, C9orf104, FCN2, FCN1, OLFM1, C9orf62, KIAA0649, C9orf116, MRPS2, LCN1, OBP2A…	hsa-mir-199b, hsa-mir-219-2, hsa-mir-126, hsa-mir-602	V_0132_LC11835_Iafrate et al. (2004), V_0133_LC11864_Iafrate et al. (2004), V_0134_LC11864_Iafrate et al. (2004), V_4657_LC11835_Wong et al. (2007), V_4658_LC11835_Wong et al. (2007), V_4659_LC11848_Wong et al. (2007), V_4660_LC11849_Wong et al. (2007), V_4661_LC11864_Wong et al. (2007), V_4662_LC11864_Wong et al. (2007), V_4663_LC11864_Wong et al. (2007)
10	p15.1	5.51	6.42	8	5	CALML5, CALML3, ASB13, C10orf18, GDI2, ANKRD16, FBXO18, IL15RA, IL2RA, RBM17, PFKFB3		
10	q11.21	43.29	44.2	16	18	BMS1, RET, CSGALNACT2, RASGEF1A, FXYD4, HNRNPF, ZNF487, ZNF239, ZNF485, ZNF32		
10	q11.22	46.84	47.76	14	5	FAM35B, SYT15, GPRIN2, ANXA8L1, PPYR1, FAM25B, BMS1P2, CTSLL7, FAM25HP		V_0764_LC12274_Sharp et al. (2005), V_2153_LC12274_Locke et al. (2006), V_4687_LC12274_Wong et al. (2007), V_4688_LC12274_Wong et al. (2007), V_4689_LC12274_Wong et al. (2007)
10	q21.3-q22.1	70.48	70.96	5	5	CCAR1, STOX1, DDX50, DDX21, KIAA1279, SRGN, VPS26A, SUPV3L1	hsa-mir-1254	
10	q24.32-q24.33	103.74	105.49	21	5	C10orf76, HPS6, LDB1, PPRC1, NOLC1, ELOVL3, PITX3, GBF1, NFKB2, PSD, FBXL15, CUEDC2, C10orf95, TMEM180, ACTR1A, SUFU, TRIM8, ARL3, SFXN2, C10orf26, CYP17A1, C10orf32, AS3MT, CNNM2, NT5C2, INA, PCGF6, TAF5, USMG5, PDCD11, CALHM2, CALHM1, CALHM3, NEURL, SH3PXD2A	hsa-mir-146b, hsa-mir-1307	
10	q26.3	133.66	135.5	30	22	PPP2R2D, BNIP3, JAKMIP3, DPYSL4, STK32C, LRRC27, PWWP2B, C10orf91, INPP5A, NKX6-2, C10orf92, C10orf93, GPR123, KNDC1, UTF1, VENTX, ADAM8, TUBGCP2, ZNF511, CALY, PRAP1, C10orf125, ECHS1, PAOX, MTG1, CYP2E1, SYCE1, FRG2B	hsa-mir-202	V_0370_LC12807_Le Caignec et al. (2005), V_2162_LC12807_Locke et al. (2006), V_4717_LC12807_Wong et al. (2007), V_4718_LC12807_Wong et al. (2007), V_4719_LC12807_Wong et al. (2007), V_4720_LC12807_Wong et al. (2007), V_4721_LC12807_Wong et al. (2007), V_4722_LC12807_Wong et al. (2007), V_4723_LC12807_Wong et al. (2007), V_4724_LC12807_Wong et al. (2007)
11	p15.5-p15.4	0.06	4.28	41	24	BET1L, SCGB1C1, ODF3, RIC8A, SIRT3, PSMD13, NLRP6, ATHL1, IFITM5, IFITM2, IFITM1, IFITM3, B4GALNT4, PKP3, SIGIRR, ANO9, PTDSS2, RNH1, HRAS, LRRC56, C11orf35, RASSF7, PHRF1, IRF7, MUPCDH, SCT, DRD4, DEAF1, TMEM80, EPS8L2, TALDO1, PDDC1, CEND1, SLC25A22, LRDD, RPLP2, PNPLA2, EFCAB4A, CD151, POLR2L, TSPAN4, CHID1, AP2A2, MUC6, MUC2, MUC5B, TOLLIP, BRSK2, DUSP8, C11orf81, KRTAP5-1, KRTAP5-3, KRTAP5-5, KRTAP5-6, CTSD, SYT8, TNNI2, LSP1, C11orf89, TNNT3, MRPL23, IGF2, INS, IGF2AS, TH, ASCL2, C11orf21, TSPAN32, CD81, TSSC4, TRPM5, KCNQ1, CDKN1C, SLC22A18, PHLDA2, NAP1L4, CARS, OSBPL5, MRGPRG, MRGPRE, ZNF195, ART5, ART1, CHRNA10, NUP98, RHOG, STIM1, RRM1	hsa-mir-210, hsa-mir-675, hsa-mir-483	V_0767_LC12925_Sharp et al. (2005), V_2163_LC12925_Locke et al. (2006), V_4725_LC12865_Wong et al. (2007), V_4726_LC12865_Wong et al. (2007), V_4728_LC12896_Wong et al. (2007), V_4729_LC12896_Wong et al. (2007), V_4730_LC12916_Wong et al. (2007)
11	p15.4	7.97	9.89	24	6	NLRP10, EIF3F, TUB, RIC3, LMO1, STK33, TRIM66, RPL27A, ST5, C11orf17, C11orf16, ASCL3, TMEM9B, NRIP3, SCUBE2, DENND5A, TMEM41B, IPO7, ZNF143, WEE1, SWAP70, SBF2		
11	p13	32.56	33.02	4	5	EIF3M, CCDC73, PRRG4, QSER1		
11	p13	33.04	33.84	11	5	DEPDC7, TCP11L1, CSTF3, HIPK3, C11orf41, C11orf91, CD59, FBXO3		
11	p11.2	44.26	48.38	49	16	EXT2, ALX4, CD82, TSPAN18, TP53I11, PRDM11, SYT13, CHST1, SLC35C1, CRY2, MAPK8IP1, PEX16, GYLTL1B, PHF21A, CREB3L1, DGKZ, MDK, CHRM4, AMBRA1, HARBI1, KIAA0652, ARHGAP1, ZNF408, F2, CKAP5, LRP4, C11orf49, ARFGAP2, PACSIN3, DDB2, ACP2, NR1H3, MADD, MYBPC3, SPI1, SLC39A13, PSMC3, RAPSN, CUGBP1, PTPMT1, KBTBD4, NDUFS3, FAM180B, C1QTNF4, MTCH2, AGBL2, FNBP4, NUP160, PTPRJ, OR4B1, OR4X2, OR4X1, OR4S1, OR4C3, OR4C45		V_4741_LC13180_Wong et al. (2007)

11	q12.2-q14.1	60.17	80.52	215	25	MS4A14, MS4A5, MS4A1, MS4A12, MS4A13, MS4A8B, MS4A15, MS4A10, CCDC86, GPR44, ZP1, PRPF19, TMEM109, TMEM132A, SLC15A3, CD6, CD5, VPS37C, PGA3, PGA5, VWCE, DDB1, DAK, CYBASC3, TMEM138, TMEM216, CPSF7, C11orf79, C11orf66, DAGLA, C11orf9, C11orf10, FEN1, FADS1, FADS2, FADS3, RAB3IL1, BEST1, FTH1, INCENP, SCGB1D1, SCGB2A1, SCGB1D2, SCGB2A2, SCGB1D4, ASRGL1, SCGB1A1, AHNAK, TUT1, MTA2, EML3, ROM1, B3GAT3, GANAB, INTS5, C11orf48, METTL12, C11orf83, UBXN1, LRRN4CL, BSCL2, GNG3, HNRNPUL2, TTC9C, ZBTB3, POLR2G, TAF6L, TMEM179B, TMEM223, NXF1, STX5, WDR74, SLC3A2, CHRM1, SLC22A6, SLC22A8, SLC22A24, SLC22A25, SLC22A10, SLC22A9, HRASLS5, LGALS12, RARRES3, HRASLS2, PLA2G16, ATL3, RTN3, C11orf84, MARK2, RCOR2, NAT11, COX8A, OTUB1, MACROD1, FLRT1, FERMT3, TRPT1, NUDT22, DNAJC4, VEGFB, FKBP2, PPP1R14B, PLCB3, BAD, GPR137, KCNK4, C11orf20, ESRRA, PRDX5, CCDC88B, RPS6KA4, SLC22A11, SLC22A12, NRXN2, RASGRP2, PYGM, SF1, MAP4K2, MEN1, CDC42BPG, EHD1, ATG2A, PPP2R5B, GPHA2, C11orf85, BATF2, ARL2, SNX15, SAC3D1, NAALADL1, CDCA5, ZFPL1, C11orf2, TM7SF2, ZNHIT2, FAU, MRPL49, SYVN1, SPDYC, CAPN1, SLC22A20, POLA2, CDC42EP2, DPF2, TIGD3, SLC25A45, FRMD8, MALAT1, SCYL1, LTBP3, SSSCA1, FAM89B, EHBP1L1, KCNK7, MAP3K11, PCNXL3, SIPA1, RELA, KAT5, RNASEH2C, OVOL1, SNX32, CFL1, MUS81, EFEMP2, CTSW, FIBP, CCDC85B, FOSL1, C11orf68, DRAP1, TSGA10IP, SART1, EIF1AD, BANF1, CST6, CATSPER1, GAL3ST3, SF3B2, PACS1, KLC2, RAB1B, CNIH2, YIF1A, TMEM151A, CD248, RIN1, BRMS1, SLC29A2, NPAS4, MRPL11, PELI3, BBS1, ZDHHC24, CTSF, CCDC87, CCS, RBM4, RBM4B, SPTBN2, C11orf80, RCE1, PC, LRFN4, C11orf86, SYT12…	hsa-mir-611, hsa-mir-1908, hsa-mir-1237, hsa-mir-192, hsa-mir-194-2, hsa-mir-612, hsa-mir-548k, hsa-mir-139, hsa-mir-326, hsa-mir-708	V_0150_LC13257_Iafrate et al. (2004), V_0151_LC13373_Iafrate et al. (2004), V_0777_LC13377_Sharp et al. (2005), V_2169_LC13288_Locke et al. (2006), V_2184_LC13377_Locke et al. (2006), V_4727_LC13373_Wong et al. (2007), V_4747_LC13245_Wong et al. (2007), V_4748_LC13245_Wong et al. (2007), V_4749_LC13256_Wong et al. (2007), V_4750_LC13267_Wong et al. (2007), V_4751_LC13267_Wong et al. (2007), V_4752_LC13273_Wong et al. (2007), V_4753_LC13273_Wong et al. (2007), V_4754_LC13285_Wong et al. (2007), V_4755_LC13316_Wong et al. (2007), V_4756_LC13329_Wong et al. (2007)
11	q14.1	82.38	82.8	3	5	RPS28, FAM181B, PRCP, C11orf82, RAB30		
11	q23.3	118.52	119.39	9	5	PHLDB1, TREH, DDX6, CXCR5, BCL9L, UPK2, FOXR1, CCDC84, RPS25, TRAPPC4, SLC37A4, HYOU1, VPS11, HMBS, H2AFX, DPAGT1, C2CD2L, HINFP, ABCG4, NLRX1, PDZD3, CCDC153, CBL, MCAM, RNF26, C1QTNF5, MFRP, USP2, THY1		
12	p13.33-p13.32	0.15	3.82	38	15	FAM138D, IQSEC3, SLC6A12, SLC6A13, KDM5A, CCDC77, B4GALNT3, NINJ2, WNK1, RAD52, ERC1, FBXL14, WNT5B, ADIPOR2, LRTM2, DCP1B, CACNA1C, FKBP4, ITFG2, NRIP2, FOXM1, C12orf32, TULP3, TEAD4, TSPAN9, RPS27P23, PRMT8, EFCAB4B		V_0161_LC13778_Iafrate et al. (2004), V_4765_LC13757_Wong et al. (2007), V_4766_LC13773_Wong et al. (2007)
12	p13.31	5.88	8.91	33	20	ANO2, VWF, CD9, PLEKHG6, TNFRSF1A, SCNN1A, LTBR, CD27, TAPBPL, VAMP1, MRPL51, NCAPD2, GAPDH, IFFO1, NOP2, CHD4, LPAR5, ACRBP, ING4, ZNF384, C12orf53, COPS7A, MLF2, PTMS, LAG3, CD4, GPR162, GNB3, CDCA3, USP5, TPI1, LRRC23, ENO2, ATN1, C12orf57, PTPN6, PHB2, EMG1, LPCAT3, C1S, C1R, C1RL, RBP5, CLSTN3, PEX5, ACSM4, CD163L1, CD163, APOBEC1, GDF3, DPPA3, CLEC4C, NANOG, SLC2A14, NANOGP1, SLC2A3, FOXJ2, C3AR1, NECAP1, CLEC4A, ZNF705A, FAM90A1, CLEC6A, CLEC4D, CLEC4E, AICDA, MFAP5	hsa-mir-200c, hsa-mir-141	
12	q11-q12	38.02	38.5	6	5			
12	q13.11-q13.12	48.03	51.04	35	8	RPAP3, RAPGEF3, SLC48A1, HDAC7, VDR, TMEM106C, COL2A1, SENP1, PFKM, ASB8, C12orf68, OR10AD1, H1FNT, ZNF641, ANP32D, C12orf54, OR8S1, LALBA, C12orf41, CCNT1, ADCY6, CACNB3, DDX23, RND1, CCDC65, FKBP11, ARF3, WNT10B, WNT1, DDN, PRKAG1, MLL2, RHEBL1, DHH, LMBR1L, TUBA1B, TUBA1A, TUBA1C, PRPH, TROAP, C1QL4, DNAJC22, SPATS2, KCNH3, MCRS1, FAM186B, PRPF40B, FMNL3, TMBIM6, KIAA1602, BCDIN3D, FAIM2, AQP2, AQP5, AQP6, RACGAP1, ACCN2, SMARCD1, GPD1, C12orf62, LASS5, LIMA1, FAM186A, LARP4, DIP2B	hsa-mir-1293	V_4778_LC14057_Wong et al. (2007)
12	q13.13	53.21	54.16	14	12	KRT79, KRT78, KRT8, KRT18, EIF4B, TENC1, SPRYD3, IGFBP6, SOAT2, CSAD, ZNF740, ITGB7, RARG, MFSD5, ESPL1, PFDN5, C12orf10, AAAS, SP7, SP1, AMHR2, PRR13, PCBP2, MAP3K12, TARBP2, NPFF, ATF7, ATP5G2, CALCOCO1		V_4780_LC14080_Wong et al. (2007)
12	q13.2-q14.1	55.94	58.23	26	6	OR6C4, OR2AP1, OR10P1, METTL7B, ITGA7, BLOC1S1, RDH5, CD63, GDF11, SARNP, ORMDL2, DNAJC14, MMP19, WIBG, DGKA, SILV, CDK2, RAB5B, SUOX, IKZF4, RPS26, ERBB3, PA2G4, ZC3H10, FAM62A, MYL6, MYL6, SMARCC2, RNF41, OBFC2B, SLC39A5, ANKRD52, COQ10A, CS, CNPY2, PAN2, IL23A, STAT2, APOF, TIMELESS, MIP, SPRYD4, GLS2, RBMS2, BAZ2A, ATP5B, PTGES3, NACA, PRIM1, HSD17B6, SDR9C7, RDH16, GPR182, ZBTB39, TAC3, MYO1A, TMEM194A, NAB2, STAT6, LRP1, NXPH4, SHMT2, NDUFA4L2, STAC3, R3HDM2, INHBC, INHBE, GLI1, ARHGAP9, MARS, DDIT3, MBD6, DCTN2, KIF5A, PIP4K2C, DTX3, SLC26A10, B4GALNT1, OS9, AGAP2, TSPAN31, CDK4, Mar-09, CYP27B1, METTL1, FAM119B, TSFM, AVIL, CTDSP2	hsa-mir-1228, hsa-mir-616, hsa-mir-26a-2	
12	q14.1-q14.3	62.81	65.24	33	5	MON2, C12orf61, PPM1H, AVPR1A, DPY19L2, TMEM5, SRGAP1, C12orf66, C12orf56, XPOT, TBK1, RASSF3, GNS, TBC1D30	hsa-let-7i, hsa-mir-548c	
12	q15	68.77	71.43	30	5	RAP1B, NUP107, SLC35E3, MDM2, CPM, CPSF6, LYZ, YEATS4, FRS2, CCT2, LRRC10, BEST3, RAB3IP, C12orf28, CNOT2, KCNMB4, PTPRB, PTPRR		V_4781_LC14179_Wong et al. (2007)
12	q24.21	114.85	115.37	7	5	TBX5, TBX3		V_4787_LC14460_Wong et al. (2007)
12	q24.21-q24.22	116.76	117.38	10	7	NCRNA00173, MAP1LC3B2, C12orf49, RNFT2, HRK, FBXW8		
12	q24.23-q24.31	120.11	125.67	69	14	PRKAB1, CIT, CCDC64, RAB35, GCN1L1, RPLP0, NME2P1, SIRT4, PLA2G1B, MSI1, COX6A1, TRIAP1, SFRS9, DYNLL1, COQ5, RNF10, POP5, CABP1, MLEC, UNC119B, ACADS, C12orf27, HNF1A, C12orf43, OASL, P2RX7, P2RX4, CAMKK2, ANAPC5, RNF34, KDM2B, ORAI1, MORN3, TMEM120B, RHOF, SETD1B, HPD, PSMD9, WDR66, BCL7A, MLXIP, IL31, LRRC43, B3GNT4, DIABLO, VPS33A, CLIP1, ZCCHC8, RSRC2, KNTC1, GPR81, NIACR1, DENR, CCDC62, HIP1R, VPS37B, ABCB9, OGFOD2, ARL6IP4, PITPNM2, MPHOSPH9, C12orf65, CDK2AP1, SBNO1, SETD8, SNRNP35, RILPL2, RILPL1, TMED2, DDX55, EIF2B1, GTF2H3, TCTN2, ATP6V0A2, DNAH10, CCDC92, ZNF664, FAM101A, NCOR2, SCARB1, UBC, DHX37, BRI3BP, AACS	hsa-mir-1178	V_4790_LC14504_Wong et al. (2007), V_4792_LC14514_Wong et al. (2007)
12	q24.33	131.62	133.78	18	17	GPR133, SFRS8, MMP17, ULK1, PUS1, EP400, EP400NL, DDX51, NOC4L, GALNT9, MUC8, FBRSL1, P2RX2, POLE, PGAM5, ANKLE2, GOLGA3, CHFR, ZNF605, ZNF26, ZNF84, ZNF140, ZNF10		V_4404_LC14595_Wong et al. (2007)
13	q34	110.77	111.97	12	6	COL4A1, COL4A2, RAB20, CARKD, CARS2, ING1, C13orf29, ANKRD10, ARHGEF7		
13	q34	111.92	115.07	29	10	ARHGEF7, C13orf16, SOX1, C13orf28, TUBGCP3, C13orf35, ATP11A, MCF2L, F7, F10, PROZ, PCID2, CUL4A, LAMP1, GRTP1, ADPRHL1, DCUN1D2, TMCO3, TFDP1, ATP4B, GRK1, FAM70B, GAS6, RASA3, CDC16, UPF3A		V_4819_LC15248_Wong et al. (2007), V_4820_LC15248_Wong et al. (2007)
14	q11.2	19.97	20.41	5	8	OR11H2, OR4Q3, OR4H12P, OR4M1, OR4N2, OR4K2, OR4K5, OR4K1		
14	q24.3	77.53	78.44	10	5	KIAA1737, ZDHHC22, TMEM63C, NGB, POMT2, GSTZ1, TMED8, C14orf174, C14orf148, C14orf133, AHSA1, ISM2, SPTLC2, ALKBH1, C14orf156, SNW1, C14orf178, ADCK1	hsa-mir-1260	

14	q32.2-q32.33	100.01	106.43	69	24	CCDC85C, HHIPL1, CYP46A1, EML1, EVL, DEGS2, YY1, SLC25A29, C14orf68, WARS, WDR25, BEGAIN, C14orf70, DLK1, DIO3, PPP2R5C, DYNC1H1, HSP90AA1, WDR20, RAGE, ZNF839, TECPR2, ANKRD9, RCOR1, TRAF3, AMN, CDC42BPB, C14orf73, TNFAIP2, EIF5, MARK3, CKB, TRMT61A, BAG5, C14orf153, XRCC3, ZFYVE21, PPP1R13B, C14orf2, TDRD9, ASPG, KIF26A, C14orf144, C14orf180, TMEM179, INF2, ADSSL1, SIVA1, AKT1, ZBTB42, RPS2P4, PLD4, AHNAK2, C14orf79, CDCA4, GPR132, JAG2, NUDT14, BRF1, BTBD6, PACS2, MTA1, CRIP2, CRIP1, C14orf80, TMEM121, IGHA2, IGHE, IGHG4, IGHA1, IGHV4-31, IGHVII-15-1, IGHM, IGHD, IGHM, FAM30A	hsa-mir-342, hsa-mir-345, hsa-mir-770, hsa-mir-493, hsa-mir-337, hsa-mir-665, hsa-mir-431, hsa-mir-433, hsa-mir-127, hsa-mir-432, hsa-mir-136, hsa-mir-370, hsa-mir-379, hsa-mir-411, hsa-mir-299, hsa-mir-380, hsa-mir-1197, hsa-mir-323, hsa-mir-758, hsa-mir-329-1, hsa-mir-329-2, hsa-mir-494, hsa-mir-543, hsa-mir-495, hsa-mir-376c, hsa-mir-654, hsa-mir-300, hsa-mir-1185-1…	V_0180_LC16001_Iafrate et al. (2004), V_0182_LC16055_Iafrate et al. (2004), V_0770_LC16055_Sharp et al. (2005), V_0771_LC16055_Sharp et al. (2005), V_0772_LC16055_Sharp et al. (2005), V_0773_LC16055_Sharp et al. (2005), V_0774_LC16055_Sharp et al. (2005), V_2176_LC16055_Locke et al. (2006), V_2177_LC16055_Locke et al. (2006), V_2178_LC16055_Locke et al. (2006), V_2179_LC16055_Locke et al. (2006), V_4847_LC16001_Wong et al. (2007), V_4848_LC16001_Wong et al. (2007), V_4849_LC16055_Wong et al. (2007), V_4850_LC16055_Wong et al. (2007), V_4851_LC16055_Wong et al. (2007), V_4852_LC16055_Wong et al. (2007), V_4853_LC16055_Wong et al. (2007), V_4854_LC16055_Wong et al. (2007), V_4855_LC16055_Wong et al. (2007), V_4856_LC16055_Wong et al. (2007), V_4857_LC16055_Wong et al. (2007), V_4858_LC16055_Wong et al. (2007), V_4859_LC16055_Wong et al. (2007), V_4860_LC16055_Wong et al. (2007), V_0377_LC16055_Bejjani et al. (2005)
15	q11.2	20.21	22.55	27	10	BCL8, OR11K1P, OR4M2, OR4N4, VSIG6	hsa-mir-1268	V_2183_LC16090_Locke et al. (2006), V_4877_LC16090_Wong et al. (2007), V_4878_LC16090_Wong et al. (2007), V_4879_LC16090_Wong et al. (2007), V_4880_LC16090_Wong et al. (2007), V_4881_LC16090_Wong et al. (2007)
15	q15.1	40.65	42.3	20	9	DISP2, C15orf23, IVD, BAHD1, CHST14, C15orf57, RPUSD2, CASC5, RAD51, FAM82A2, GCHFR, DNAJC17, C15orf62, ZFYVE19, PPP1R14D, SPINT1, RHOV, VPS18, DLL4, CHAC1, INO80, FAM92A2, EXD1, OIP5, NUSAP1, NDUFAF1, RTF1, ITPKA, LTK, RPAP1, TYRO3, MGA, MAPKBP1, JMJD7, SPTBN5, EHD4, PLA2G4E	hsa-mir-626	
15	q22.31-q23	64.17	67.85	35	10	DAPK2, FAM96A, SNX1, SNX22, PPIB, CSNK1G1, KIAA0101, TRIP4, ZNF609, RBPMS2, PIF1, ANKDD1A, SPG21, MTFMT, RASL12, PDCD7, CLPX, CILP, PARP16, IGDCC3, IGDCC4, DPP8, PTPLAD1, C15orf44, SLC24A1, DENND4A, RAB11A, MEGF11, DIS3L, TIPIN, MAP2K1, SNAPC5, RPL4, ZWILCH, LCTL, SMAD6, SMAD3, IQCH, C15orf61, MAP2K5	hsa-mir-1272	
15	q24.1-q24.2	74.99	75.33	4	5	CYP1A1, CYP1A2, CSK, LMAN1L, CPLX3, ULK3, SCAMP2, MPI, C15orf17, COX5A, RPP25, SCAMP5, PPCDC		V_4905_LC16412_Wong et al. (2007)
15	q26.1	89.83	90.94	9	10	FANCI, POLG, RHCG, C15orf42, KIF7, PLIN, PEX11A, WDR93, MESP1, MESP2, ANPEP, C15orf38, ZNF710, IDH2, CIB1, C15orf58, TTLL13, NGRN, GABARAPL3, ZNF774, IQGAP1	hsa-mir-9-3	
16	p13.3-q11.1	0.06	35.2	363	38	WASH4P, POLR3K, SNRNP25, RHBDF1, MPG, C16orf35, HBZ, HBM, HBA2, HBA1, HBQ1, LUC7L, ITFG3, RGS11, PDIA2, AXIN1, MRPL28, TMEM8, NME4, RAB11FIP3, SOLH, C16orf11, PIGQ, RAB40C, WFIKKN1, C16orf13, C16orf14, WDR90, RHOT2, RHBDL1, STUB1, WDR24, FBXL16, METRN, FAM173A, CCDC78, HAGHL, NARFL, MSLN, MSLNL, RPUSD1, CHTF18, GNG13, LMF1, SOX8, SSTR5, C1QTNF8, CACNA1H, TPSG1, TPSB2, TPSAB1, TPSD1, PRSS29P, UBE2I, BAIAP3, C16orf42, GNPTG, UNKL, C16orf91, CCDC154, CLCN7, C16orf38, TELO2, IFT140, TMEM204, CRAMP1L, HN1L, MAPK8IP3, NME3, MRPS34, EME2, SPSB3, NUBP2, IGFALS, HAGH, FAHD1, C16orf73, HS3ST6, SEPX1, RPL3L, NDUFB10, RPS2, RNF151, TBL3, NOXO1, GFER, SYNGR3, ZNF598, NPW, NTHL1, TSC2, PKD1, RAB26, TRAF7, CASKIN1, C16orf79, PGP, E4F1, DNASE1L2, DCI, RNPS1, ABCA3, ABCA17P, CCNF, C16orf59, NTN3, TBC1D24, ATP6V0C, AMDHD2, CEMP1, PDPK1, KCTD5, PRSS27, SRRM2, TCEB2, PRSS33, PRSS21, ZG16B, PRSS22, FLYWCH2, FLYWCH1, KREMEN2, PKMYT1, PAQR4, CLDN9, CLDN6, TNFRSF12A, HCFC1R1, THOC6, CCDC64B, MMP25, IL32, ZSCAN10, ZNF205, ZNF213, OR1F1, ZNF200, MEFV, ZNF263, TIGD7, ZNF75A, OR2C1, ZNF434, ZNF174, ZNF597, NAT15, C16orf90, CLUAP1, NLRC3, BTBD12, DNASE1, TRAP1, CREBBP, ADCY9, SRL, TFAP4, GLIS2, CORO7, VASN, DNAJA3, NMRAL1, HMOX2, C16orf5, FAM100A, MGRN1, NUDT16L1, ANKS3, C16orf71, ZNF500, Sep-12, ROGDI, UBN1, PPL, SEC14L5, NAGPA, C16orf89, ALG1, FAM86A, TMEM114, C16orf68, ABAT, TMEM186, PMM2, CARHSP1, USP7, C16orf72, GRIN2A, ATF7IP2, EMP2, TEKT5, NUBP1, CIITA, CLEC16A, SOCS1, TNP2, PRM3, PRM2, PRM1, C16orf75, LITAF, SNN, TXNDC11, ZC3H7A, RSL1D1, TNFRSF17, RUNDC2A, SNX29, CPPED1, ERCC4, MKL2, BFAR, PLA2G10, ABCC6P2, NOMO1, NPIP, PDXDC1, NTAN1, RRN3, PKD1P6, MPV17L, C16orf45, KIAA0430, NDE1, MYH11, C16orf63, ABCC1, ABCC6, NOMO3, XYLT1, NOMO2, RPS15A, ARL6IP1, SMG1, TMC7, COQ7, ITPRIPL2, SYT7, TMC5, GDE1, C16orf62, C16orf88, IQCK, GPRC5B, GPR139, GP2, UMOD, PDILT, ACSM5, ACSM2A, ACSM2B, ACSM1, THUMPD1, ACSM3, ERI2, DCUN1D3, LYRM1…	hsa-mir-662, hsa-mir-1225, hsa-mir-940, hsa-mir-548h-2, hsa-mir-193b, hsa-mir-365-1, hsa-mir-1972, hsa-mir-484	V_0195_LC16821_Iafrate et al. (2004), V_0196_LC16821_Iafrate et al. (2004), V_0197_LC16821_Iafrate et al. (2004), V_0793_LC16761_Sharp et al. (2005), V_0794_LC16821_Sharp et al. (2005), V_0795_LC16821_Sharp et al. (2005), V_0796_LC16821_Sharp et al. (2005), V_2203_LC16733_Locke et al. (2006), V_2204_LC16736_Locke et al. (2006), V_2205_LC16736_Locke et al. (2006), V_2206_LC16761_Locke et al. (2006), V_2207_LC16761_Locke et al. (2006), V_2208_LC16802_Locke et al. (2006), V_2209_LC16817_Locke et al. (2006), V_2210_LC16821_Locke et al. (2006), V_2211_LC16821_Locke et al. (2006), V_2212_LC16821_Locke et al. (2006), V_2213_LC16821_Locke et al. (2006), V_2214_LC16821_Locke et al. (2006), V_2215_LC16821_Locke et al. (2006), V_4440_LC16821_Wong et al. (2007), V_4779_LC16593_Wong et al. (2007), V_4912_LC16593_Wong et al. (2007), V_4913_LC16593_Wong et al. (2007), V_4914_LC16593_Wong et al. (2007), V_4915_LC16593_Wong et al. (2007), V_4916_LC16593_Wong et al. (2007), V_4917_LC16593_Wong et al. (2007), V_4918_LC16593_Wong et al. (2007), V_4919_LC16593_Wong et al. (2007), V_4920_LC16652_Wong et al. (2007), V_4921_LC16658_Wong et al. (2007), V_4922_LC16660_Wong et al. (2007), V_4923_LC16730_Wong et al. (2007), V_4924_LC16730_Wong et al. (2007), V_4925_LC16730_Wong et al. (2007), V_4926_LC16734_Wong et al. (2007), V_4927_LC16736_Wong et al. (2007), V_4928_LC16736_Wong et al. (2007), V_4929_LC16736_Wong et al. (2007), V_4930_LC16736_Wong et al. (2007), V_4931_LC16758_Wong et al. (2007), V_4932_LC16761_Wong et al. (2007), V_4933_LC16761_Wong et al. (2007), V_4934_LC16761_Wong et al. (2007), V_4935_LC16781_Wong et al. (2007), V_4936_LC16785_Wong et al. (2007), V_4937_LC16802_Wong et al. (2007), V_4938_LC16802_Wong et al. (2007), V_4939_LC16808_Wong et al. (2007), V_4940_LC16814_Wong et al. (2007), V_4941_LC16818_Wong et al. (2007), V_4942_LC16818_Wong et al. (2007), V_4943_LC16821_Wong et al. (2007), V_4944_LC16821_Wong et al. (2007), V_4945_LC16821_Wong et al. (2007)…
16	q21-q22.1	66.64	69.45	26	5	CMTM3, CMTM4, DYNC1LI2, CCDC79, NAE1, CA7, CDH16, RRAD, CES2, CES3, CES8, CBFB, C16orf70, B3GNT9, TRADD, FBXL8, HSF4, NOL3, EXOC3L, E2F4, ELMO3, LRRC29, TMEM208, FHOD1, SLC9A5, PLEKHG4, KCTD19, LRRC36, TPPP3, ZDHHC1, HSD11B2, ATP6V0D1, AGRP, FAM65A, CTCF, RLTPR, ACD, PARD6A, C16orf48, C16orf86, GFOD2, RANBP10, TSNAXIP1, CENPT, THAP11, NUTF2, EDC4, NRN1L, PSKH1, CTRL, PSMB10, LCAT, SLC12A4, DPEP3, DPEP2, DDX28, DUS2L, NFATC3, ESRP2, PLA2G15, SLC7A6, SLC7A6OS, PRMT7, SMPD3, ZFP90, CDH3, CDH1, TMCO7, HAS3, CHTF8, CIRH1A, SNTB2, VPS4A, PDF, COG8, NIP7, TMED6, TERF2	hsa-mir-328	V_0797_LC16959_Sharp et al. (2005), V_2216_LC16959_Locke et al. (2006), V_4963_LC16959_Wong et al. (2007), V_4964_LC16959_Wong et al. (2007), V_4965_LC16963_Wong et al. (2007)
16	q24.2-q24.3	87.83	90.04	22	8	SLC7A5, CA5A, BANP, ZNF469, ZFPM1, C16orf85, ZC3H18, IL17C, CYBA, MVD, SNAI3, RNF166, C16orf84, FAM38A, CDT1, APRT, GALNS, TRAPPC2L, CBFA2T3, ACSF3, CDH15, ZNF778, ANKRD11, SPG7, RPL13, CPNE7, DPEP1, CHMP1A, C16orf55, CDK10, SPATA2L, C16orf7, ZNF276, FANCA, SPIRE2, TCF25, TUBB3, DEF8		V_0200_LC17076_Iafrate et al. (2004), V_4977_LC17076_Wong et al. (2007), V_4978_LC17076_Wong et al. (2007)
17	p13.3-p13.1	0	9.13	100	22	DOC2BL, RPH3AL, C17orf97, FAM101B, VPS53, FAM57A, GEMIN4, GLOD4, RNMTL1, NXN, TIMM22, ABR, BHLHA9, TUSC5, YWHAE, CRK, MYO1C, INPP5K, PITPNA, SLC43A2, SCARF1, RILP, PRPF8, TLCD2, WDR81, SERPINF2, SERPINF1, SMYD4, RPA1, RTN4RL1, DPH1, HIC1, SMG6, SRR, TSR1, SGSM2, MNT, METT10D, PAFAH1B1, KIAA0664, GARNL4, OR1D4, OR1D2, OR1G1, OR1A2, OR1A1, OR3A2, OR3A1, OR1E1, OR3A3, OR1E2, SPATA22, ASPA, TRPV3, SHPK, CTNS, TAX1BP3, TMEM93, P2RX5, ITGAE, GSG2, C17orf85, CAMKK1, P2RX1, ATP2A3, ZZEF1, CYB5D2, ANKFY1, SPNS3, SPNS2, MYBBP1A, GGT6, SMTNL2, ALOX15, PELP1, ARRB2, MED11, CXCL16, ZMYND15, TM4SF5, VMO1, GLTPD2, PSMB6, PLD2, MINK1, CHRNE, GP1BA, SLC25A11, RNF167, PFN1, ENO3, SPAG7, CAMTA2, INCA1, KIF1C, GPR172B, ZFP3, ZNF232, USP6, ZNF594, C17orf87, RABEP1, NUP88, RPAIN, C1QBP, DHX33, DERL2, MIS12, NLRP1, WSCD1, AIPL1, FAM64A, PITPNM3, KIAA0753, TXNDC17, MED31, C17orf100, SLC13A5, XAF1, FBXO39, TEKT1, ALOX12, RNASEK, C17orf49, BCL6B, SLC16A13, SLC16A11, CLEC10A, ASGR2, ASGR1, DLG4, ACADVL, DVL2, PHF23, GABARAP, DULLARD, C17orf81, CLDN7, SLC2A4, YBX2, EIF5A, GPS2, NEURL4, ACAP1, KCTD11, TMEM95, TNK1, PLSCR3, C17orf61, NLGN2, SPEM1, C17orf74, TMEM102, FGF11, CHRNB1, ZBTB4, AMAC1L3, POLR2A, TNFSF12, SENP3, EIF4A1, CD68, MPDU1, SOX15, FXR2, SAT2, SHBG, ATP1B2, TP53, WRAP53, EFNB3, DNAH2, KDM6B, TMEM88, LSMD1, CYB5D1, CHD3, KCNAB3, TRAPPC1, CNTROB, GUCY2D, ALOX15B,	hsa-mir-22, hsa-mir-132, hsa-mir-212, hsa-mir-1253, hsa-mir-195, hsa-mir-497, hsa-mir-324	V_2217_LC17259_Locke et al. (2006), V_4979_LC17159_Wong et al. (2007), V_4980_LC17159_Wong et al. (2007), V_4981_LC17250_Wong et al. (2007), V_4982_LC17265_Wong et al. (2007), V_4983_LC17269_Wong et al. (2007), V_4984_LC17276_Wong et al. (2007), V_4985_LC17280_Wong et al. (2007), V_4986_LC17280_Wong et al. (2007), V_4987_LC17280_Wong et al. (2007), V_4988_LC17315_Wong et al. (2007)

						ALOX12B, ALOXE3, HES7, PER1, VAMP2, TMEM107, C17orf59, AURKB, C17orf68, PFAS, SLC25A35, RANGRF, ARHGEF15, ODF4, KRBA2, RPL26, NDEL1, MYH10, CCDC42, SPDYE4, MFSD6L, PIK3R6, PIK3R5, NTN1		
17	p11.2	16.78	18.45	19	17	TNFRSF13B, MPRIP, C17orf84, PLD6, FLCN, COPS3, NT5M, MED9, RASD1, PEMT, RAI1, SMCR5, SREBF1, TOM1L2, LRRC48, ATPAF2, C17orf39, DRG2, MYO15A, ALKBH5, LLGL1, FLII, SMCR7, TOP3A, SMCR8, SHMT1, EVPLL, LGALS9C, CCDC144B	hsa-mir-33b	V_2219_LC17388_Locke et al. (2006), V_4990_LC17383_Wong et al. (2007), V_4992_LC17388_Wong et al. (2007)
17	p11.2	18.81	20.07	15	10	PRPSAP2, SLC5A10, FAM83G, GRAP, EPN2, B9D1, MAPK7, MFAP4, RNF112, SLC47A1, ALDH3A2, SLC47A2, ALDH3A1, ULK2, AKAP10, CYTSB	hsa-mir-1180	V_4994_LC17394_Wong et al. (2007)
17	p11.1	21.77	21.99	4	9	FAM27L		V_4998_LC17406_Wong et al. (2007)
17	q12-q21.33	36.17	49.15	160	12	TBC1D3, TBC1D3E, MRPL45, GPR179, SOCS7, C17orf96, MLLT6, CISD3, PCGF2, PSMB3, PIP4K2B, CCDC49, C17orf98, RPL23, LASP1, FBXO47, PLXDC1, CACNB1, RPL19, STAC2, FBXL20, MED1, CRKRS, NEUROD2, PPP1R1B, STARD3, TCAP, PNMT, PERLD1, ERBB2, C17orf37, GRB7, IKZF3, ZPBP2, GSDMB, ORMDL3, GSDMA, PSMD3, CSF3, MED24, THRA, NR1D1, MSL1, CASC3, RAPGEFL1, WIPF2, CDC6, RARA, GJD3, TOP2A, IGFBP4, TNS4, CCR7, SMARCE1, KRT222P, KRT24, KRT25, KRT26, KRT27, KRT28, KRT10, TMEM99, KRT12, KRT20, KRT23, KRT39, KRT40, KRTAP3-3, KRTAP3-2, KRTAP3-1, KRTAP1-5, KRTAP1-4, KRTAP1-3, KRTAP1-1, KRTAP2-2, KRTAP2-1, KRTAP2-4, KRTAP4-9, KRTAP4-8, KRTAP4-11, KRTAP4-12, KRTAP4-6, KRTAP4-5, KRTAP4-4, KRTAP4-3, KRTAP4-2, KRTAP9-2, KRTAP9-3, KRTAP9-8, KRTAP9-6, KRTAP9-7, KRTAP16-1, KRTAP17-1, KRT33A, KRT33B, KRT34, KRT31, KRT37, KRT38, KRT32, KRT35, KRT36, KRT13, KRT15, KRT19, KRT9, KRT14, KRT16, KRT17, EIF1, GAST, HAP1, JUP, FKBP10, NT5C3L, KLHL10, KLHL11, ACLY, TTC25, CNP, NKIRAS2, ZNF385C, DHX58, KAT2A, HSPB9, RAB5C, KCNH4, HCRT, GHDC, STAT5B, STAT5A, STAT3, PTRF, ATP6V0A1, NAGLU, HSD17BP1, HSD17B1, COASY, MLX, PSMC3IP, FAM134C, TUBG1, TUBG2, PLEKHH3, CCR10, CNTNAP1, EZH1, RAMP2, VPS25, WNK4, CCDC56, CNTD1, BECN1, PSME3, AOC2, AOC3, G6PC, AARSD1, RUNDC1, RPL27, IFI35, VAT1, RND2, BRCA1, NBR2, TMEM106A, ARL4D, DHX8, ETV4, MEOX1, SOST, DUSP3, MPP3, CD300LG, MPP2, C17orf88, PPY, PYY, NAGS, TMEM101, LSM12, G6PC3…	hsa-mir-152, hsa-mir-1203, hsa-mir-10a, hsa-mir-196a-1	V_0205_LC17492_Iafrate et al. (2004), V_0206_LC17502_Iafrate et al. (2004), V_0207_LC17522_Iafrate et al. (2004), V_0208_LC17538_Iafrate et al. (2004), V_0209_LC17565_Iafrate et al. (2004), V_0801_LC17522_Sharp et al. (2005), V_0802_LC17522_Sharp et al. (2005), V_0803_LC17522_Sharp et al. (2005), V_0804_LC17530_Sharp et al. (2005), V_2225_LC17522_Locke et al. (2006), V_2226_LC17522_Locke et al. (2006), V_2227_LC17522_Locke et al. (2006), V_2228_LC17522_Locke et al. (2006), V_2229_LC17530_Locke et al. (2006), V_5007_LC17508_Wong et al. (2007), V_5008_LC17512_Wong et al. (2007), V_5009_LC17516_Wong et al. (2007), V_5010_LC17522_Wong et al. (2007), V_5011_LC17522_Wong et al. (2007), V_5012_LC17522_Wong et al. (2007), V_5014_LC17522_Wong et al. (2007), V_5015_LC17522_Wong et al. (2007), V_5016_LC17543_Wong et al. (2007), V_5017_LC17552_Wong et al. (2007), V_5018_LC17559_Wong et al. (2007)
17	q22-q23.1	57.25	57.7	5	6	PRR11, C17orf71, GDPD1, YPEL2, DHX40, CLTC		V_2230_LC17608_Locke et al. (2006), V_5020_LC17608_Wong et al. (2007)
17	q23.2-q24.2	59.14	66.63	101	8	BCAS3, TBX2, C17orf82, TBX4, BRIP1, MED13, TBC1D3P2, EFCAB3, METTL2A, TLK2, MRC2, Mar-10, TANC2, CYB561, ACE, KCNH6, WDR68, CCDC44, MAP3K3, LIMD2, STRADA, CCDC47, DDX42, FTSJ3, PSMC5, SMARCD2, CSH2, GH2, CSH1, CSHL1, GH1, CD79B, C17orf72, ICAM2, ERN1, TEX2, POLG2, DDX5, CCDC45, SMURF2, PLEKHM1P, LRRC37A3, GNA13, RGS9, AXIN2, CCDC46, APOH, PRKCA, CACNG5, CACNG4, CACNG1, HELZ, PSMD12, PITPNC1, NOL11, BPTF, C17orf58, KPNA2, AMZ2, ARSG, SLC16A6, WIPI1, PRKAR1A, FAM20A	hsa-mir-633, hsa-mir-634, hsa-mir-548d-2, hsa-mir-635	V_0210_LC17626_Iafrate et al. (2004), V_0211_LC17666_Iafrate et al. (2004), V_0806_LC17642_Sharp et al. (2005), V_2231_LC17631_Locke et al. (2006), V_2232_LC17640_Locke et al. (2006), V_5022_LC17631_Wong et al. (2007), V_5023_LC17631_Wong et al. (2007), V_5024_LC17631_Wong et al. (2007), V_5026_LC17636_Wong et al. (2007), V_5027_LC17640_Wong et al. (2007)
17	q24.3-q25.3	69.99	81.02	136	28	SOX9, SLC39A11, SSTR2, COG1, FAM104A, C17orf80, CPSF4L, CDC42EP4, SDK2, RPL38, TTYH2, DNAI2, KIF19, BTBD17, GPRC5C, CD300A, CD300LB, CD300C, CD300LD, C17orf77, CD300E, RAB37, CD300LF, SLC9A3R1, NAT9, TMEM104, GRIN2C, FDXR, FADS6, USH1G, OTOP2, OTOP3, C17orf28, CDR2L, ICT1, ATP5H, KCTD2, SLC16A5, ARMC7, NT5C, HN1, SUMO2, NUP85, GGA3, MRPS7, MIF4GD, SLC25A19, GRB2, KIAA0195, CASKIN2, TSEN54, LLGL2, MYO15B, MYO15B, RECQL5, SAP30BP, ITGB4, GALK1, H3F3B, UNK, UNC13D, WBP2, TRIM47, TRIM65, MRPL38, FBF1, ACOX1, CDK3, EVPL, SRP68, GALR2, ZACN, EXOC7, FOXJ1, RNF157, FAM100B, QRICH2, PRPSAP1, SPHK1, UBE2O, AANAT, RHBDF2, CYGB, PRCD, SNORD1C, ST6GALNAC2, ST6GALNAC1, MXRA7, JMJD6, C17orf95, SFRS2, MFSD11, MGAT5B, SEC14L1, TNRC6C, TMC6, TMC8, C17orf99, SYNGR2, TK1, AFMID, BIRC5, SOCS3, PGS1, DNAH17, CYTH1, USP36, TIMP2, LGALS3BP, CANT1, C1QTNF1, ENGASE, ENPP7, CBX2, CBX8, CBX4, TBC1D16, CCDC40, GAA, EIF4A3, CARD14, SGSH, SLC26A11, KIAA1618, RNF213, NPTX1, CHMP6, BAIAP2, AATK, AZI1, C17orf56, C17orf89, SLC38A10, C17orf55, TMEM105, BAHCC1, ACTG1, FSCN2, C17orf70, NPLOC4, TSPAN10, PDE6G, C17orf90, CCDC137, ARL16, HGS, MRPL12, SLC25A10, GCGR, DYSFIP1, P4HB, ARHGDIA, THOC4, ANAPC11, NPB, PCYT2, SIRT7, MAFG, PYCR1, MYADML2, NOTUM, ASPSCR1, STRA13, LRRC45, RAC3, DCXR, RFNG, GPS1, DUS1L, FASN, CCDC57, SLC16A3, CSNK1D, CD7, SECTM1, TEX19, UTS2R, C17orf101, HEXDC, C17orf62, NARF, FOXK2, WDR45L, RAB40B, FN3KRP, FN3K, TBCD, ZNF750, B3GNTL1	hsa-mir-636, hsa-mir-657, hsa-mir-338, hsa-mir-1250	V_0212_LC17741_Iafrate et al. (2004), V_0213_LC17753_Iafrate et al. (2004), V_0807_LC17750_Sharp et al. (2005), V_2233_LC17750_Locke et al. (2006), V_2234_LC17753_Locke et al. (2006), V_2235_LC17756_Locke et al. (2006), V_4327_LC17763_Wong et al. (2007), V_5030_LC17713_Wong et al. (2007), V_5031_LC17717_Wong et al. (2007), V_5032_LC17720_Wong et al. (2007), V_5033_LC17737_Wong et al. (2007), V_5034_LC17743_Wong et al. (2007), V_5035_LC17750_Wong et al. (2007), V_5036_LC17763_Wong et al. (2007), V_5039_LC17763_Wong et al. (2007), V_5040_LC17763_Wong et al. (2007), V_5041_LC17763_Wong et al. (2007), V_5042_LC17763_Wong et al. (2007), V_5043_LC17763_Wong et al. (2007)
18	p11.21	12.57	13.14	7	5	SPIRE1, CEP76, PSMG2, PTPN2, SEH1L, CEP192		
18	q12.1	28.56	28.95	4	5	DSC3, DSC2, DSC1, DSG1		
18	q12.3-q21.1	41.17	45.02	39	38	SETBP1, SLC14A2, SLC14A1, SIGLEC15, KIAA1632, PSTPIP2, ATP5A1, HAUS1, C18orf25, RNF165, LOXHD1, ST8SIA5, PIAS2, KATNAL2, TCEB3CL2, TCEB3CL, TCEB3C, TCEB3B, HDHD2, IER3IP1		V_5054_LC18222_Wong et al. (2007), V_5055_LC18222_Wong et al. (2007), V_5056_LC18250_Wong et al. (2007)
18	q21.33-q22.1	59.2	62.46	34	6	CDH20, RNF152, KIAA1468, TNFRSF11A, ZCCHC2, PHLPP, BCL2, KDSR, VPS4B, SERPINB5, SERPINB12, SERPINB13, SERPINB4, SERPINB3, SERPINB11, SERPINB7, SERPINB10, HMSD, SERPINB8		V_5059_LC18395_Wong et al. (2007), V_5060_LC18434_Wong et al. (2007)
18	q22.1	63.22	64.1	12	6	CDH7		
18	q22.3	72.07	72.99	10	5	C18orf51, CNDP2, CNDP1, ZNF407, C18orf33, ZADH2, TSHZ1		
18	q23	75.79	77.88	29	16	SALL3, ATP9B, NFATC1, CTDP1, KCNG2, PQLC1, TXNL4A, C18orf22, ADNP2		
19	p13.3-p12	0.12	20.51	252	30	PPAP2C, MIER2, THEG, FAM148C, SHC2, ODF3L2, MADCAM1, C19orf20, CDC34, GZMM, BSG, HCN2, POLRMT, FGF22, RNF126, FSTL3, PRSSL1, PALM, C19orf21, PTBP1, AZU1, PRTN3, ELANE, CFD, MED16, C19orf22, KISS1R, ARID3A, WDR18, GRIN3B, C19orf6, CNN2, ABCA7, HMHA1, POLR2E, GPX4, SBNO2, STK11, C19orf26, ATP5D, MIDN, C19orf23, CIRBP, C19orf24, MUM1, EFNA2, NDUFS7, GAMT, DAZAP1, RPS15, APC2, C19orf25, PCSK4, REEP6, ADAMTSL5, PLK5P, MEX3D, MBD3, UQCR, TCF3, ONECUT3, ATP8B3, REXO1, KLF16, FAM108A1, SCAMP4, ADAT3, CSNK1G2, C19orf34, BTBD2, MKNK2, MOBKL2A, C19orf36, AP3D1, DOT1L, PLEKHJ1, SF3A2, AMH, JSRP1, OAZ1, C19orf35, LINGO3, LSM7, TMPRSS9, TIMM13, LMNB2, GADD45B, DIRAS1, SLC39A3, SGTA, THOP1, ZNF554, ZNF555, ZNF556, ZNF77, ZNF57, TLE6, AES, GNA11, GNA15, S1PR4, NCLN, BRUNOL5, NFIC, DOHH, RAX2, FZR1, C19orf28, C19orf71, HMG20B, GIPC3, C19orf64, TBXA2R, C19orf29OS, PIP5K1C, TJP3, APBA3, MRPL54, MATK, ZFR2, ATCAY, ITGB1BP3, DAPK3, EEF2, PIAS4, ZBTB7A, MAP2K2, CREB3L3, SIRT6, ANKRD24, EBI3, CCDC94, SHD, TMIGD2, FSD1, STAP2, MPND, SH3GL1, CHAF1A, UBXN6, KIAA1881, LRG1, SEMA6B, TNFAIP8L1, C19orf10, FEM1A, TICAM1, M6PRBP1, ARRDC5, C19orf31, KDM4B, PTPRS, ZNRF4, SAFB2, SAFB, C19orf70, HSD11B1L, RPL36, LONP1, TMEM146, DUS3L, NRTN, FUT6, FUT3, FUT5, NDUFA11, CAPS, RANBP3, RFX2, ACSBG2, MLLT1, ACER1, CLPP, ALKBH7, PSPN, GTF2F1, KHSRP, SLC25A41, SLC25A23, CRB3, DENND1C, TUBB4, TNFSF9, CD70, TNFSF14, C3, GPR108, TRIP10, SH2D3A, VAV1, EMR1, EMR4P, MBD3L2, ZNF557, INSR, ARHGEF18, PEX11G, C19orf45, ZNF358, MCOLN1, PNPLA6, KIAA1543, XAB2, PCP2, STXBP2, RETN, C19orf59, TRAPPC5, FCER2, CLEC4G…	hsa-mir-1909, hsa-mir-1227, hsa-mir-637, hsa-mir-7-3, hsa-mir-220b, hsa-mir-1181, hsa-mir-1238, hsa-mir-638, hsa-mir-199a-1, hsa-mir-24-2, hsa-mir-27a, hsa-mir-23a, hsa-mir-181c, hsa-mir-181d, hsa-mir-639, hsa-mir-1470, hsa-mir-640	V_0220_LC18794_Iafrate et al. (2004), V_0808_LC18794_Sharp et al. (2005), V_2237_LC18671_Locke et al. (2006), V_2238_LC18783_Locke et al. (2006), V_2239_LC18794_Locke et al. (2006), V_2240_LC18794_Locke et al. (2006), V_4400_LC18834_Wong et al. (2007), V_5065_LC18671_Wong et al. (2007), V_5066_LC18671_Wong et al. (2007), V_5067_LC18671_Wong et al. (2007), V_5068_LC18671_Wong et al. (2007), V_5069_LC18671_Wong et al. (2007), V_5070_LC18730_Wong et al. (2007), V_5071_LC18730_Wong et al. (2007), V_5072_LC18736_Wong et al. (2007), V_5073_LC18746_Wong et al. (2007), V_5074_LC18749_Wong et al. (2007), V_5075_LC18752_Wong et al. (2007), V_5076_LC18770_Wong et al. (2007), V_5077_LC18773_Wong et al. (2007), V_5078_LC18783_Wong et al. (2007), V_5079_LC18794_Wong et al. (2007), V_5080_LC18794_Wong et al. (2007), V_5081_LC18794_Wong et al. (2007), V_5082_LC18794_Wong et al. (2007), V_5083_LC18794_Wong et al. (2007), V_5084_LC18813_Wong et al. (2007), V_5085_LC18818_Wong et al. (2007), V_5086_LC18821_Wong et al. (2007), V_5087_LC18821_Wong et al. (2007), V_5088_LC18841_Wong et al. (2007), V_5089_LC18844_Wong et al. (2007), V_5090_LC18847_Wong et al. (2007), V_5091_LC18881_Wong et al. (2007), V_5092_LC18883_Wong et al. (2007), V_5093_LC18883_Wong et al. (2007)
19	q13.11-	33.38	43.1	122	21	CCDC123, C19orf40, RHPN2, GPATCH1, WDR88, LRP3, SLC7A10, CEBPG, PEPD, CHST8, KCTD15, LSM14A,	hsa-mir-641	V_5097_LC18975_Wong et al. (2007), V_5098_LC18976_Wong et al. (2007), V_5099_LC18991_Wong et al.

	q13.2					KIAA0355, GPI, PDCD2L, UBA2, WTIP, SCGBL, ZNF181, ZNF599, ZNF30, ZNF792, GRAMD1A, SCN1B, HPN, FXYD3, LGI4, FXYD1, FXYD7, FXYD5, FAM187B, LSR, USF2, HAMP, MAG, CD22, FFAR1, FFAR3, FFAR2, KRTDAP, DMKN, GAPDHS, TMEM147, ATP4A, HAUS5, RBM42, ETV2, COX6B1, UPK1A, ZBTB32, TMEM149, U2AF1L4, PSENEN, LIN37, HSPB6, C19orf55, SNX26, PRODH2, KIRREL2, APLP1, NFKBID, HCST, TYROBP, LRFN3, C19orf46, CLIP3, THAP8, WDR62, POLR2I, TBCB, CAPNS1, COX7A1, ZNF565, ZNF146, ZFP14, ZFP82, ZNF566, ZNF529, ZNF382, ZNF461, ZNF567, ZNF790, ZNF345, ZNF568, ZNF420, ZNF585A, ZNF585B, ZNF383, ZNF527, ZNF569, ZNF570, ZNF793, ZNF540, ZNF571, ZFP30, ZNF781, ZNF607, ZNF573, WDR87, SIPA1L3, DPF1, PPP1R14A, SPINT2, C19orf33, YIF1B, KCNK6, C19orf15, PSMD8, GGN, SPRED3, FAM98C, RASGRP4, RYR1, MAP4K1, EIF3K, ACTN4, CAPN12, LGALS7, LGALS7B, LGALS4, ECH1, HNRNPL, RINL, SIRT2, NFKBIB, FBXO17, MRPS12, FBXO27, PAK4, NCCRP1, SYCN, IL28B, IL28A, IL29, LRFN1, GMFG, SAMD4B, PAF1, MED29, ZFP36, PLEKHG2, RPS16, SUPT5H, TIMM50, DLL3, EID2B, EID2, LGALS13, LGALS14, CLC, LEUTX…		(2007)
19	q13.31-q13.41	43.78	51.62	103	23	CD177, CD177P, TEX101, LYPD3, PHLDB3, ETHE1, ZNF575, XRCC1, IRGQ, ZNF576, ZNF428, CADM4, PLAUR, IRGC, C19orf61, ZNF221, KCNN4, LYPD5, ZNF404, ZNF45, ZNF155, ZNF230, ZNF223, ZNF284, ZNF224, ZNF227, ZNF233, ZNF235, ZFP112, ZNF285A, ZNF229, ZNF180, CEACAM20, PVR, CEACAM19, CEACAM16, BCL3, CBLC, BCAM, PVRL2, TOMM40, APOE, APOC1, APOC4, APOC2, CLPTM1, RELB, SFRS16, ZNF296, GEMIN7, LRRC68, NKPD1, TRAPPC6A, BLOC1S3, EXOC3L2, MARK4, CKM, KLC3, ERCC2, PPP1R13L, CD3EAP, ERCC1, FOSB, RTN2, VASP, OPA3, GPR4, EML2, GIPR, SNRPD2, QPCTL, FBXO46, SIX5, DMPK, DMWD, RSHL1, SYMPK, FOXA3, IRF2BP1, MYPOP, NANOS2, NOVA2, CCDC61, PGLYRP1, IGFL4, IGFL3, IGFL2, HIF3A, PPP5C, CCDC8, PNMAL1, PNMAL2, CALM3, PTGIR, GNG8, DACT3, PRKD2, STRN4, FKRP, SLC1A5, AP2S1, GRLF1, NPAS1, TMEM160, ZC3H4, SAE1, BBC3, CCDC9, C5AR1, GPR77, DHX34, MEIS3, SLC8A2, KPTN, NAPA, ZNF541, GLTSCR1, EHD2, GLTSCR2, SEPW1, TPRX1, CRX, SULT2A1, BSPH1…	hsa-mir-330, hsa-mir-642, hsa-mir-769, hsa-mir-220c, hsa-mir-150	V_0221_LC19039_Iafrate et al. (2004), V_2243_LC19026_Locke et al. (2006), V_2244_LC19026_Locke et al. (2006), V_2245_LC19036_Locke et al. (2006), V_5100_LC19016_Wong et al. (2007), V_5101_LC19026_Wong et al. (2007), V_5102_LC19026_Wong et al. (2007), V_5103_LC19048_Wong et al. (2007)
19	q13.42-q13.43	53.96	59.08	65	14	ZNF761, ZNF813, ZNF331, DPRX, NLRP12, MYADM, PRKCG, CACNG7, CACNG8, CACNG6, VSTM1, NDUFA3, OSCAR, TFPT, PRPF31, CNOT3, LENG1, TMC4, MBOAT7, TSEN34, RPS9, LILRB3, LILRB5, LILRB2, LILRA3, LILRA5, LILRA4, LAIR1, TTYH1, LENG8, LENG9, CDC42EP5, LAIR2, KIR3DX1, LILRB1, LILRA1, LILRB4, KIR2DL4, KIR2DL1, KIR3DL1, KIR2DS4, FCAR, NCR1, NLRP7, NLRP2, GP6, RDH13, EPS8L1, PPP1R12C, TNNT1, TNNI3, C19orf51, SYT5, PTPRH, TMEM86B, HSPBP1, BRSK1, TMEM224, SUV420H2, COX6B2, FAM71E2, IL11, TMEM190, RPL28, UBE2S, ISOC2, ZNF628, NAT14, SBK2, ZNF579, FIZ1, ZNF524, ZNF784, ZNF580, ZNF581, CCDC106, U2AF2, EPN1, NLRP9, NLRP11, NLRP4, NLRP13, NLRP8, NLRP5, ZNF787, ZNF444, GALP, ZSCAN5B, ZSCAN5C, ZSCAN5A, ZNF542, ZNF582, ZNF583, ZNF667, ZNF471, ZFP28, ZNF470, ZNF71, ZNF835, PEG3, USP29, ZIM3, DUXA, ZNF264, AURKC, ZNF805, ZNF460, ZNF543, ZNF304, ZNF547, ZNF548, ZNF17, ZNF749, VN1R1, ZNF772, ZNF419, ZNF773, ZNF549, ZNF550, ZNF416, ZIK1, ZNF530, ZNF134, ZNF211, ZSCAN4, ZNF551, ZNF154, ZNF671, ZNF776, ZNF586, ZNF418, ZNF552, ZNF587, ZNF814, ZNF417, ZNF256, C19orf18, ZNF606, ZSCAN1, ZNF135, ZSCAN18, ZNF329, ZNF274, ZNF544, ZNF8, ZSCAN22, A1BG, ZNF497, ZNF837, RPS5, ZNF324B, ZNF132, ZNF324, ZNF446, SLC27A5, ZBTB45, TRIM28, CHMP2A, UBE2M, MZF1	hsa-mir-512-1, hsa-mir-512-1, hsa-mir-1323, hsa-mir-498, hsa-mir-520e, hsa-mir-515-1, hsa-mir-519e, hsa-mir-520f, hsa-mir-515-1, hsa-mir-519c, hsa-mir-1283-1, hsa-mir-520a, hsa-mir-526b, hsa-mir-519b, hsa-mir-525, hsa-mir-523, hsa-mir-518f, hsa-mir-520b, hsa-mir-518b, hsa-mir-526a-1, hsa-mir-520c, hsa-mir-518c, hsa-mir-524, hsa-mir-517a, hsa-mir-519d, hsa-mir-521-2, hsa-mir-520d, hsa-mir-517b, hsa-mir-520g, hsa-mir-516b-2…	V_2246_LC19081_Locke et al. (2006), V_2247_LC19092_Locke et al. (2006), V_5107_LC19073_Wong et al. (2007), V_5108_LC19073_Wong et al. (2007), V_5109_LC19078_Wong et al. (2007), V_5110_LC19081_Wong et al. (2007), V_5111_LC19081_Wong et al. (2007), V_5112_LC19081_Wong et al. (2007), V_5113_LC19081_Wong et al. (2007), V_5114_LC19090_Wong et al. (2007), V_5115_LC19131_Wong et al. (2007)
20	p12.2	10.44	11.05	6	7	C20orf94, JAG1, C20orf187		
20	p11.21	23.23	23.64	3	5	NXT1, GZF1, NAPB, CSTL1, CST11, CST8, CST9L, CST9, CST3		
20	q11.21	29.83	31.01	16	11	DEFB115, DEFB116, DEFB117, DEFB118, DEFB119, DEFB123, DEFB124, REM1, HM13, ID1, COX4I2, BCL2L1, TPX2, MYLK2, FOXS1, DUSP15, TTLL9, PDRG1, XKR7, C20orf160, HCK, TM9SF4, PLAGL2, POFUT1, KIF3B, ASXL1	hsa-mir-1825	V_5132_LC19553_Wong et al. (2007), V_5133_LC19567_Wong et al. (2007)
20	q11.21	31.5	31.89	3	5	EFCAB8, SPAG4L, BPIL1, BPIL3, C20orf185, C20orf186, C20orf70, C20orf71, PLUNC, C20orf114		
20	q11.21-q12	31.92	37.81	75	7	CDK5RAP1, SNTA1, CBFA2T2, NECAB3, C20orf144, C20orf134, E2F1, PXMP4, ZNF341, CHMP4B, RALY, EIF2S2, AHCY, ASIP, ITCH, DYNLRB1, MAP1LC3A, PIGU, TP53INP2, NCOA6, GGT7, ACSS2, GSS, MYH7B, TRPC4AP, EDEM2, PROCR, EIF6, MMP24, FAM83C, UQCC, GDF5OS, GDF5, CEP250, C20orf173, ERGIC3, SPAG4, CPNE1, ROMO1, RBM39, PHF20, SCAND1, C20orf152, EPB41L1, C20orf4, DLGAP4, MYL9, TGIF2, C20orf24, SLA2, NDRG3, DSN1, C20orf117, C20orf118, SAMHD1, RBL1, C20orf132, RPN2, GHRH, MANBAL, SRC, BLCAP, NNAT, CTNNBL1, VSTM2L, KIAA0406, RPRD1B, TGM2, KIAA1755, BPI, LBP, KIAA1219, ADIG, C20orf95, SLC32A1, ACTR5, PPP1R16B, FAM83D, DHX35	hsa-mir-644, hsa-mir-499, hsa-mir-1289-1	V_5134_LC19585_Wong et al. (2007), V_5135_LC19601_Wong et al. (2007), V_5136_LC19617_Wong et al. (2007)
20	q13.12	43.02	44.57	19	5	HNF4A, C20orf62, TTPAL, SERINC3, PKIG, ADA, WISP2, KCNK15, RIMS4, YWHAB, PABPC1L, TOMM34, STK4, KCNS1, WFDC5, WFDC12, PI3, SEMG1, SEMG2, SLPI, MATN4, RBPJL, SDC4, SYS1, TP53TG5, PIGT, WFDC2, SPINT3, WFDC6, WFDC8, WFDC9, WFDC10A, WFDC11, WFDC10B, WFDC13, SPINT4, C20orf168, WFDC3, DNTTIP1, UBE2C, TNNC2, SNX21, ACOT8, ZSWIM3, ZSWIM1, C20orf165, NEURL2, CTSA, PLTP, PCIF1		
20	q13.12	45.21	46.05	9	5	SLC13A3, TP53RK, SLC2A10, EYA2, ZMYND8		V_2251_LC19741_Locke et al. (2006), V_5139_LC19754_Wong et al. (2007)
20	q13.13	46.68	49.72	38	9	PREX1, ARFGEF2, CSE1L, STAU1, DDX27, ZNFX1, KCNB1, PTGIS, B4GALT5, SLC9A8, SPATA2, RNF114, SNAI1, TMEM189, CEBPB, PTPN1, FAM65C, PARD6B, BCAS4, ADNP, DPM1, MOCS3, KCNG1	hsa-mir-645, hsa-mir-1302-5	V_5140_LC19784_Wong et al. (2007), V_5141_LC19791_Wong et al. (2007)
20	q13.2	51.95	53.09	15	7	TSHZ2, ZNF217, BCAS1, CYP24A1, PFDN4, DOK5		
20	q13.33	58.67	59.04	3	5		hsa-mir-646	
20	q13.33	59.73	62.96	40	27	CDH4, TAF4, LSM14B, PSMA7, SS18L1, GTPBP5, HRH3, OSBPL2, ADRM1, LAMA5, RPS21, CABLES2, C20orf151, GATA5, C20orf166, SLCO4A1, C20orf90, NTSR1, C20orf20, OGFR, COL9A3, TCFL5, DIDO1, C20orf11, SLC17A9, BHLHE23, YTHDF1, BIRC7, NKAIN4, ARFGAP1, COL20A1, CHRNA4, KCNQ2, EEF1A2, C20orf149, PTK6, SRMS, C20orf195, GMEB2, STMN3, RTEL1, ARFRP1, ZGPAT, LIME1, SLC2A4RG, ZBTB46, C20orf181, TPD52L2, C20orf135, DNAJC5, UCKL1, UCKL1OS, ZNF512B, SAMD10, PRPF6, SOX18, TCEA2, RGS19, OPRL1, C20orf201, NPBWR2, MYT1, PCMTD2	hsa-mir-1257, hsa-mir-1-1, hsa-mir-133a-2, hsa-mir-124-3, hsa-mir-941-1, hsa-mir-941-1, hsa-mir-941-1, hsa-mir-941-1, hsa-mir-1914, hsa-mir-647	V_2252_LC19985_Locke et al. (2006), V_5144_LC19966_Wong et al. (2007), V_5145_LC19985_Wong et al. (2007), V_5146_LC19985_Wong et al. (2007), V_5147_LC19985_Wong et al. (2007), V_5148_LC19985_Wong et al. (2007), V_5149_LC19985_Wong et al. (2007), V_5150_LC19985_Wong et al. (2007)
21	q22.3	43.41	48.1	65	24	ZNF295, UMODL1, C21orf128, ABCG1, TFF3, TFF2, TFF1, TMPRSS3, UBASH3A, RSPH1, SLC37A1, PDE9A, WDR4, NDUFV3, PKNOX1, CBS, U2AF1, CRYAA, C21orf136, SIK1, HSF2BP, RRP1B, PDXK, CSTB, RRP1, AGPAT3, TRAPPC10, C21orf33, C21orf32, ICOSLG, DNMT3L, AIRE, PFKL, C21orf2, TRPM2, LRRC3, C21orf30, C21orf29, C21orf90, KRTAP10-1, KRTAP10-2, KRTAP10-3, KRTAP10-4, KRTAP10-6, KRTAP10-7, KRTAP10-8, KRTAP10-9, KRTAP10-10, KRTAP10-11, KRTAP12-4, KRTAP12-2, KRTAP12-1, KRTAP10-12, UBE2G2, SUMO3, PTTG1IP, ITGB2, C21orf67, C21orf69, C21orf70, ADARB1, POFUT2, C21orf86, COL18A1, NCRNA00175, SLC19A1, PCBP3, COL6A1, COL6A2, FTCD, C21orf56, LSS, MCM3AP, C21orf57, C21orf58, PCNT, DIP2A, S100B, PRMT2		V_5162_LC20269_Wong et al. (2007), V_5163_LC20269_Wong et al. (2007)
22	q11.1	16.06	16.46	12	9	POTEH, OR11H1		

22	q11.1-q11.22	17.43	22.42	55	8	GAB4, IL17RA, CECR6, CECR5, CECR1, CECR2, SLC25A18, ATP6V1E1, BCL2L13, BID, C22orf37, MICAL3, PEX26, TUBA8, USP18, DGCR6, PRODH, DGCR2, DGCR14, TSSK2, GSC2, SLC25A1, CLTCL1, HIRA, MRPL40, UFD1L, CDC45L, CLDN5, RPL7AP70, Sep-05, GP1BB, TBX1, GNB1L, C22orf29, TXNRD2, COMT, ARVCF, C22orf25, DGCR8, TRMT2A, RANBP1, ZDHHC8, RTN4R, DGCR6L, GGTLC3, TMEM191B, RIMBP3, USP41, ZNF74, KLHL22, MED15, POM121L4P, TOP3B, SERPIND1, SNAP29, CRKL, AIFM3, LZTR1, THAP7, P2RX6, SLC7A4, POM121L7, GGT2, RIMBP3B, HIC2, RIMBP3C, UBE2L3, YDJC, CCDC116, SDF2L1, PPIL2, YPEL1, MAPK1, PPM1F, IGLV4-69	hsa-mir-648, hsa-mir-185, hsa-mir-1306, hsa-mir-1286, hsa-mir-649, hsa-mir-301b, hsa-mir-130b	V_0816_LC20342_Sharp et al. (2005), V_0817_LC20342_Sharp et al. (2005), V_0818_LC20342_Sharp et al. (2005), V_2030_LC20342_Urban et al (2006), V_2031_LC20342_Urban et al (2006), V_2034_LC20342_Urban et al (2006), V_2261_LC20342_Locke et al. (2006), V_2262_LC20342_Locke et al. (2006), V_2263_LC20342_Locke et al. (2006), V_2264_LC20342_Locke et al. (2006), V_2265_LC20342_Locke et al. (2006), V_2266_LC20342_Locke et al. (2006), V_2267_LC20342_Locke et al. (2006), V_2268_LC20342_Locke et al. (2006), V_5168_LC20342_Wong et al. (2007), V_5169_LC20342_Wong et al. (2007), V_5170_LC20342_Wong et al. (2007), V_5171_LC20342_Wong et al. (2007), V_5172_LC20342_Wong et al. (2007), V_5173_LC20342_Wong et al. (2007), V_5174_LC20342_Wong et al. (2007), V_5175_LC20342_Wong et al. (2007), V_5176_LC20342_Wong et al. (2007), V_5177_LC20342_Wong et al. (2007), V_5178_LC20342_Wong et al. (2007), V_5179_LC20381_Wong et al. (2007)
22	q12.1-q12.2	29.49	31.77	19	8	KREMEN1, EMID1, RHBDD3, EWSR1, GAS2L1, RASL10A, AP1B1, RFPL1, NEFH, THOC5, NIPSNAP1, NF2, CABP7, ZMAT5, ASCC2, MTMR3, HORMAD2, LIF, OSM, TBC1D10A, SF3A1, CCDC157, RNF215, SEC14L2, SEC14L3, SEC14L4, GAL3ST1, PES1, TCN2, SLC35E4, DUSP18, OSBP2, MORC2, TUG1, SMTN, INPP5J, PLA2G3, RNF185, LIMK2, PIK3IP1, PATZ1		V_0236_LC20439_Iafrate et al. (2004)
22	q12.3-q13.33	36.63	51.19	147	20	APOL2, APOL1, MYH9, TXN2, FOXRED2, EIF3D, CACNG2, RABL4, PVALB, NCF4, CSF2RB, C22orf33, TST, MPST, KCTD17, TMPRSS6, IL2RB, C1QTNF6, SSTR3, RAC2, CYTH4, ELFN2, MFNG, CARD10, CDC42EP1, LGALS2, GGA1, PDXP, LGALS1, NOL12, TRIOBP, H1F0, GCAT, GALR3, ANKRD54, EIF3L, MICALL1, C22orf23, POLR2F, SOX10, PICK1, SLC16A8, BAIAP2L2, PLA2G6, MAFF, TMEM184B, CSNK1E, KCNJ4, KDELR3, DDX17, DMC1, CBY1, TOMM22, JOSD1, GTPBP1, UNC84B, DNAL4, NPTXR, CBX6, APOBEC3A, APOBEC3D, APOBEC3F, APOBEC3H, CBX7, PDGFB, RPL3, SYNGR1, MAP3K7IP1, MGAT3, SMCR7L, ATF4, RPS19BP1, CACNA1I, ENTHD1, GRAP2, FAM83F, TNRC6B, SGSM3, MKL1, MCHR1, SLC25A17, ST13, XPNPEP3, DNAJB7, RBX1, EP300, L3MBTL2, CHADL, RANGAP1, ZC3H7B, TEF, TOB2, PHF5A, ACO2, POLR3H, CSDC2, PMM1, PPPDE2, XRCC6, NHP2L1, MEI1, CCDC134, SREBF2, TNFRSF13C, CENPM, Sep-03, WBP2NL, NAGA, FAM109B, C22orf32, NDUFA6, CYP2D6, CYP2D7P1, TCF20, NFAM1, SERHL, RRP7A, SERHL2, POLDIP3, CYB5R3, A4GALT, PACSIN2, TTLL1, BIK, MCAT, TSPO, TTLL12, SCUBE1, MPPED1, EFCAB6, SULT4A1, PNPLA5, PNPLA3, SAMM50, PARVB, PARVG, KIAA1644, LDOC1L, ARHGAP8, PHF21B, NUP50, C22orf9, UPK3A, FAM118A, SMC1B, RIBC2, FBLN1, ATXN10, WNT7B, C22orf26, PPARA, C22orf40, PKDREJ, TTC38, GTSE1, TRMU, CELSR1, GRAMD4, CERK, TBC1D22A, FAM19A5, C22orf34, BRD1, ZBED4, ALG12, CRELD2, PIM3, IL17REL, TTLL8, MLC1, MOV10L1, PANX2, TRABD, TUBGCP6, HDAC10, MAPK12, MAPK11, PLXNB2, FAM116B, SAPS2, SBF1, ADM2, MIOX, LMF2, NCAPH2, SCO2, TYMP, ODF3B, KLHDC7B, C22orf41, CPT1B, CHKB, MAPK8IP2, ARSA, SHANK3, ACR	hsa-mir-658, hsa-mir-659, hsa-mir-1281, hsa-mir-33a, hsa-mir-1249, hsa-let-7a-3, hsa-let-7b	V_0239_LC20651_Iafrate et al. (2004), V_2037_LC20505_Urban et al (2006), V_2038_LC20505_Urban et al (2006), V_5185_LC20500_Wong et al. (2007), V_5186_LC20500_Wong et al. (2007), V_5187_LC20514_Wong et al. (2007), V_5188_LC20524_Wong et al. (2007), V_5189_LC20524_Wong et al. (2007), V_5190_LC20580_Wong et al. (2007), V_5191_LC20603_Wong et al. (2007), V_5192_LC20651_Wong et al. (2007), V_5193_LC20651_Wong et al. (2007)
23	p22.33	0.63	3.11	23	10	CRLF2, CSF2RA, IL3RA, SLC25A6, ASMTL, P2RY8, SFRS17A, ASMT, DHRSX, ZBED1, CD99, XG, GYG2, ARSD, ARSE, ARSH, ARSF		
23	q27.1-q27.2	140.09	140.86	8	5	SPANXB1, LDOC1, SPANXC, SPANXA2, SPANXA1, SPANXD		V_0255_LC21142_Iafrate et al. (2004), V_0827_LC21138_Sharp et al. (2005), V_2282_LC21138_Locke et al. (2006)
23	q27.3	143.32	143.75	6	5			
23	q28	149.87	154.4	56	25	MTMR1, CD99L2, HMGB3, GPR50, VMA21, PASD1, PRRG3, FATE1, CNGA2, MAGEA4, GABRE, MAGEA10, GABRA3, GABRQ, MAGEA6, CSAG3, MAGEA2B, CSAG4, CSAG1, MAGEA2, CSAG2, MAGEA3, CETN2, NSDHL, ZNF185, PNMA5, PNMA3, PNMA6A, PNMA6B, MAGEA1, ZNF275, TREX2, HAUS7, BGN, ATP2B3, FAM58A, DUSP9, PNCK, SLC6A8, BCAP31, ABCD1, PLXNB3, SRPK3, IDH3G, SSR4, PDZD4, L1CAM, AVPR2, ARHGAP4, ARD1A, RENBP, HCFC1, TMEM187, IRAK1, MECP2, OPN1LW, TEX28P2, OPN1MW, TEX28P1, OPN1MW2, TEX28, TKTL1, FLNA, EMD, RPL10, DNASE1L1, TAZ, ATP6AP1, GDI1, FAM50A, PLXNA3, LAGE3, UBL4A, SLC10A3, FAM3A, G6PD, IKBKG, CXorf52, CTAG1A, CTAG1B, CXorf52B, CTAG2, GAB3, DKC1, MPP1, F8, H2AFB1, F8A1, FUNDC2, MTCP1NB, BRCC3	hsa-mir-224, hsa-mir-452, hsa-mir-105-1, hsa-mir-767, hsa-mir-105-2, hsa-mir-1184	
24	p11.2	2.71	3.26	8	8	RPS4Y1, ZFY		

Supplementary Table 6: Most frequent (in five or more cases) chromosomal losses observed in 50 papillary carcinomas.

Chromosome	Cytobands	Start (Mb)	End (Mb)	Number of BACs	Papillary carcinomas (n=50)	Genes	mi-RNAs	aCGH CNVs
1	p36.33-p36.31	0.01	6.27	62	21	WASH5P, OR4F5, OR4F29, OR4F16, SAMD11, NOC2L, KLHL17, PLEKHN1, C1orf170, HES4, ISG15, AGRN, C1orf159, TTLL10, TNFRSF18, TNFRSF4, SDF4, B3GALT6, FAM132A, UBE2J2, SCNN1D, ACAP3, PUSL1, CPSF3L, GLTPD1, TAS1R3, DVL1, MXRA8, AURKAIP1, CCNL2, MRPL20, VWA1, ATAD	hsa-mir-1302-2, hsa-mir-1977, hsa-mir-200b, hsa-mir-200a, hsa-mir-429, hsa-mir-551a	V_0001_LC0020_Iafrate et al. (2004), V_0002_LC0028_Iafrate et al. (2004), V_0675_LC0001_Sharp et al. (2005), V_2041_LC0001_Locke et al. (2006), V_2042_LC0028_Locke et al. (2006), V_4189_LC0001_Wong et al. (2007), V_4190_LC0001_Wong et al. (2007), V_4191_L
1	p36.31-p36.23	6.64	7.83	13	6	TAS1R1, ZBTB48, KLHL21, PHF13, THAP3, DNAJC11, CAMTA1, VAMP3		V_4203_LC0113_Wong et al. (2007)
1	p36.23	8.33	8.92	5	5	SLC45A1, RERE, ENO1		V_0003_LC0126_Iafrate et al. (2004)
1	p36.22	11.21	12.01	9	5	FRAP1, ANGPTL7, UBIAD1, PTCHD2, FBXO2, FBXO44, FBXO6, MAD2L2, C1orf187, AGTRAP, C1orf167, MTHFR, CLCN6, NPPA, NPPB, KIAA2013, PLOD1		
1	p36.22-p36.13	12.68	16.75	29	7	DHRS3, AADACL4, AADACL3, C1orf158, PRAMEF12, PRAMEF1, PRAMEF11, HNRNPCL1, PRAMEF2, PRAMEF4, PRAMEF10, PRAMEF7, PRAMEF22, PRAMEF3, PRAMEF5, PRAMEF8, PRAMEF9, PRAMEF13, PRAMEF18, PRAMEF16, PRAMEF21, PRAMEF15, PRAMEF14, PRAMEF19, PRAMEF17, PRAMEF20, LRRC38,		V_0004_LC0152_Iafrate et al. (2004), V_0677_LC0152_Sharp et al. (2005), V_4206_LC0165_Wong et al. (2007), V_4207_LC0177_Wong et al. (2007), V_4208_LC0177_Wong et al. (2007), V_4403_LC0152_Wong et al. (2007)
1	p36.13-p36.12	16.79	23.77	76	9	NBPF1, MSTP9, CROCC, MFAP2, ATP13A2, SDHB, PADI2, PADI1, PADI3, PADI4, PADI6, RCC2, ARHGEF10L, ACTL8, IGSF21, KLHDC7A, PAX7, TAS1R2, ALDH4A1, IFFO2, UBR4, KIAA0090, MRTO4, AKR7L, AKR7A3, AKR7A2, PQLC2, CAPZB, C1orf151, NBL1, HTR6, TMCO4, RNF186, OTUD3, PL	hsa-mir-1290, hsa-mir-1256	V_0005_LC0177_Iafrate et al. (2004), V_0679_LC0177_Sharp et al. (2005), V_2044_LC0177_Locke et al. (2006), V_2045_LC0219_Locke et al. (2006), V_2046_LC0230_Locke et al. (2006), V_4207_LC0177_Wong et al. (2007), V_4209_LC0177_Wong et al. (2007), V_4210_LC0
1	p36.11-p35.2	24.35	31.95	91	11	MYOM3, IL22RA1, IL28RA, GRHL3, C1orf201, NIPAL3, RCAN3, C1orf130, SRRM1, CLIC4, RUNX3, SYF2, C1orf63, RHD, TMEM50A, RHCE, TMEM57, LDLRAP1, MAN1C1, SEPN1, FAM54B, C1orf135, PAQR7, STMN1, PAFAH2, EXTL1, SLC30A2, TRIM63, PDIK1L, GRRP1, ZNF593, CNKSR1, CATSPE	hsa-mir-1976	V_0680_LC0248_Sharp et al. (2005), V_2047_LC0248_Locke et al. (2006), V_4217_LC0248_Wong et al. (2007), V_4218_LC0253_Wong et al. (2007)
1	p35.1-p34.3	33.96	35.27	16	8	CSMD2, C1orf94, GJB5, GJB4, GJB3, GJA4	hsa-mir-552	
1	p12-q21.1	119.84	145.08	39	33	HAO2, HSD3B2, HSD3B1, ZNF697, PHGDH, HMGCS2, REG4, ADAM30, NOTCH2, FAM72B, FCGR1B, PPIAL4G, FAM72D, SRGAP2P2, PPIAL4B, NBPF9, PDE4DIP		V_0683_LC0751_Sharp et al. (2005), V_0684_LC0752_Sharp et al. (2005), V_0685_LC0752_Sharp et al. (2005), V_2050_LC0752_Locke et al. (2006), V_4244_LC0743_Wong et al. (2007), V_4245_LC0743_Wong et al. (2007), V_4246_LC0743_Wong et al. (2007), V_4247_LC0752
2	p25.3	2.47	2.91	4	6			
2	p25.3	3.66	4.36	11	5	COLEC11, ALLC		
2	p24.1	22	23.93	19	6	KLHL29		
2	p21	45.89	46.29	3	5	PRKCE		
2	p16.3	48.83	52.64	36	7	STON1, LHCGR, FSHR, NRXN1		
2	p12	78.29	78.82	4	5			
2	p12-p11.2	78.89	85.18	70	8	REG3G, REG1B, REG1A, REG3A, CTNNA2, LRRTM1, SUCLG1, DNAH6, TMSB10		V_0020_LC1992_Iafrate et al. (2004), V_4290_LC1992_Wong et al. (2007)
2	p11.2	86.94	88.38	24	8	VPS24, RMND5A, CD8A, CD8B, RGPD1, PLGLB1, PLGLB2, RGPD2, KRCC1, SMYD1		V_4291_LC2035_Wong et al. (2007), V_4292_LC2035_Wong et al. (2007), V_4293_LC2035_Wong et al. (2007), V_4294_LC2035_Wong et al. (2007)
2	p11.2-q11.2	88.59	96.87	58	14	C2orf51, EIF2AK3, RPIA, IGKV2-19, IGKC, IGKV4-1, IGKV1-5, IGKV3D-15, TEKT4, MAL, MRPS5, ZNF514, ZNF2, PROM2, KCNIP3, FAHD2A, TRIM43, ADRA2B, ASTL, DUSP2, STARD7		V_2057_LC2046_Locke et al. (2006), V_2058_LC2046_Locke et al. (2006), V_4295_LC2046_Wong et al. (2007), V_4296_LC2046_Wong et al. (2007), V_4297_LC2046_Wong et al. (2007), V_4298_LC2046_Wong et al. (2007), V_4299_LC2057_Wong et al. (2007), V_4300_LC2064_W
2	q11.2	97.57	99.84	27	8	FAM178B, FAHD2B, ANKRD36B, COX5B, ACTR1B, ZAP70, TMEM131, VWA3B, CNGA3, INPP4A, C2orf64, UNC50, MGAT4A, C2orf55, TSGA10, MRPL30, LIPT1, MITD1		V_4301_LC2072_Wong et al. (2007)
2	q13	110.64	110.99	8	5	LIMS3, MALL, NPHP1		
2	q14.1	115.24	115.85	6	5	DPP10		
2	q14.1	117.09	117.93	9	6			
2	q14.2	119.17	120.41	12	5	EN1, MARCO, C1QL2, STEAP3, C2orf76, DBI, TMEM37, SCTR		
2	q14.2-q14.3	120.91	123.76	25	7	EPB41L5, RALB, INHBB, GLI2, TFCP2L1, CLASP1, MKI67IP, TSN		
2	q14.3	125.26	125.81	4	5	CNTNAP5		
2	q21.1-q21.2	132.28	132.99	9	8	CCDC74A, C2orf27A, C2orf27B, ZNF72, C21orf99		
2	q21.2-q23.3	134.29	150.67	174	8	MGAT5, TMEM163, ACMSD, CCNT2, YSK4, RAB3GAP1, ZRANB3, R3HDM1, UBXN4, LCT, MCM6, DARS, CXCR4, THSD7B, HNMT, SPOPL, NXPH2, LRP1B, KYNU, ARHGAP15, GTDC1, ZEB2, ACVR2A, ORC4L, MBD5, EPC2, KIF5C, LYPD6B, LYPD6	hsa-mir-128-1	V_4309_LC2319_Wong et al. (2007)
2	q23.3	151.33	151.64	3	5	RND3		V_4310_LC2333_Wong et al. (2007)
2	q37.2-q37.3	236.32	237.3	9	5	AGAP1, GBX2, ASB18, IQCA1		

2	q37.3	239.15	241.23	23	6	PER2, TRAF3IP1, ASB1, HDAC4, NDUFA10, OR6B2, PRR21, OR6B3, MYEOV2, OTOS		V_0031_LC2814_Iafrate et al. (2004), V_4330_LC2814_Wong et al. (2007)
4	p16.3-p16.1	3.39	6.24	32	8	RGS12, HGFAC, DOK7, LRPAP1, ADRA2C, OTOP1, TMEM128, LYAR, ZNF509, STX18, MSX1, CYTL1, STK32B, C4orf6, EVC2, EVC, CRMP1, C4orf50, JAKMIP1		V_4371_LC4159_Wong et al. (2007), V_4372_LC4159_Wong et al. (2007)
4	p16.1	8.52	9.85	12	8	GPR78, CPZ, HMX1, FAM90A2P, USP17, DEFB131, DRD5, SLC2A9	hsa-mir-548i-2	V_0698_LC4236_Sharp et al. (2005), V_0699_LC4236_Sharp et al. (2005), V_2068_LC4236_Locke et al. (2006), V_2069_LC4236_Locke et al. (2006), V_2070_LC4236_Locke et al. (2006), V_4376_LC4234_Wong et al. (2007), V_4377_LC4236_Wong et al. (2007), V_4378_LC423
4	p11-q12	49.06	53.53	17	6	DCUN1D4, LRRC66, SGCB, SPATA18, USP46		V_4394_LC4709_Wong et al. (2007), V_4395_LC4720_Wong et al. (2007), V_4396_LC4722_Wong et al. (2007), V_4397_LC4723_Wong et al. (2007)
4	q35.2	190.35	190.9	11	12	HSP90AA4P, FRG1		V_4424_LC6244_Wong et al. (2007), V_4425_LC6244_Wong et al. (2007)
6	p25.3	0.13	1.7	16	5	DUSP22, IRF4, EXOC2, HUS1B, FOXQ1, FOXF2, FOXC1, GMDS		V_0070_LC7931_Iafrate et al. (2004), V_0071_LC7931_Iafrate et al. (2004), V_4483_LC7931_Wong et al. (2007), V_4484_LC7948_Wong et al. (2007), V_0374_LC7931_Bejjani et al. (2005)
6	p25.1	5.42	6.34	11	7	FARS2, C6orf202, NRN1, F13A1		V_0072_LC7984_Iafrate et al. (2004)
7	q11.21	64.88	65.23	12	6			
7	q11.23	74.09	74.61	5	5	GTF2I, STAG3L2, NCF1, GTF2IRD2, PMS2L5, WBSCR16, GTF2IRD2B, NCF1C		V_4544_LC9609_Wong et al. (2007)
7	q11.23-q22.1	75.94	101.99	279	8	YWHAG, SRCRB4D, ZP3, UPK3B, POMZP3, PMS2L11, CCDC146, FGL2, PION, PTPN12, RSBN1L, TMEM60, PHTF2, MAGI2, GNAI1, CD36, GNAT3, SEMA3C, HGF, CACNA2D1, PCLO, SEMA3E, SEMA3A, SEMA3D, GRM3, KIAA1324L, DMTF1, C7orf23, CROT, ABCB4, ABCB1, RUNDC3B, SLC25A40, DBF4,	hsa-mir-1285-1, hsa-mir-653, hsa-mir-489, hsa-mir-591, hsa-mir-25, hsa-mir-93, hsa-mir-106b	V_0105_LC9667_Iafrate et al. (2004), V_0106_LC9682_Iafrate et al. (2004), V_0107_LC9766_Iafrate et al. (2004), V_0723_LC9631_Sharp et al. (2005), V_0724_LC9769_Sharp et al. (2005), V_2104_LC9753_Locke et al. (2006), V_2105_LC9769_Locke et al. (2006), V_45
7	q22.1-q32.1	102.2	128.02	250	7	POLR2J3, RASA4, POLR2J2, FAM185A, FBXL13, LRRC17, ARMC10, NAPEPLD, DPY19L2P2, PMPCB, DNAJC2, PSMC2, SLC26A5, RELN, ORC5L, LHFPL3, MLL5, SRPK2, PUS7, RINT1, EFCAB10, ATXN7L1, SYPL1, NAMPT, PIK3CG, PRKAR2B, HBP1, COG5, GPR22, DUS4L, BCAP29, SLC26A4, CBLL1,	hsa-mir-592, hsa-mir-593, hsa-mir-129-1	V_0108_LC9826_Iafrate et al. (2004), V_2106_LC9769_Locke et al. (2006), V_4554_LC9806_Wong et al. (2007), V_4555_LC9863_Wong et al. (2007), V_4556_LC9887_Wong et al. (2007), V_4557_LC9892_Wong et al. (2007), V_4558_LC9916_Wong et al. (2007)
7	q32.2-q36.3	129.39	159.12	344	10	NRF1, UBE2H, ZC3HC1, KLHDC10, TMEM209, C7orf45, CPA2, CPA4, CPA5, CPA1, TSGA14, MEST, COPG2, TSGA13, KLF14, MKLN1, PODXL, PLXNA4, CHCHD3, EXOC4, LRGUK, SLC35B4, AKR1B1, AKR1B10, BPGM, CALD1, AGBL3, TMEM140, C7orf49, WDR91, STRA8, CNOT4, NUP205, SLC13A4, F	hsa-mir-182, hsa-mir-96, hsa-mir-183, hsa-mir-335, hsa-mir-29a, hsa-mir-29b-1, hsa-mir-490, hsa-mir-548f-4, hsa-mir-1975, hsa-mir-671, hsa-mir-153-2, hsa-mir-595	V_0110_LC10016_Iafrate et al. (2004), V_0111_LC10099_Iafrate et al. (2004), V_0725_LC10016_Sharp et al. (2005), V_0726_LC10016_Sharp et al. (2005), V_0727_LC10049_Sharp et al. (2005), V_0728_LC10049_Sharp et al. (2005), V_0729_LC10082_Sharp et al. (2005),
8	p23.3-p12	0.05	35.65	359	17	OR4F21, ZNF596, FAM87A, FBXO25, C8orf42, ERICH1, C8orf68, CLN8, ARHGEF10, KBTBD11, MYOM2, CSMD1, MCPH1, ANGPT2, AGPAT5, XKR5, DEFB1, DEFA6, DEFA4, DEFA1, DEFT1P, DEFA3, DEFA5, FAM90A3, FAM90A13, FAM90A5, FAM90A20, DEFB108P2, DEFB103A, SPAG11B, DEFB104B, D	hsa-mir-596, hsa-mir-548i-3, hsa-mir-597, hsa-mir-124-1, hsa-mir-598, hsa-mir-383, hsa-mir-320a, hsa-mir-548h-4	V_0116_LC10436_Iafrate et al. (2004), V_0731_LC10225_Sharp et al. (2005), V_0732_LC10225_Sharp et al. (2005), V_0733_LC10380_Sharp et al. (2005), V_0734_LC10380_Sharp et al. (2005), V_0735_LC10380_Sharp et al. (2005), V_0736_LC10380_Sharp et al. (2005), V
8	q11.1	46.85	47.42	6	6			V_4590_LC10569_Wong et al. (2007)
9	p24.3	0.03	0.32	3	5	FAM138C, FOXD4, CBWD1, C9orf66, DOCK8		V_0125_LC11024_Iafrate et al. (2004)
9	p11.2-q21.11	38.57	71.51	77	31	ANKRD18A, C9orf122, CNTNAP3, FAM75A1, ZNF658B, FAM75A2, FAM74A1, FAM75A3, FAM74A3, ZNF658, FAM74A2, FAM75A4, FAM75A5, ANKRD20A2, CBWD7, FOXD4L2, ANKRD20A1, FAM75A6, CNTNAP3B, FAM27C, FAM27A, FAM27E2, FAM27E1, FAM27D1, FAM75A7, FAM27B, ANKRD20A3, FOXD4L6,	hsa-mir-1299	V_0742_LC11330_Sharp et al. (2005), V_0743_LC11344_Sharp et al. (2005), V_0744_LC11330_Sharp et al. (2005), V_0745_LC11330_Sharp et al. (2005), V_0746_LC11330_Sharp et al. (2005), V_0747_LC11330_Sharp et al. (2005), V_0748_LC11330_Sharp et al. (2005), V_0
9	q32-q33.2	117.57	122.86	53	10	TNFSF8, TNC, Dec-01, PAPPA, ASTN2, TRIM32, TLR4, DBC1		V_4653_LC11698_Wong et al. (2007)
10	p11.1-q11.21	38.44	42.9	7	7	HSD17B7P2		V_0763_LC12261_Sharp et al. (2005), V_2152_LC12261_Locke et al. (2006), V_4677_LC12257_Wong et al. (2007), V_4678_LC12257_Wong et al. (2007), V_4679_LC12257_Wong et al. (2007), V_4680_LC12257_Wong et al. (2007), V_4771_LC12261_Wong et al. (2007)
10	q11.22	46.18	49.55	36	9	FAM21C, AGAP4, PTPN20A, FRMPD2L2, FAM35B, SYT15, GPRIN2, ANXA8L1, PPYR1, FAM25B, BMS1P2, CTSLL7, FAM25HP, FAM21B, ASAH2C, BMS1P6, FAM25G, ANXA8, ZNF488, RBP3, GDF2, GDF10, PTPN20B, FRMPD2L1, CTGLF9P, FAM25C, BMS1P7, FRMPD2, MAPK8		V_0136_LC12274_Iafrate et al. (2004), V_0764_LC12274_Sharp et al. (2005), V_2153_LC12274_Locke et al. (2006), V_2154_LC12274_Locke et al. (2006), V_2155_LC12288_Locke et al. (2006), V_4681_LC12274_Wong et al. (2007), V_4682_LC12274_Wong et al. (2007), V_4
10	q11.22-q11.23	49.64	50.18	7	6	MAPK8, ARHGAP22, WDFY4, LRRC18		
10	q23.1-q23.2	87.21	88.12	7	6	GRID1	hsa-mir-346	
10	q25.1	106.28	107.24	9	5	SORCS3		
10	q26.2	130.04	130.43	3	5			
10	q26.3	130.66	133.92	34	8	MGMT, EBF3, GLRX3, TCERG1L, PPP2R2D, BNIP3		V_4716_LC12779_Wong et al. (2007), V_4717_LC12807_Wong et al. (2007)
11	p11.2-p11.12	48.9	49.54	6	6	UBTFL7, FOLH1, TYRL		
11	q13.4-q25	72.7	134.93	626	31	FCHSD2, P2RY2, P2RY6, ARHGEF17, RELT, FAM168A, RAB6A, MRPL48, CHCHD8, PAAF1, DNAJB13, UCP2, UCP3, C2CD3, PPME1, P4HA3, PGM2L1, KCNE3, POLD3, CHRDL2, RNF169, XRRA1, SPCS2, NEU3, OR2AT4, SLCO2B1, ARRB1, RPS3, KLHL35, GDPD5, SERPINH1, MAP6, MOGAT2, DGAT2, UV	hsa-mir-326, hsa-mir-708, hsa-mir-1261, hsa-mir-1304, hsa-mir-548l, hsa-mir-34b, hsa-mir-34c, hsa-mir-125b-1, hsa-let-7a-2, hsa-mir-100	V_0151_LC13373_Iafrate et al. (2004), V_0152_LC13403_Iafrate et al. (2004), V_0154_LC13475_Iafrate et al. (2004), V_0155_LC13522_Iafrate et al. (2004), V_0156_LC13530_Iafrate et al. (2004), V_0158_LC13592_Iafrate et al. (2004), V_0159_LC13605_Iafrate et a
12	p13.31	5.45	6.05	8	6	NTF3, ANO2		

12	q24.31-q24.33	124.89	132.29	81	8	NCOR2, SCARB1, UBC, DHX37, BRI3BP, AACS, TMEM132B, SLC15A4, GLT1D1, TMEM132D, FZD10, PIWIL1, RIMBP2, STX2, RAN, GPR133, SFRS8		V_0769_LC14595_Sharp et al. (2005), V_2172_LC14595_Locke et al. (2006), V_4404_LC14595_Wong et al. (2007), V_4793_LC14538_Wong et al. (2007), V_4794_LC14556_Wong et al. (2007), V_4795_LC14556_Wong et al. (2007), V_4796_LC14595_Wong et al. (2007)
13	q12.11-q12.13	19.02	27.47	81	6	TUBA3C, TPTE2, MPHOSPH8, PSPC1, ZMYM5, ZMYM2, GJA3, GJB2, GJB6, CRYL1, IFT88, IL17D, N6AMT2, XPO4, LATS2, SAP18, C13orf3, MRP63, ZDHHC20, EFHA1, FGF9, SGCG, SACS, TNFRSF19, MIPEP, SPATA13, PARP4, ATP12A, RNF17, CENPJ, TPTE2P1, PABPC3, FAM123A, MTMR6, NUPL		V_0167_LC14662_lafrate et al. (2004), V_4797_LC14674_Wong et al. (2007), V_4899_LC14682_Wong et al. (2007)
13	q12.3	29.26	30.41	10	6	SLC46A3, KIAA0774, SLC7A1, UBL3		
13	q12.3-q21.33	31.05	70.16	430	9	HMGB1, USPL1, ALOX5AP, C13orf33, C13orf26, HSPH1, B3GALTL, RXFP2, FRY, BRCA2, N4BP2L1, N4BP2L2, PDS5B, KL, STARD13, RFC3, NBEA, MAB21L1, DCLK1, C13orf38, SPG20, CCNA1, C13orf36, RFXAP, SMAD9, ALG5, EXOSC8, FAM48A, CSNK1A1L, POSTN, TRPC4, UFM1, FREM2, STOM	hsa-mir-320d-1, hsa-mir-621, hsa-mir-16-1, hsa-mir-15a	V_0168_LC14853_lafrate et al. (2004), V_0169_LC14892_lafrate et al. (2004), V_0170_LC14945_lafrate et al. (2004), V_2173_LC14935_Locke et al. (2006), V_4480_LC14964_Wong et al. (2007), V_4798_LC14797_Wong et al. (2007), V_4799_LC14805_Wong et al. (2007),
13	q21.33-q31.1	72.33	85.19	132	9	DACH1, C13orf37, C13orf34, DIS3, PIBF1, KLF5, KLF12, TBC1D4, COMMD6, UCHL3, LMO7, KCTD12, IRG1, CLN5, FBXL3, MYCBP2, SCEL, SLAIN1, EDNRB, POU4F1, RNF219, RBM26, NDFIP2, SPRY2, PTMAP5, SLITRK1		V_0171_LC15037_lafrate et al. (2004), V_0172_LC15055_lafrate et al. (2004), V_4812_LC15022_Wong et al. (2007), V_4813_LC15063_Wong et al. (2007)
13	q31.1	86.38	87.22	8	5			
13	q31.1-q31.2	87.46	87.91	4	5			
13	q31.2-q34	89.41	115.07	260	9	GPC5, GPC6, DCT, TGDS, GPR180, SOX21, ABCC4, CLDN10, DZIP1, DNAJC3, UGCGL2, HS6ST3, OXGR1, MBNL2, RAP2A, IPO5, FARP1, RNF113B, STK24, SLC15A1, DOCK9, UBAC2, GPR18, GPR183, TM9SF2, CLYBL, ZIC5, ZIC2, PCCA, A2LD1, TMTC4, NALCN, ITGBL1, FGF14, TPP2, C13orf39	hsa-mir-622, hsa-mir-17, hsa-mir-18a, hsa-mir-19a, hsa-mir-20a, hsa-mir-19b-1, hsa-mir-92a-1, hsa-mir-623, hsa-mir-1267	V_4814_LC15122_Wong et al. (2007), V_4815_LC15123_Wong et al. (2007), V_4816_LC15155_Wong et al. (2007), V_4817_LC15210_Wong et al. (2007), V_4818_LC15212_Wong et al. (2007), V_4819_LC15248_Wong et al. (2007), V_4820_LC15248_Wong et al. (2007), V_0361_LC1
14	q11.2	19.97	20.41	5	5	OR11H2, OR4Q3, OR4H12P, OR4M1, OR4N2, OR4K2, OR4K5, OR4K1		
14	q23.1-q32.12	59.35	93.86	328	10	DAAM1, GPR135, C14orf149, C14orf100, C14orf38, RTN1, LRRC9, C14orf135, DHRS7, PPM1A, C14orf39, SIX6, SIX1, SIX4, MNAT1, TRMT5, SLC38A6, TMEM30B, PRKCH, HIF1A, SNAPC1, SYT16, KCNH5, RHOJ, GPHB5, PPP2R5E, RPL31P5, WDR89, SGPP1, SYNE2, ESR2, MTHFD1, AKAP5, Z	hsa-mir-548h-1, hsa-mir-625, hsa-mir-1260	V_0178_LC15831_lafrate et al. (2004), V_4838_LC15719_Wong et al. (2007), V_4839_LC15767_Wong et al. (2007), V_4840_LC15786_Wong et al. (2007), V_4841_LC15841_Wong et al. (2007), V_4842_LC15858_Wong et al. (2007), V_4844_LC15916_Wong et al. (2007), V_4845_
15	q11.2	20.01	22.82	39	17	VSIG7, BCL8, OR11K1P, OR4M2, OR4N4, VSIG6	hsa-mir-1268	V_2183_LC16090_Locke et al. (2006), V_4873_LC16090_Wong et al. (2007), V_4874_LC16090_Wong et al. (2007), V_4875_LC16090_Wong et al. (2007), V_4877_LC16090_Wong et al. (2007), V_4878_LC16090_Wong et al. (2007), V_4879_LC16090_Wong et al. (2007), V_4880_LC
15	q11.2	24.26	25.02	11	6	C15orf2		
15	q13.1	28.53	28.73	5	5	HERC2, GOLGA8F		V_2186_LC16139_Locke et al. (2006), V_4886_LC16139_Wong et al. (2007), V_4887_LC16139_Wong et al. (2007)
16	p11.2-p11.1	31.91	33.83	17	10	ZNF267, IGHV2OR16-5, TP53TG3		V_0195_LC16821_lafrate et al. (2004), V_0794_LC16821_Sharp et al. (2005), V_0795_LC16821_Sharp et al. (2005), V_0796_LC16821_Sharp et al. (2005), V_2210_LC16821_Locke et al. (2006), V_2211_LC16821_Locke et al. (2006), V_2212_LC16821_Locke et al. (2006), V
16	p11.1-q24.3	34.28	90.04	593	42	CCNYL3, SHCBP1, VPS35, ORC6L, MYLK3, C16orf87, GPT2, DNAJA2, NETO2, ITFG1, PHKB, ABCC12, ABCC11, LONP2, SIAH1, N4BP1, CBLN1, C16orf78, ZNF423, TMEM188, HEATR3, PAPD5, ADCY7, BRD7, NKD1, SNX20, NOD2, CYLD, SALL1, TOX3, CHD9, RBL2, AKTIP, RPGRIP1L, FTO, IRX	hsa-mir-138-2, hsa-mir-328, hsa-mir-1538, hsa-mir-140, hsa-mir-1972, hsa-mir-1910	V_0196_LC16821_lafrate et al. (2004), V_0197_LC16821_lafrate et al. (2004), V_0198_LC16863_lafrate et al. (2004), V_0199_LC17071_lafrate et al. (2004), V_0200_LC17076_lafrate et al. (2004), V_0678_LC16967_Sharp et al. (2005), V_0797_LC16959_Sharp et al. (
17	p13.2-p13.1	5.38	7.03	11	7	DERL2, MIS12, NLRP1, WSCD1, AIPL1, FAM64A, PITPNM3, KIAA0753, TXNDC17, MED31, C17orf100, SLC13A5, XAF1, FBXO39, TEKT1, ALOX12, RNASEK, C17orf49, BCL6B, SLC16A13, SLC16A11, CLEC10A, ASGR2	hsa-mir-195, hsa-mir-497	
17	p13.1-p11.2	7.92	16.99	94	9	GUCY2D, ALOX15B, ALOX12B, ALOXE3, HES7, PER1, VAMP2, TMEM107, C17orf59, AURKB, C17orf68, PFAS, SLC25A35, RANGRF, ARHGEF15, ODF4, KRBA2, RPL26, NDEL1, MYH10, CCDC42, SPDYE4, MFSD6L, PIK3R6, PIK3R5, NTN1, STX8, WDR16, USP43, DHRS7C, GLP2R, RCVRN, GAS7, MYH1	hsa-mir-744, hsa-mir-548h-3, hsa-mir-1288	V_0798_LC17354_Sharp et al. (2005), V_2218_LC17354_Locke et al. (2006), V_4988_LC17315_Wong et al. (2007), V_4989_LC17333_Wong et al. (2007)
17	p11.2-p11.1	20.03	21.84	25	9	CYTSB, CCDC144C, FAM106B, CDRT15L2, CCDC144NL, USP22, DHRS7B, TMEM11, C17orf103, MAP2K3, KCNJ12, C17orf51, FAM27L		V_4995_LC17400_Wong et al. (2007), V_4996_LC17400_Wong et al. (2007), V_4997_LC17400_Wong et al. (2007), V_4998_LC17406_Wong et al. (2007)
17	q11.2-q12	31.18	33.21	24	8	MYO1D, TMEM98, SPACA3, ACCN1, CCL2, CCL7, CCL11, CCL8, CCL13, CCL1, C17orf102, TMEM132E		V_0799_LC17457_Sharp et al. (2005), V_0800_LC17457_Sharp et al. (2005), V_2220_LC17457_Locke et al. (2006), V_2221_LC17457_Locke et al. (2006), V_2222_LC17457_Locke et al. (2006), V_2223_LC17457_Locke et al. (2006), V_5001_LC17457_Wong et al. (2007), V_50
18	p11.32	1.36	2.52	11	5			

18	p11.31	5.4	5.76	3	5	EPB41L3		
18	p11.21-p11.1	14.3	15.31	12	8	POTEC, ANKRD30B		V_5046_LC17976_Wong et al. (2007)
18	q22.3-q23	71.64	73.49	19	6	FBXO15, C18orf55, CYB5A, C18orf51, CNDP2, CNDP1, ZNF407, C18orf33, ZADH2, TSHZ1, C18orf62		V_5062_LC18530_Wong et al. (2007)
19	p13.2	8.65	9.17	16	28	ADAMTS10, ACTL9, OR2Z1, ZNF558, MBD3L1, MUC16		V_0220_LC18794_Iafrate et al. (2004), V_0808_LC18794_Sharp et al. (2005), V_2239_LC18794_Locke et al. (2006), V_2240_LC18794_Locke et al. (2006), V_5079_LC18794_Wong et al. (2007), V_5080_LC18794_Wong et al. (2007), V_5081_LC18794_Wong et al. (2007), V_50
19	q11-q12	27.83	30.18	30	10	UQCRFS1, VSTM2B, POP4, PLEKHF1		
19	q12	30.5	31.72	19	6	C19orf2, ZNF536		
19	q13.2-q13.31	43.09	43.93	7	10	CEACAM8, PSG3, PSG8, PSG1, PSG6, PSG7, PSG5, PSG9, CD177, CD177P, TEX101		V_5099_LC18991_Wong et al. (2007)
19	q13.33	50.45	50.95	8	6	SIGLEC11, SIGLECP16, VRK3, ZNF473, C19orf41, MYH14, KCNC3, NAPSB, NAPSA, NR1H2, POLD1, SPIB, MYBPC2		V_5103_LC19048_Wong et al. (2007)
19	q13.42	54.89	55.29	6	6	TTYH1, LENG8, LENG9, CDC42EP5, LAIR2, KIR3DX1, LILRB1, LILRA1, LILRB4, KIR2DL4, KIR2DL1		V_2246_LC19081_Locke et al. (2006), V_2247_LC19092_Locke et al. (2006), V_5112_LC19081_Wong et al. (2007), V_5113_LC19081_Wong et al. (2007), V_5114_LC19090_Wong et al. (2007)
21	q11.1-q11.2	10.91	15.4	13	12	TPTE, BAGE, POTED		V_0810_LC20058_Sharp et al. (2005), V_0811_LC20058_Sharp et al. (2005), V_2254_LC20058_Locke et al. (2006), V_2255_LC20058_Locke et al. (2006), V_5157_LC20058_Wong et al. (2007), V_5158_LC20061_Wong et al. (2007)
22	q11.1	16.06	16.39	10	10	POTEH		
22	q11.21-q13.1	18.17	37.93	196	8	BCL2L13, BID, C22orf37, MICAL3, PEX26, TUBA8, USP18, DGCR6, PRODH, DGCR2, DGCR14, TSSK2, GSC2, SLC25A1, CLTCL1, HIRA, MRPL40, UFD1L, CDC45L, CLDN5, RPL7AP70, Sep-05, GP1BB, TBX1, GNB1L, C22orf29, TXNRD2, COMT, ARVCF, C22orf25, DGCR8, TRMT2A, RANBP1, ZDHHC	hsa-mir-648, hsa-mir-185, hsa-mir-1306, hsa-mir-1286, hsa-mir-649, hsa-mir-301b, hsa-mir-130b, hsa-mir-650, hsa-mir-548j	V_0235_LC20386_Iafrate et al. (2004), V_0236_LC20439_Iafrate et al. (2004), V_0237_LC20476_Iafrate et al. (2004), V_0688_LC20386_Sharp et al. (2005), V_0816_LC20342_Sharp et al. (2005), V_0817_LC20342_Sharp et al. (2005), V_0818_LC20342_Sharp et al. (2005
22	q13.1	38.2	39.8	15	5	H1F0, GCAT, GALR3, ANKRD54, EIF3L, MICALL1, C22orf23, POLR2F, SOX10, PICK1, SLC16A8, BAIAP2L2, PLA2G6, MAFF, TMEM184B, CSNK1E, KCNJ4, KDELR3, DDX17, DMC1, CBY1, TOMM22, JOSD1, GTPBP1, UNC84B, DNAL4, NPTXR, CBX6, APOBEC3A, APOBEC3D, APOBEC3F, APOBEC3H, CBX	hsa-mir-658, hsa-mir-659	V_5187_LC20514_Wong et al. (2007)
22	q13.1	40.22	40.81	7	5	ENTHD1, GRAP2, FAM83F, TNRC6B, SGSM3, MKL1		V_5189_LC20524_Wong et al. (2007)
22	q13.2-q13.33	43.75	50.65	66	10	MPPED1, EFCAB6, SULT4A1, PNPLA5, PNPLA3, SAMM50, PARVB, PARVG, KIAA1644, LDOC1L, ARHGAP8, PHF21B, NUP50, C22orf9, UPK3A, FAM118A, SMC1B, RIBC2, FBLN1, ATXN10, WNT7B, C22orf26, PPARA, C22orf40, PKDREJ, TTC38, GTSE1, TRMU, CELSR1, GRAMD4, CERK, TBC1D22A, FA	hsa-mir-1249, hsa-let-7a-3, hsa-let-7b	V_0239_LC20651_Iafrate et al. (2004), V_5190_LC20580_Wong et al. (2007), V_5191_LC20603_Wong et al. (2007), V_5192_LC20651_Wong et al. (2007), V_5193_LC20651_Wong et al. (2007)
23	p22.33	0.63	1.69	8	5	CRLF2, CSF2RA, IL3RA, SLC25A6, ASMTL, P2RY8		
23	p22.33	1.89	4.14	20	5	DHRSX, ZBED1, CD99, XG, GYG2, ARSD, ARSE, ARSH, ARSF, CXorf28, MXRA5, PRKX		V_0820_LC20665_Sharp et al. (2005), V_2274_LC20665_Locke et al. (2006)
23	p22.31-p22.2	9.21	10.48	12	6	TBL1X, GPR143, SHROOM2, WWC3, CLCN4, MID1		V_2275_LC20696_Locke et al. (2006)
23	q22.3	104.62	105.27	5	6	IL1RAPL2, NRK		V_0250_LC21009_Iafrate et al. (2004)
23	q28	147.75	152.88	50	5	AFF2, IDS, MAGEA9B, HSFX1, TMEM185A, MAGEA11, MAGEA9, MAGEA8, CXorf40A, MAMLD1, MTM1, MTMR1, CD99L2, HMGB3, GPR50, VMA21, PASD1, PRRG3, FATE1, CNGA2, MAGEA4, GABRE, MAGEA10, GABRA3, GABRQ, MAGEA6, CSAG3, MAGEA2B, CSAG4, CSAG1, MAGEA2, CSAG2, MAGEA3, CETN2	hsa-mir-224, hsa-mir-452, hsa-mir-105-1, hsa-mir-767, hsa-mir-105-2	
23	q28	153.32	153.65	4	5	MECP2, OPN1LW, TEX28P2, OPN1MW, TEX28P1, OPN1MW2, TEX28, TKTL1, FLNA, EMD, RPL10, DNASE1L1, TAZ		
23	q28	153.78	155.19	16	11	IKBKG, CXorf52, CTAG1A, CTAG1B, CXorf52B, CTAG2, GAB3, DKC1, MPP1, F8, H2AFB1, F8A1, FUNDC2, MTCP1NB, BRCC3, VBP1, RAB39B, CLIC2, H2AFB2, F8A2, F8A3, H2AFB3, TMLHE, SPRY3, VAMP7	hsa-mir-1184, hsa-mir-1184, hsa-mir-1184	V_0825_LC21225_Sharp et al. (2005), V_0828_LC21214_Sharp et al. (2005)

Supplementary Table 7: Regions differentially gained between papillary carcinomas and grade- and ER-matched IDC-NSTs (multi-Fisher's exact test $p < 0.05$).

Chromosome	Cytobands	Start (Mb)	End (Mb)	Number of BACs	papillary carcinomas (n=50)	IDC-NSTs (n=50)	Genes	mi-RNAs	aCGH CNVs
1	p12	120.45	120.65	4	7	24	NOTCH2		V_4246_LC0743_Wong et al. (2007)
1	q21.1-q21.3	143.51	153.27	86	22	40	PPIAL4G, FAM72D, SRGAP2P2, PPIAL4B, NBPF9, PDE4DIP, SEC22B, NOTCH2NL, HFE2, TXNIP, POLR3GL, ANKRD34A, LIX1L, RBM8A, GNRHR2, PEX11B, ITGA10, ANKRD35, PIAS3, NUDT17, POLR3C, RNF115, CD160, PDZK1, GPR89A, GPR89C, NBPF8, NBPF8, NBPF12, PRKAB2, FMO5, CHD1L, BC	hsa-mir-554	V_0685_LC0752_Sharp et al. (2005), V_2050_LC0752_Locke et al. (2006), V_2051_LC0752_Locke et al. (2006), V_2052_LC0752_Locke et al. (2006), V_4249_LC0752_Wong et al. (2007), V_4250_LC0752_Wong et al. (2007), V_4251_LC0752_Wong et al. (2007), V_4252_LC0752
1	q23.1-q32.1	156.92	204.46	488	28	41	ARHGEF11, ETV3, FCRL5, FCRL4, FCRL3, FCRL2, FCRL1, CD5L, KIRREL, CD1D, CD1A, CD1C, CD1B, CD1E, OR10T2, OR10K2, OR10K1, OR10R2, OR6Y1, OR6P1, OR10X1, OR10Z1, SPTA1, OR6K2, OR6K3, OR6K6, OR6N1, OR6N2, MNDA, PYHIN1, IFI16, AIM2, CADM3, DARC, OR10J3, FCER1A,	hsa-mir-556, hsa-mir-921, hsa-mir-1255b-2, hsa-mir-557, hsa-mir-1295, hsa-mir-214, hsa-mir-199a-2, hsa-mir-488, hsa-mir-1278, hsa-mir-181b-1, hsa-mir-181a-1, hsa-mir-1231	V_0014_LC0941_Iafrate et al. (2004), V_0015_LC0954_Iafrate et al. (2004), V_0686_LC1055_Sharp et al. (2005), V_0687_LC1055_Sharp et al. (2005), V_2053_LC1052_Locke et al. (2006), V_2054_LC1055_Locke et al. (2006), V_2055_LC1055_Locke et al. (2006), V_4258
1	q32.1-q42.12	207.14	225.97	191	25	42	FCAMR, C1orf116, YOD1, PFKFB2, C4BPB, C4BPA, CD55, CR2, CR1, CR1L, CD46, C1orf132, CD34, PLXNA2, CAMK1G, LAMB3, G0S2, HSD11B1, TRAF3IP3, C1orf74, IRF6, C1orf107, SYT14, C1orf133, SERTAD4, HHAT, KCNH1, RCOR3, TRAF5, C1orf97, RD3, SLC30A1, NEK2, LPGAT1, INT	hsa-mir-29c, hsa-mir-29b-2, hsa-mir-205, hsa-mir-215, hsa-mir-194-1, hsa-mir-320b-2	V_4270_LC1176_Wong et al. (2007)
1	q42.12-q42.13	226.33	227.81	18	22	36	ACBD3, MIXL1, LIN9, PARP1, C1orf95, ITPKB, PSEN2, CABC1, CDC42BPA, ZNF678		
1	q42.13-q43	228.87	241.83	142	24	41	RHOU, TMEM78, RAB4A, SPHAR, C1orf96, ACTA1, NUP133, ABCB10, TAF5L, URB2, GALNT2, PGBD5, COG2, AGT, CAPN9, C1orf198, TTC13, ARV1, FAM89A, TRIM67, C1orf131, GNPAT, EXOC8, C1orf124, EGLN1, TSNAX, DISC1, SIPA1L2, KIAA1383, C1orf57, PCNXL2, KCNK1, SLC35F3, C1o	hsa-mir-1182, hsa-mir-1537	V_0016_LC1285_Iafrate et al. (2004), V_4271_LC1296_Wong et al. (2007), V_4272_LC1302_Wong et al. (2007)
1	q43-q44	243.55	248.88	66	21	39	SDCCAG8, AKT3, ZNF238, C1orf100, ADSS, C1orf101, PPPDE1, FAM36A, C1orf199, HNRNPU, EFCAB2, KIF26B, SMYD3, TFB2M, C1orf71, SCCPDH, AHCTF1, ZNF695, ZNF670, ZNF669, C1orf229, ZNF124, ZNF496, NLRP3, OR2B11, C1orf150, OR2C3, OR2G2, OR2G3, OR13G1, OR14A2, OR6F1		V_0017_LC1401_Iafrate et al. (2004), V_2056_LC1401_Locke et al. (2006)
6	q27	170.39	170.76	5	9	0	DLL1, FAM120B		
7	p22.3	0.96	1.36	6	32	15	ADAP1, CYP2W1, C7orf50, GPR146, GPER, ZFAND2A, UNCX	hsa-mir-339	V_0093_LC9158_Iafrate et al. (2004), V_4519_LC9158_Wong et al. (2007), V_4520_LC9158_Wong et al. (2007)
7	q11.21	65.03	65.23	4	3	16			
7	q21.3	95.04	96.55	10	1	11	PON2, ASB4, PDK4, DYNC1I1, SLC25A13, SHFM1	hsa-mir-591	
7	q31.2-q31.31	117.13	118.14	8	0	10	CFTR, CTTNBP2, LSM8, ANKRD7		
11	p15.4	3.06	3.23	2	15	3	CARS, OSBPL5		
11	p15.4	3.46	3.58	2	13	2			
15	q22.31	65	65.75	7	10	0	RBPMS2, PIF1, ANKDD1A, SPG21, MTFMT, RASL12, PDCD7, CLPX, CILP, PARP16, IGDCC3, IGDCC4, DPP8	hsa-mir-1272	
16	q11.1	35.13	35.28	2	4	18			

17	p13.3	0	2.54	38	22	6	DOC2BL, RPH3AL, C17orf97, FAM101B, VPS53, FAM57A, GEMIN4, GLOD4, RNMTL1, NXN, TIMM22, ABR, BHLHA9, TUSC5, YWHAE, CRK, MYO1C, INPP5K, PITPNA, SLC43A2, SCARF1, RILP, PRPF8, TLCD2, WDR81, SERPINF2, SERPINF1, SMYD4, RPA1, RTN4RL1, DPH1, HIC1, SMG6, SRR, TSR1,	hsa-mir-22, hsa-mir-132, hsa-mir-212	V_4979_LC17159_Wong et al. (2007), V_4980_LC17159_Wong et al. (2007)
17	p13.2	4.55	4.79	8	18	5	PELP1, ARRB2, MED11, CXCL16, ZMYND15, TM4SF5, VMO1, GLTPD2, PSMB6, PLD2, MINK1		V_4985_LC17280_Wong et al. (2007), V_4986_LC17280_Wong et al. (2007), V_4987_LC17280_Wong et al. (2007)
18	q21.1	44.4	44.71	5	38	20	PIAS2, KATNAL2, TCEB3CL2, TCEB3CL, TCEB3C, TCEB3B, HDHD2, IER3IP1		
19	p13.3	0.96	4.53	40	30	16	ARID3A, WDR18, GRIN3B, C19orf6, CNN2, ABCA7, HMHA1, POLR2E, GPX4, SBNO2, STK11, C19orf26, ATP5D, MIDN, C19orf23, CIRBP, C19orf24, MUM1, EFNA2, NDUFS7, GAMT, DAZAP1, RPS15, APC2, C19orf25, PCSK4, REEP6, ADAMTSL5, PLK5P, MEX3D, MBD3, UQCR, TCF3, ONECUT3, AT	hsa-mir-1909, hsa-mir-1227, hsa-mir-637	V_2237_LC18671_Locke et al. (2006), V_5065_LC18671_Wong et al. (2007), V_5066_LC18671_Wong et al. (2007), V_5067_LC18671_Wong et al. (2007), V_5068_LC18671_Wong et al. (2007), V_5069_LC18671_Wong et al. (2007), V_5070_LC18730_Wong et al. (2007), V_5071_LC
19	p13.2	7.08	8.69	14	26	9	ZNF557, INSR, ARHGEF18, PEX11G, C19orf45, ZNF358, MCOLN1, PNPLA6, KIAA1543, XAB2, PCP2, STXBP2, RETN, C19orf59, TRAPPC5, FCER2, CLEC4G, CD209, CLEC4M, EVI5L, LRRC8E, MAP2K7, SNAPC2, CTXN1, TIMM44, ELAVL1, CCL25, FBN3, LASS4, CD320, NDUFA7, RPS28P9, KANK3,		V_0808_LC18794_Sharp et al. (2005), V_2238_LC18783_Locke et al. (2006), V_2239_LC18794_Locke et al. (2006), V_5078_LC18783_Wong et al. (2007), V_5079_LC18794_Wong et al. (2007), V_5080_LC18794_Wong et al. (2007)
19	p13.11	17.01	18.9	32	30	12	CPAMD8, HAUS8, MYO9B, USE1, OCEL1, NR2F6, USHBP1, ANKLE1, ABHD8, MRPL34, DDA1, ANO8, GTPBP3, PLVAP, BST2, FAM125A, TMEM221, NXNL1, SLC27A1, PGLS, FAM129C, GLT25D1, UNC13A, MAP1S, FCHO1, B3GNT3, JAK3, RPL18A, SLC5A5, CCDC124, KCNN1, ARRDC2, IL12RB1, MAST3,		V_5091_LC18881_Wong et al. (2007), V_5092_LC18883_Wong et al. (2007), V_5093_LC18883_Wong et al. (2007)
19	q13.32-q13.33	45.34	48.2	33	23	9	PVRL2, TOMM40, APOE, APOC1, APOC4, APOC2, CLPTM1, RELB, SFRS16, ZNF296, GEMIN7, LRRC68, NKPD1, TRAPPC6A, BLOC1S3, EXOC3L2, MARK4, CKM, KLC3, ERCC2, PPP1R13L, CD3EAP, ERCC1, FOSB, RTN2, VASP, OPA3, GPR4, EML2, GIPR, SNRPD2, QPCTL, FBXO46, SIX5, DMPK, DMWD,	hsa-mir-330, hsa-mir-642, hsa-mir-769	V_2243_LC19026_Locke et al. (2006), V_5100_LC19016_Wong et al. (2007), V_5101_LC19026_Wong et al. (2007), V_5102_LC19026_Wong et al. (2007)
19	q13.33	48.76	49.12	4	23	9	ZNF114, CCDC114, EMP3, TMEM143, SYNGR4, KDELR1, GRIN2D, GRWD1, KCNJ14, CYTH2, LMTK3, SULT2B1, FAM83E, SPACA4	hsa-mir-220c	V_2245_LC19036_Locke et al. (2006)
19	q13.33	50.37	51.34	15	22	7	PNKP, AKT1S1, TBC1D17, IL4I1, NUP62, SIGLEC11, ATF5, SIGLECP16, VRK3, ZNF473, C19orf41, MYH14, KCNC3, NAPSB, NAPSA, NR1H2, POLD1, SPIB, MYBPC2, FAM71E1, C19orf63, JOSD2, ASPDH, LRRC4B, SYT3, SHANK1, CLEC11A, GPR32, ACPT, C19orf48, KLK1, KLK15		V_5103_LC19048_Wong et al. (2007)
20	q13.2	52.16	52.59	5	7	21	ZNF217, BCAS1		
21	q22.3	45.72	46.3	7	23	8	AIRE, PFKL, C21orf2, TRPM2, LRRC3, C21orf30, C21orf29, C21orf90, KRTAP10-1, KRTAP10-2, KRTAP10-3, KRTAP10-4, KRTAP10-6, KRTAP10-7, KRTAP10-8, KRTAP10-9, KRTAP10-10, KRTAP10-11, KRTAP12-4, KRTAP12-2, KRTAP12-1, KRTAP10-12, UBE2G2, SUMO3, PTTG1IP		
21	q22.3	47.02	47.94	14	24	7	PCBP3, COL6A1, COL6A2, FTCD, C21orf56, LSS, MCM3AP, C21orf57, C21orf58, PCNT, DIP2A		
22	q12.3-q13.1	37.08	38.76	18	20	6	CACNG2, RABL4, PVALB, NCF4, CSF2RB, C22orf33, TST, MPST, KCTD17, TMPRSS6, IL2RB, C1QTNF6, SSTR3, RAC2, CYTH4, ELFN2, MFNG, CARD10, CDC42EP1, LGALS2, GGA1, PDXP, LGALS1, NOL12, TRIOBP, H1F0, GCAT, GALR3, ANKRD54, EIF3L, MICALL1, C22orf23, POLR2F, SOX10, PI	hsa-mir-658, hsa-mir-659	V_2037_LC20505_Urban et al (2006), V_2038_LC20505_Urban et al (2006), V_5187_LC20514_Wong et al. (2007)
23	q28	152.71	153.8	17	25	10	TREX2, HAUS7, BGN, ATP2B3, FAM58A, DUSP9, PNCK, SLC6A8, BCAP31, ABCD1, PLXNB3, SRPK3, IDH3G, SSR4, PDZD4, L1CAM, AVPR2, ARHGAP4, ARD1A, RENBP, HCFC1, TMEM187, IRAK1, MECP2, OPN1LW, TEX28P2, OPN1MW, TEX28P1, OPN1MW2, TEX28, TKTL1, FLNA, EMD, RPL10, DNASE1L		

Supplementary Table 8: Regions differentially lost between papillary carcinomas and grade- and ER-matched IDC-NSTs (multi-Fisher's exact test $p < 0.05$).

Chromosome	Cytobands	Start (Mb)	End (Mb)	Number of BACs	papillary carcinomas (n=50)	IDC-NSTs (n=50)	Genes	mi-RNAs	aCGH CNVs
1	p36.32	2.7	3.39	14	9	31	TTC34, ACTRT2, PRDM16, ARHGEF16		V_4194_LC0040_Wong et al. (2007), V_4195_LC0040_Wong et al. (2007), V_4196_LC0040_Wong et al. (2007)
1	p36.32-p36.31	4.02	5.83	24	11	28	AJAP1		V_4198_LC0097_Wong et al. (2007)
1	p35.1-p34.3	33.96	35.27	16	8	25	CSMD2, C1orf94, GJB5, GJB4, GJB3, GJA4	hsa-mir-552	
1	p34.3	35.5	36.28	8	1	11	ZMYM1, SFPQ, ZMYM4, KIAA0319L, NCDN, PSMB2, TFAP2E, C1orf216, CLSPN, EIF2C4		
1	p34.3	37.11	39.41	26	4	16	GRIK3, ZC3H12A, C1orf149, SNIP1, DNALI1, GNL2, RSPO1, C1orf109, CDCA8, EPHA10, MANEAL, YRDC, C1orf122, MTF1, INPP5B, SF3A3, FHL3, UTP11L, POU3F1, RRAGC, MYCBP, GJA9, RHBDL2		V_0006_LC0305_Iafrate et al. (2004)
1	p34.3-p34.2	39.63	41.15	19	0	9	MACF1, BMP8A, PABPC4, HEYL, NT5C1A, HPCAL4, PPIE, BMP8B, OXCT2, TRIT1, MYCL1, MFSD2, CAP1, PPT1, RLF, TMCO2, ZMPSTE24, COL9A2, SMAP2, ZNF643, ZNF642, DEM1, ZNF684, RIMS3		V_4219_LC0315_Wong et al. (2007)
1	p32.3	51.1	56.07	49	4	18	FAF1, CDKN2C, C1orf185, RNF11, TTC39A, EPS15, OSBPL9, NRD1, RAB3B, TXNDC12, KTI12, BTF3L4, ZFYVE9, CC2D1B, ORC1L, PRPF38A, ZCCHC11, GPX7, C1orf163, ZYG11B, ZYG11A, ECHDC2, SCP2, PODN, SLC1A7, CPT2, C1orf123, MAGOH, LRP8, DMRTB1, GLIS1, TMEM48, YIPF1, DIO1		V_4223_LC0373_Wong et al. (2007), V_4224_LC0373_Wong et al. (2007), V_4225_LC0378_Wong et al. (2007)
1	p32.2	57.89	58.05	2	2	13	DAB1		
3	p25.3	10.37	10.97	5	0	9	ATP2B2, SLC6A11	hsa-mir-885	
6	p21.33-p21.32	31.46	32.19	7	0	8	LTB, APOM, LY6G6C, LSM2, HSPA1A, EHMT2, C4B, TNXB, ATF6B, PRRT1, RNF5, GPSM3	hsa-mir-1236	V_4492_LC8203_Wong et al. (2007)
6	p21.2	36.7	37.3	5	0	8	RAB44, CPNE5, PPIL1, C6orf89, PI16, MTCH1, FGD2, COX6A1P2, PIM1, TMEM217, TBC1D22B		
6	p21.2-p21.1	40.03	40.93	11	2	13	LRFN2		
6	p21.1	40.93	44.24	40	0	14	UNC5CL, BZRPL1, APOBEC2, C6orf130, NFYA, TREML1, TREM2, TREML2, TREML4, TREM1, NCR2, FOXP4, MDFI, TFEB, PGC, FRS3, PRICKLE4, TOMM6, USP49, MED20, BYSL, CCND3, TAF8, C6orf132, GUCA1A, GUCA1B, MRPS10, TRERF1, UBR2, PRPH2, TBCC, KIAA0240, RPL7L1, C6orf226, P		
6	q11.1	62.23	62.79	7	0	8	KHDRBS2		V_0080_LC8417_Iafrate et al. (2004), V_0081_LC8420_Iafrate et al. (2004)
6	q11.1-q12	63.07	64.97	25	0	11	FKBP1C, LGSN, PTP4A1, PHF3, EYS		
6	q13	73.28	73.79	5	0	8	KCNQ5		V_0087_LC8488_Iafrate et al. (2004)
6	q13-q14.1	74.19	80.27	71	0	10	MTO1, EEF1A1, SLC17A5, CD109, COL12A1, COX7A2, TMEM30A, FILIP1, SENP6, MYO6, IMPG1, HTR1B, IRAK1BP1, PHIP, HMGN3, LCA5		V_4498_LC8515_Wong et al. (2007)
6	q14.3-q15	87.82	91.24	32	1	14	ZNF292, GJB7, C6orf162, C6orf163, C6orf164, C6orf165, SLC35A1, RARS2, ORC3L, AKIRIN2, SPACA1, CNR1, RNGTT, PNRC1, PM20D2, GABRR1, GABRR2, UBE2J1, RRAGD, ANKRD6, MDN1, CASP8AP2, GJA10, BACH2, MAP3K7		V_4500_LC8569_Wong et al. (2007)
6	q16.3-q21	105.27	105.68	4	2	13	HACE1, C6orf220, LIN28B, BVES, C6orf112, POPDC3		
6	q23.2-q24.1	134.16	142.74	81	2	11	TCF21, TBPL1, SLC2A12, SGK1, ALDH8A1, HBS1L, MYB, AHI1, PDE7B, FAM54A, BCLAF1, MAP7, MAP3K5, PEX7, SLC35D3, IL20RA, IL22RA2, IFNGR1, OLIG3, TNFAIP3, PERP, KIAA1244, PBOV1, HEBP2, NHSL1, CCDC28A, ECT2L, REPS1, C6orf115, HECA, TXLNB, CITED2, NMBR, VTA1, GPR	hsa-mir-548a-2	

6	q24.2-q24.3	143.39	146.36	36	1	11	AIG1, ADAT2, PEX3, FUCA2, PHACTR2, LTV1, FAM164B, PLAGL1, SF3B5, STX11, UTRN, EPM2A, FBXO30, SHPRH, GRM1		
6	q24.3-q25.1	146.92	150.23	38	2	12	C6orf103, STXBP5, SAMD5, SASH1, UST, MAP3K7IP2, SUMO4, ZC3H12D, PPIL4, C6orf72, KATNA1, LATS1, NUP43, PCMT1, LRP11, RAET1E		V_4510_LC8882_Wong et al. (2007)
6	q25.1-q27	151.67	170.03	217	6	22	AKAP12, ZBTB2, RMND1, C6orf211, C6orf97, ESR1, SYNE1, MYCT1, VIP, FBXO5, MTRF1L, RGS17, OPRM1, IPCEF1, MAGI1, RBM16, TIAM2, TFB1M, CLDN20, NOX3, ARID1B, C6orf35, ZDHHC14, SNX9, SYNJ2, SERAC1, GTF2H5, TULP4, TMEM181, DYNLT1, SYTL3, EZR, C6orf99, RSPH3, TAG	hsa-mir-1202, hsa-mir-1913	V_2098_LC9057_Locke et al. (2006), V_4512_LC8905_Wong et al. (2007), V_4513_LC8977_Wong et al. (2007), V_4514_LC8985_Wong et al. (2007), V_4515_LC9007_Wong et al. (2007), V_4516_LC9028_Wong et al. (2007), V_4517_LC9032_Wong et al. (2007)
6	q27	170.33	170.76	6	1	11	DLL1, FAM120B		
9	q11	42.23	42.28	2	30	15			V_0752_LC11330_Sharp et al. (2005), V_2140_LC11330_Locke et al. (2006), V_4637_LC11330_Wong et al. (2007)
9	q11	42.93	43.16	6	30	15	ANKRD20A1		V_2149_LC11330_Locke et al. (2006)
9	q11-q12	44.97	46.08	8	31	15	FAM27C, FAM27A, FAM27E2		V_0744_LC11330_Sharp et al. (2005), V_0745_LC11330_Sharp et al. (2005), V_0746_LC11330_Sharp et al. (2005)…
9	q33.3-q34.11	130.1	132.11	23	0	11	GARNL3, SLC2A8, ZNF79, RPL12, LRSAM1, FAM129B, STXBP1, TTC16, C9orf117, TOR2A, SH2D3C, CDK9, FPGS, ENG, AK1, ST6GALNAC6, ST6GALNAC4, PIP5KL1, DPM2, FAM102A, NAIF1, SLC25A25, PTGES2, LCN2, C9orf16, CIZ1, DNM1, GOLGA2, C9orf119, TRUB2, COQ4, SLC27A4, TMSL4,	hsa-mir-199b, hsa-mir-219-2	
9	q34.11-q34.3	132.41	141.06	95	4	19	PRRX2, PTGES, TOR1B, TOR1A, C9orf78, USP20, FNBP1, GPR107, FREQ, HMCN2, ASS1, FUBP3, PRDM12, EXOSC2, ABL1, QRFP, FIBCD1, LAMC3, AIF1L, NUP214, FAM78A, PPAPDC3, BAT2L, POMT1, UCK1, RAPGEF1, MED27, NTNG2, SETX, TTF1, C9orf171, BARHL1, DDX31, GTF3C4, C9orf98	hsa-mir-126, hsa-mir-602	V_0132_LC11835_Iafrate et al. (2004), V_0133_LC11864_Iafrate et al. (2004), V_0134_LC11864_Iafrate et al. (2004), V_4657_LC11835_Wong et al. (2007), V_4658_LC11835_Wong et al. (2007), V_4659_LC11848_Wong et al. (2007), V_4660_LC11849_Wong et al. (2007), V
10	q11.21	43.46	43.88	7	0	8	RET, CSGALNACT2, RASGEF1A, FXYD4		
10	q22.2-q22.3	77.23	78.23	12	0	9	C10orf11	hsa-mir-606	
11	p15.5	0.25	1.29	8	0	9	PSMD13, NLRP6, ATHL1, IFITM5, IFITM2, IFITM1, IFITM3, B4GALNT4, PKP3, SIGIRR, ANO9, PTDSS2, RNH1, HRAS, LRRC56, C11orf35, RASSF7, PHRF1, IRF7, MUPCDH, SCT, DRD4, DEAF1, TMEM80, EPS8L2, TALDO1, PDDC1, CEND1, SLC25A22, LRDD, RPLP2, PNPLA2, EFCAB4A, CD151, P	hsa-mir-210	V_4725_LC12865_Wong et al. (2007), V_4726_LC12865_Wong et al. (2007)
11	q13.1	63.8	63.96	2	2	13	MACROD1, FLRT1		
11	q13.1	64.85	65.54	5	1	11	CDCA5, ZFPL1, C11orf2, TM7SF2, ZNHIT2, FAU, MRPL49, SYVN1, SPDYC, CAPN1, SLC22A20, POLA2, CDC42EP2, DPF2, TIGD3, SLC25A45, FRMD8, MALAT1, SCYL1, LTBP3, SSSCA1, FAM89B, EHBP1L1, KCNK7, MAP3K11, PCNXL3, SIPA1, RELA, KAT5, RNASEH2C	hsa-mir-612	
11	q13.1-q13.2	65.63	66.46	6	0	10	MUS81, EFEMP2, CTSW, FIBP, CCDC85B, FOSL1, C11orf68, DRAP1, TSGA10IP, SART1, EIF1AD, BANF1, CST6, CATSPER1, GAL3ST3, SF3B2, PACS1, KLC2, RAB1B, CNIH2, YIF1A, TMEM151A, CD248, RIN1, BRMS1, SLC29A2, NPAS4, MRPL11, PELI3, BBS1, ZDHHC24, CTSF, CCDC87, CCS, RB		V_4754_LC13285_Wong et al. (2007)
11	q13.2	66.78	67.36	6	0	9	SYT12, RHOD, KDM2A, ADRBK1, ANKRD13D, SSH3, POLD4, CLCF1, RAD9A, PPP1CA, TBC1D10C, ATPGD1, RPS6KB2, PTPRCAP, CORO1B, GPR152, CABP4, TMEM134, AIP, PITPNM1, CDK2AP2, CABP2, GSTP1		V_2169_LC13288_Locke et al. (2006)
11	q13.3-q13.4	69.41	70.56	12	0	9	CCND1, ORAOV1, FGF19, FGF4, FGF3, ANO1, FADD, PPFIA1, CTTN, SHANK2	hsa-mir-548k	
12	q13.13	52.52	52.9	4	0	8	KRT80, KRT7, KRT81, KRT86, KRT83, KRT85, KRT84, KRT82, KRT75, KRT6B, KRT6C, KRT6A		
12	q13.13	53.32	53.65	3	0	8	KRT18, EIF4B, TENC1, SPRYD3, IGFBP6, SOAT2, CSAD, ZNF740, ITGB7, RARG, MFSD5		
12	q13.13	54.41	54.6	3	0	8	HOXC4, HOXC6, HOXC5, SMUG1	hsa-mir-615	
16	q22.2	70.81	71.22	4	35	20	VAC14, HYDIN		

17	p13.3-p13.1	0	7.97	89	7	32	DOC2BL, RPH3AL, C17orf97, FAM101B, VPS53, FAM57A, GEMIN4, GLOD4, RNMTL1, NXN, TIMM22, ABR, BHLHA9, TUSC5, YWHAE, CRK, MYO1C, INPP5K, PITPNA, SLC43A2, SCARF1, RILP, PRPF8, TLCD2, WDR81, SERPINF2, SERPINF1, SMYD4, RPA1, RTN4RL1, DPH1, HIC1, SMG6, SRR, TSR1,	hsa-mir-22, hsa-mir-132, hsa-mir-212, hsa-mir-1253, hsa-mir-195, hsa-mir-497, hsa-mir-324	V_2217_LC17259_Locke et al. (2006), V_4979_LC17159_Wong et al. (2007), V_4980_LC17159_Wong et al. (2007), V_4981_LC17250_Wong et al. (2007), V_4982_LC17265_Wong et al. (2007), V_4983_LC17269_Wong et al. (2007), V_4984_LC17276_Wong et al. (2007), V_4985_LC
17	p13.1	8.21	9.73	17	8	23	ARHGEF15, ODF4, KRBA2, RPL26, NDEL1, MYH10, CCDC42, SPDYE4, MFSD6L, PIK3R6, PIK3R5, NTN1, STX8, WDR16, USP43, DHRS7C, GLP2R		
17	p13.1-p12	10.26	10.94	7	8	22	MYH13, MYH8, MYH4, MYH1, MYH2, MYH3, SCO1, C17orf48, TMEM220		
17	p11.2	18.28	18.56	3	4	17	EVPLL, LGALS9C, CCDC144B, TBC1D28		V_2219_LC17388_Locke et al. (2006), V_4992_LC17388_Wong et al. (2007), V_4993_LC17390_Wong et al. (2007)
17	p11.2	20.17	20.74	9	5	21	CYTSB, CCDC144C, FAM106B, CDRT15L2		V_4995_LC17400_Wong et al. (2007), V_4996_LC17400_Wong et al. (2007), V_4997_LC17400_Wong et al. (2007)
17	p11.2	20.91	21.09	2	5	18	USP22, DHRS7B		
17	p11.2-p11.1	21.15	21.53	9	9	25	C17orf103, MAP2K3, KCNJ12, C17orf51		
17	q12	35.34	35.94	6	1	11	AATF, ACACA, C17orf78, TADA2L, DUSP14, AP1GBP1		
17	q12-q21.2	37.89	39.23	13	0	9	C17orf37, GRB7, IKZF3, ZPBP2, GSDMB, ORMDL3, GSDMA, PSMD3, CSF3, MED24, THRA, NR1D1, MSL1, CASC3, RAPGEFL1, WIPF2, CDC6, RARA, GJD3, TOP2A, IGFBP4, TNS4, CCR7, SMARCE1, KRT222P, KRT24, KRT25, KRT26, KRT27, KRT28, KRT10, TMEM99, KRT12, KRT20, KRT23, KRT39,		V_0206_LC17502_Iafrate et al. (2004), V_5007_LC17508_Wong et al. (2007)
17	q21.2-q21.31	39.35	41.35	25	0	11	KRTAP9-2, KRTAP9-3, KRTAP9-8, KRTAP9-6, KRTAP9-7, KRTAP16-1, KRTAP17-1, KRT33A, KRT33B, KRT34, KRT31, KRT37, KRT38, KRT32, KRT35, KRT36, KRT13, KRT15, KRT19, KRT9, KRT14, KRT16, KRT17, EIF1, GAST, HAP1, JUP, FKBP10, NT5C3L, KLHL10, KLHL11, ACLY, TTC25, CN		V_5008_LC17512_Wong et al. (2007), V_5009_LC17516_Wong et al. (2007), V_5010_LC17522_Wong et al. (2007)
17	q21.31	41.51	43.57	24	1	12	DHX8, ETV4, MEOX1, SOST, DUSP3, MPP3, CD300LG, MPP2, C17orf88, PPY, PYY, NAGS, TMEM101, LSM12, G6PC3, HDAC5, C17orf53, ASB16, C17orf65, TMUB2, ATXN7L3, UBTF, SLC4A1, RUNDC3A, SLC25A39, GRN, FAM171A2, ITGA2B, GPATCH8, FZD2, CCDC43, DBF4B, ADAM11, GJC1, HIG		V_0207_LC17522_Iafrate et al. (2004), V_0801_LC17522_Sharp et al. (2005), V_0802_LC17522_Sharp et al. (2005), V_0803_LC17522_Sharp et al. (2005), V_0804_LC17530_Sharp et al. (2005), V_2225_LC17522_Locke et al. (2006), V_2226_LC17522_Locke et al. (2006), V
17	q21.31-q21.33	43.67	49.15	69	2	18	C17orf69, CRHR1, MAPT, KIAA1267, LRRC37A, LRRC37A2, ARL17P1, NSF, WNT3, WNT9B, GOSR2, RPRML, LRRC37A4, CDC27, MYL4, ITGB3, C17orf57, NPEPPS, KPNB1, TBKBP1, TBX21, OSBPL7, MRPL10, LRRC46, SCRN2, SP6, SP2, PNPO, ATAD4, CDK5RAP3, COPZ2, NFE2L1, CBX1, SNX11,	hsa-mir-152, hsa-mir-1203, hsa-mir-10a, hsa-mir-196a-1	V_0208_LC17538_Iafrate et al. (2004), V_0209_LC17565_Iafrate et al. (2004), V_5016_LC17543_Wong et al. (2007), V_5017_LC17552_Wong et al. (2007), V_5018_LC17559_Wong et al. (2007)
17	q25.1	71.46	72.27	10	2	14	SDK2, RPL38, TTYH2		V_5032_LC17720_Wong et al. (2007)
17	q25.1	72.76	73.69	11	0	8	SLC9A3R1, NAT9, TMEM104, GRIN2C, FDXR, FADS6, USH1G, OTOP2, OTOP3, C17orf28, CDR2L, ICT1, ATP5H, KCTD2, SLC16A5, ARMC7, NT5C, HN1, SUMO2, NUP85, GGA3, MRPS7, MIF4GD, SLC25A19, GRB2, KIAA0195, CASKIN2, TSEN54, LLGL2, MYO15B, MYO15B, RECQL5, SAP30BP		
17	q25.1	73.66	74.04	6	0	8	SAP30BP, ITGB4, GALK1, H3F3B, UNK, UNC13D, WBP2, TRIM47, TRIM65, MRPL38, FBF1, ACOX1, CDK3, EVPL, SRP68		V_5033_LC17737_Wong et al. (2007)
17	q25.3	75.97	77.1	15	0	10	TNRC6C, TMC6, TMC8, C17orf99, SYNGR2, TK1, AFMID, BIRC5, SOCS3, PGS1, DNAH17, CYTH1, USP36, TIMP2, LGALS3BP, CANT1, C1QTNF1, ENGASE		V_4327_LC17763_Wong et al. (2007), V_5036_LC17763_Wong et al. (2007), V_5039_LC17763_Wong et al. (2007), V_5040_LC17763_Wong et al. (2007)
17	q25.3	77.64	81.02	37	0	12	ENPP7, CBX2, CBX8, CBX4, TBC1D16, CCDC40, GAA, EIF4A3, CARD14, SGSH, SLC26A11, KIAA1618, RNF213, NPTX1, CHMP6, BAIAP2, AATK, AZI1, C17orf56, C17orf89, SLC38A10, C17orf55, TMEM105, BAHCC1, ACTG1, FSCN2, C17orf70, NPLOC4, TSPAN10, PDE6G, C17orf90, CCDC137,	hsa-mir-657, hsa-mir-338, hsa-mir-1250	V_5043_LC17763_Wong et al. (2007)

19	p13.3	0.12	4.85	49	0	10	PPAP2C, MIER2, THEG, FAM148C, SHC2, ODF3L2, MADCAM1, C19orf20, CDC34, GZMM, BSG, HCN2, POLRMT, FGF22, RNF126, FSTL3, PRSSL1, PALM, C19orf21, PTBP1, AZU1, PRTN3, ELANE, CFD, MED16, C19orf22, KISS1R, ARID3A, WDR18, GRIN3B, C19orf6, CNN2, ABCA7, HMHA1, POLR2	hsa-mir-1909, hsa-mir-1227, hsa-mir-637, hsa-mir-7-3	V_2237_LC18671_Locke et al. (2006), V_5065_LC18671_Wong et al. (2007), V_5066_LC18671_Wong et al. (2007), V_5067_LC18671_Wong et al. (2007), V_5068_LC18671_Wong et al. (2007), V_5069_LC18671_Wong et al. (2007), V_5070_LC18730_Wong et al. (2007), V_5071_LC
19	p13.2	9.87	11.73	27	0	10	ZNF846, FBXL12, UBL5, PIN1, OLFM2, COL5A3, RDH8, C3P1, C19orf66, ANGPTL6, PPAN, EIF3G, DNMT1, S1PR2, MRPL4, ICAM1, ICAM4, ICAM5, FDX1L, RAVER1, ICAM3, TYK2, CDC37, PDE4A, KEAP1, S1PR5, ATG4D, KRI1, CDKN2D, AP1M2, SLC44A2, ILF3, QTRT1, DNM2, TMED1, C19orf3	hsa-mir-1181, hsa-mir-1238, hsa-mir-638, hsa-mir-199a-1	V_5084_LC18813_Wong et al. (2007), V_5085_LC18818_Wong et al. (2007), V_5086_LC18821_Wong et al. (2007), V_5087_LC18821_Wong et al. (2007)
19	q12-q13.11	31.7	32.7	10	4	17	TSHZ3		V_5096_LC18924_Wong et al. (2007)
20	q11.21	30.41	30.47	2	0	9	MYLK2, FOXS1, DUSP15, TTLL9		
21	q22.3	44.94	47.87	44	0	12	HSF2BP, RRP1B, PDXK, CSTB, RRP1, AGPAT3, TRAPPC10, C21orf33, C21orf32, ICOSLG, DNMT3L, AIRE, PFKL, C21orf2, TRPM2, LRRC3, C21orf30, C21orf29, C21orf90, KRTAP10-1, KRTAP10-2, KRTAP10-3, KRTAP10-4, KRTAP10-6, KRTAP10-7, KRTAP10-8, KRTAP10-9, KRTAP10-10, KRT		
22	q11.1	16.88	17.25	3	4	17	KCNMB3L, CCT8L2		V_0814_LC20342_Sharp et al. (2005), V_0815_LC20342_Sharp et al. (2005), V_2258_LC20342_Locke et al. (2006), V_2259_LC20342_Locke et al. (2006), V_2260_LC20342_Locke et al. (2006)
22	q11.1	17.28	17.72	4	4	19	XKR3, GAB4, IL17RA, CECR6, CECR5, CECR1		
22	q11.1-q11.21	17.72	18.61	13	5	18	CECR1, CECR2, SLC25A18, ATP6V1E1, BCL2L13, BID, C22orf37, MICAL3, PEX26, TUBA8	hsa-mir-648	V_2261_LC20342_Locke et al. (2006), V_5168_LC20342_Wong et al. (2007)
22	q11.21	18.92	19.15	2	5	18	PRODH, DGCR2, DGCR14, TSSK2, GSC2		V_5169_LC20342_Wong et al. (2007)
22	q11.21-q11.22	21.34	22.75	10	7	22	TOP3B, AIFM3, LZTR1, THAP7, P2RX6, SLC7A4, POM121L7, GGT2, RIMBP3B, HIC2, RIMBP3C, UBE2L3, YDJC, CCDC116, SDF2L1, PPIL2, YPEL1, MAPK1, PPM1F, IGLV4-69, IGLV8-61, IGLV4-60, IGLV6-57, IGLV11-55, IGLV10-54, VPREB1, IGLV5-52, IGLV7-46, IGLV5-45, IGLV1-44, IGL	hsa-mir-649, hsa-mir-301b, hsa-mir-130b	V_0818_LC20342_Sharp et al. (2005), V_2030_LC20342_Urban et al (2006), V_2031_LC20342_Urban et al (2006), V_2032_LC20386_Urban et al (2006), V_2033_LC20386_Urban et al (2006), V_2034_LC20342_Urban et al (2006), V_2035_LC20386_Urban et al (2006), V_2036_LC
22	q11.23	23.89	25.86	20	6	20	IGLL1, C22orf43, RGL4, ZNF70, VPREB3, C22orf15, CHCHD10, MMP11, SMARCB1, DERL3, SLC2A11, GSTT2B, DDTL, DDT, GSTT2, GSTT1, CABIN1, SUSD2, GGT5, CYTSA, ADORA2A, UPB1, C22orf13, SNRPD3, GGT1, C22orf36, PIWIL3, SGSM1, TMEM211, CRYBB3, CRYBB2, LRP5L		V_0819_LC20395_Sharp et al. (2005), V_2029_LC20395_Urban et al (2006), V_2269_LC20395_Locke et al. (2006), V_2270_LC20395_Locke et al. (2006), V_2271_LC20395_Locke et al. (2006), V_2272_LC20395_Locke et al. (2006), V_2273_LC20404_Locke et al. (2006)
22	q12.1	27.49	28.26	9	6	20	MN1, PITPNB		
22	q12.3	32.49	35.63	32	8	26	SLC5A1, C22orf42, RFPL2, SLC5A4, RFPL3, RFPL3S, C22orf28, BPIL2, FBXO7, SYN3, TIMP3, LARGE, ISX		V_0237_LC20476_Iafrate et al. (2004), V_5181_LC20466_Wong et al. (2007), V_5182_LC20466_Wong et al. (2007), V_5183_LC20479_Wong et al. (2007)
22	q12.3-q13.1	36.55	39.65	33	5	20	APOL3, APOL4, APOL2, APOL1, MYH9, TXN2, FOXRED2, EIF3D, CACNG2, RABL4, PVALB, NCF4, CSF2RB, C22orf33, TST, MPST, KCTD17, TMPRSS6, IL2RB, C1QTNF6, SSTR3, RAC2, CYTH4, ELFN2, MFNG, CARD10, CDC42EP1, LGALS2, GGA1, PDXP, LGALS1, NOL12, TRIOBP, H1F0, GCAT, GAL	hsa-mir-658, hsa-mir-659	V_2037_LC20505_Urban et al (2006), V_2038_LC20505_Urban et al (2006), V_5185_LC20500_Wong et al. (2007), V_5186_LC20500_Wong et al. (2007), V_5187_LC20514_Wong et al. (2007)
22	q13.1	39.72	40.28	4	4	19	SYNGR1, MAP3K7IP1, MGAT3, SMCR7L, ATF4, RPS19BP1, CACNA1I, ENTHD1		V_5188_LC20524_Wong et al. (2007), V_5189_LC20524_Wong et al. (2007)
22	q13.1-q13.31	40.75	47.09	61	7	22	TNRC6B, SGSM3, MKL1, MCHR1, SLC25A17, ST13, XPNPEP3, DNAJB7, RBX1, EP300, L3MBTL2, CHADL, RANGAP1, ZC3H7B, TEF, TOB2, PHF5A, ACO2, POLR3H, CSDC2, PMM1, PPPDE2, XRCC6, NHP2L1, MEI1, CCDC134, SREBF2, TNFRSF13C, CENPM, Sep-03, WBP2NL, NAGA, FAM109B, C22orf32	hsa-mir-1281, hsa-mir-33a, hsa-mir-1249, hsa-let-7a-3, hsa-let-7b	V_5190_LC20580_Wong et al. (2007), V_5191_LC20603_Wong et al. (2007)
22	q13.31-q13.33	47.4	50.21	30	10	34	TBC1D22A, FAM19A5, C22orf34, BRD1		V_0239_LC20651_Iafrate et al. (2004), V_5192_LC20651_Wong et al. (2007), V_5193_LC20651_Wong et al. (2007)
22	q13.33	50.82	51.19	5	3	16	SAPS2, SBF1, ADM2, MIOX, LMF2, NCAPH2, SCO2, TYMP, ODF3B, KLHDC7B, C22orf41, CPT1B, CHKB, MAPK8IP2, ARSA, SHANK3, ACR		

Supplementary Table 9: Comparison of regions harbouring chromosomal gains between encapsulated, solid and invasive papillary carcinomas.

Regions differentially gained in EPC and SPC groups									
Chromosome	Cytobands	Start (Mb)	End (Mb)	Number of BACs	EPC (n=42)	SPC (n=5)	Genes	mi-RNAs	aCGH CNVs
4	p16.2	5.69	5.73	2	0	2	EVC2, EVC		
6	q27	170.39	171.01	7	5	4	DLL1, FAM120B, PSMB1, TBP, PDCD2		
18	q23	76.24	77.24	13	5	4	SALL3, ATP9B, NFATC1		

Regions differentially gained in EPC and IPC groups									
Chromosome	Cytobands	Start (Mb)	End (Mb)	Number of BACs	EPC (n=42)	IPC (n=13)	Genes	mi-RNAs	aCGH CNVs
17	p11.2	19.23	20.03	12	3	6	EPN2, B9D1, MAPK7, MFAP4, RNF112, SLC47A1, ALDH3A2, SLC47A2, ALDH3A1, ULK2, AKAP10, CYTSB	hsa-mir-1180	

Regions differentially gained in IPC and SPC groups									
Chromosome	Cytobands	Start (Mb)	End (Mb)	Number of BACs	IPC (n=13)	SPC (n=5)	Genes	mi-RNAs	aCGH CNVs
4	p16.3	1.05	1.32	3	2	4	RNF212, TMED11P, SPON2, CTBP1, C4orf42, MAEA		
6	q27	170.33	171.01	8	0	4	DLL1, FAM120B, PSMB1, TBP, PDCD2		
18	q23	76.24	77.24	13	2	4	SALL3, ATP9B, NFATC1		
22	q13.2	41.52	42.87	15	0	3	EP300, L3MBTL2, CHADL, RANGAP1, ZC3H7B, TEF, TOB2, PHF5A, ACO2, POLR3H, CSDC2, PMM1, PPPDE2, XRCC6, NHP2L1, MEI1, CCDC134, SREBF2, TNFRSF13C, CENPM, Sep-03, WBP2NL, NAGA, FAM109B, C22orf32, NDUFA6, CYP2D6, CYP2D7P1, TCF20, NFAM1	hsa-mir-33a	

Supplementary Table 10: Comparison of regions harbouring chromosomal losses between encapsulated, solid and invasive papillary carcinomas. Of note, no region differentially lost in solid and invasive papillary carcinomas were revealed.

Regions differentially lost in EPC and SPC groups									
Chromosome	**Cytobands**	**Start (Mb)**	**End (Mb)**	**Number of BACs**	**EPC (n=42)**	**SPC (n=5)**	**Genes**	**mi-RNAs**	**aCGH CNVs**
11	p15.4	5.91	8.22	24	0	2	TRIM5, OR52E5, OR56A3, OR52L1, OR56A4, OR56A1, OR52L2P, OR56B4, OR52W1, C11orf42, FAM160A2, CNGA4, CCKBR, PRKCDBP, SMPD1, APBB1, HPX, TRIM3, ARFIP2, FXC1, DNHD1, RRP8, ILK, TAF10, TPP1, DCHS1, MRPL17, OR2AG2, OR2AG1, OR6A2, OR10A5, OR10A2, OR10A4, OR2D2, OR2D3, ZNF215, ZNF214, NLRP14, RBMXL2, SYT9, OLFML1, PPFIBP2, CYB5R2, OVCH2, OR10AB1P, OR5P2, OR5P3, OR10A6, OR10A3, NLRP10, EIF3F, TUB, RIC3	hsa-mir-302e	
11	p15.4	8.72	9.01	2	0	2	ST5, C11orf17, C11orf16, ASCL3, TMEM9B, NRIP3		
11	p15.4	10.37	10.68	4	0	2	AMPD3, RNF141, LYVE1, MRVI1		
11	p15.3-p15.2	11.71	13.93	20	0	2	USP47, DKK3, MICAL2, MICALCL, PARVA, TEAD1, RASSF10, ARNTL, BTBD10, PTH, FAR1		V_0144_LC12977_Iafrate et al. (2004)
16	q12.1	47.31	47.54	2	21	0	ITFG1, PHKB		
16	q21	65.41	65.91	6	30	2			
16	q23.1	74.47	74.59	3	28	1	GLG1		
16	q23.1	75.81	76.7	8	27	1	CNTNAP4		
16	q23.1	76.99	77.48	5	28	1	MON1B, ADAMTS18		
17	p13.2-p13.1	6.44	6.84	2	2	3	PITPNM3, KIAA0753, TXNDC17, MED31, C17orf100, SLC13A5, XAF1, FBXO39, TEKT1		

Regions differentially lost in EPC and IPC groups									
Chromosome	**Cytobands**	**Start (Mb)**	**End (Mb)**	**Number of BACs**	**EPC (n=42)**	**IPC (n=13)**	**Genes**	**mi-RNAs**	**aCGH CNVs**
5	q21.3	104.66	105.35	7	0	4			V_4472_LC7288_Wong et al. (2007)
9	q21.13	76.53	77.15	8	0	4	RORB		V_4643_LC11388_Wong et al. (2007)
9	q31.1	103.45	106.26	25	0	4	BAAT, MRPL50, ZNF189, ALDOB, C9orf125, RNF20, GRIN3A, PPP3R2, C9orf107, CYLC2		V_4650_LC11572_Wong et al. (2007)

16	q11.2-q12.1	46.99	47.46	4	20	2	DNAJA2, NETO2, ITFG1		
16	q21	63.29	64.07	6	28	6			V_4961_LC16934_Wong et al. (2007)
16	q21	65.15	65.31	2	29	6	CDH11		
16	q21	66.03	66.28	3	30	7			
16	q23.1	74.34	74.66	4	28	5	PSMD7, NPIPL2, CLEC18B, GLG1, RFWD3		
16	q23.1	75.81	76.34	4	27	5	CNTNAP4		
16	q23.1	76.46	76.7	3	27	5	CNTNAP4		
16	q23.1	77.48	78.19	10	31	8	NUDT7, VAT1L, CLEC3A, WWOX		
16	q23.1-q23.2	78.51	79.27	13	31	8	WWOX		V_4968_LC17023_Wong et al. (2007)
16	q23.2	79.73	80.05	3	31	8			
18	q22.2-q22.3	68.09	72.99	53	1	5	GTSCR1, CBLN2, NETO1, FBXO15, C18orf55, CYB5A, C18orf51, CNDP2, CNDP1, ZNF407, C18orf33, ZADH2, TSHZ1		V_5062_LC18530_Wong et al. (2007)
18	q23	73.55	75.95	23	0	4	ZNF516, ZNF236, MBP, GALR1		V_5064_LC18537_Wong et al. (2007)
23	q26.3	134.64	134.98	4	0	4	DDX26B, CT45A3, CT45A5, SAGE1		V_0826_LC21120_Sharp et al. (2005), V_2281_LC21120_Locke et al. (2006)

Les études génomiques à haut débit utilisant les puces à ADN ont été largement utilisées en cancérologie pour identifier les aberrations génétiques de nombreux cancers et pour tenter d'identifier de nouvelles cibles thérapeutiques.

Devant l'extrême hétérogénéité des cancers du sein, nous avons choisi d'en étudier l'un des types particuliers. En effet, ces types particuliers, bien que rares, présentent l'intérêt d'être très homogènes entre eux et constituent donc de bons modèles d'étude de la carcinogenèse mammaire [12, 13].

Ce travail s'inscrit par ailleurs dans le cadre de la perspective d'une nouvelle classification des cancers du sein, incluant, en plus des critères morphologiques actuellement utilisés, des critères moléculaires.

Les carcinomes papillaires du sein n'ont, jusqu'à ce jour, pas fait l'objet d'analyse génomique à haut débit, du fait sans doute de leur relative rareté et de leur bon pronostic. Or, la prise en charge diagnostique et thérapeutique de ce type de cancer constitue souvent un véritable challenge pour le pathologiste et les cliniciens, notamment en raison de la controverse portant sur la nature exacte de ces lésions, certaines d'entre elles ayant été longtemps considérées comme des carcinomes *in situ*, et donc comme des lésions non invasives [22, 29, 30].

Notre étude portant sur 64 carcinomes papillaires du sein a montré qu'ils constituent dans la très grande majorité des cas des tumeurs de bas grade histologique, exprimant les RO et RP et sans surexpression de l'oncogène *HER2*. Leur phénotype moléculaire selon Sorlie et Nielsen est de type luminal, phénotype concordant avec leur bon pronostic.

Nous avons également rapporté, dans les carcinomes papillaires, un taux significativement moins élevé de métastases ganglionnaires et d'invasions lympho-vasculaires, facteurs de mauvais pronostic, que dans les CCI-NSTs équivalents en termes de grade histologique et de statut hormonal.

Du point de vue immunohistochimique, l'expression de la CCND1, protéine clé du cycle cellulaire permettant le passage de la phase G_1 à la phase S, était significativement plus fréquente dans les carcinomes papillaires que dans les CCI-NSTs. Ces résultats sont en accord avec les données de la littérature, décrivant une association entre l'expression de la CCND1 et les tumeurs de bas grade histologique et œstrogéno-dépendantes, de bon pronostic [41, 42]. De même, l'expression significativement plus élevée de la p53 dans les CCI-NSTs que dans les carcinomes papillaires confirme le bon pronostic des carcinomes papillaires, puisque l'expression de la p53 est observée dans les cancers du sein les plus agressifs, en particulier de phénotype basal [3, 43].

L'analyse génomique de 50 carcinomes papillaires du sein par CGH array a montré qu'ils ont un profil CGH relativement simple, caractérisé par un petit nombre d'altérations génomiques, limitées à quelques gains et pertes de bras chromosomiques ou chromosomes entiers et à de rares amplifications géniques.

La comparaison du profil génomique des carcinomes papillaires à celui des CCI-NSTs équivalents en termes de grade histologique et de statut hormonal a montré qu'ils sont très similaires, suggérant que ces deux types de tumeurs appartiendraient au même spectre lésionnel plutôt qu'à deux entités génomiques distinctes. En particulier, parmi les carcinomes papillaires de bas grade histologique de notre série, 82% présentaient l'altération génomique caractéristique des CCI-NSTs œstrogéno-dépendants de bas grade histologique, *i.e.* la perte du bras long du chromosome 16 (16q-) [44-46].

De plus, l'analyse non supervisée par clustering comprenant les 50 carcinomes papillaires et 50 CCI-NSTs équivalents n'a pas permis de mettre en évidence deux groupes tumoraux distincts.

Nous avons donc ici montré que les carcinomes papillaires appartiennent à la famille des néoplasies mammaires de bas grade, dans laquelle ont été décrits les carcinomes lobulaires,

tubuleux et les CCI-NSTs de bas grade histologique [9, 10, 47]. Toutefois, leur analyse génomique en CGH ne nous a pas permis de les distinguer des CCI-NSTs équivalents.

La théorie selon laquelle les carcinomes papillaires et les CCI-NSTs appartiendraient au même spectre lésionnel est corroborée par le fait qu'histologiquement, les carcinomes papillaires encapsulés ont souvent tendance à perdre leurs caractéristiques papillaires et à acquérir la morphologie de CCI-NSTs lorsqu'ils envahissent le tissu conjonctif voisin [1, 22].

D'autre part, il est intéressant de noter que le profil CGH des carcinomes papillaires présente moins d'altérations génomiques que celui des CCI-NSTs équivalents, et que les gains et pertes partiels de 1q, 6q, 17p, 19p et 22q sont observés plus fréquemment dans les carcinomes papillaires, alors que les gains et pertes des bras entiers de ces mêmes chromosomes sont plus souvent observés dans les CCI-NSTs. Ces différentes altérations génomiques pourraient soulever l'hypothèse d'une progression génomique entre les carcinomes papillaires et les CCI-NSTs, les carcinomes papillaires encapsulés acquérant les altérations génomiques des CCI-NSTs lorsqu'ils envahissent les tissus adjacents.

Il est intéressant de noter que, contrairement aux carcinomes micro-papillaires et aux carcinomes mucineux, le carcinome papillaire est le premier type particulier de cancer du sein dont l'analyse en CGH ne permet pas de le distinguer clairement des CCI-NSTs du point de vue génomique.

Néanmoins, on peut aussi envisager que les différences morphologiques observées entre carcinomes papillaires et CCI-NSTs soient dues à des mécanismes génétiques non détectables en CGH (réarrangements structuraux ou mutations somatiques) ou de type épigénétique.

La comparaison des trois variantes de carcinomes papillaires, *i.e.* carcinomes papillaires encapsulés, solides et invasifs a montré qu'elles sont très similaires, à la fois du point de vue immunohistochimique et génomique.

Une différence immunohistochimique significative est cependant à noter : la moindre expression des RP dans les carcinomes papillaires solides et invasifs que dans les carcinomes encapsulés, alors que les trois variantes exprimaient constamment les RO. Les carcinomes mammaires RO+/RP- étant associés à un moins bon pronostic que les carcinomes RO+/RP+, cette observation pourrait témoigner d'un meilleur pronostic des carcinomes papillaires encapsulés par rapport aux deux autres variantes [48].

La comparaison du profil génomique des trois variantes de carcinomes papillaires a essentiellement montré qu'une perte en 16q était plus fréquemment observée dans les carcinomes papillaires encapsulés que dans les deux autres variantes. Cette observation est toutefois d'interprétation délicate puisque 100% des carcinomes encapsulés de notre étude étaient de bas grade histologique, contre 80% et 69% des carcinomes solides et invasifs, respectivement.

Par ailleurs, l'analyse non supervisée par clustering des 50 carcinomes papillaires n'a pas permis de mettre en évidence trois groupes de tumeurs distincts.

Cette similitude entre les carcinomes papillaires invasifs et les deux autres variantes de carcinomes papillaires suggère que les carcinomes papillaires encapsulés et solides correspondraient à des formes bien limitées de carcinome invasif.

La théorie de Collins et al semble ainsi confirmée par l'analyse génomique [30].

Il serait donc judicieux de prendre en charge de la même manière ces trois types de carcinomes papillaires, à savoir comme des tumeurs de bas grade histologique et de bon pronostic.

En conclusion, cette étude de 64 cas de carcinomes papillaires mammaires a montré qu'il s'agit de carcinomes le plus souvent de bas grade histologique, exprimant les récepteurs hormonaux et sans surexpression du gène *HER2*, et donc de phénotype moléculaire luminal. Leur profil génomique en CGH array se caractérise par un nombre limité d'altérations génomiques et est très proche de celui des CCI-NSTs équivalents en termes de grade histologique et de statut hormonal.

Ceci suggère que les carcinomes papillaires appartiendraient au même spectre lésionnel que les CCI-NSTs de bas grade histologique et n'en seraient donc pas une entité génomiquement distincte.

D'autre part, nous avons montré que les trois variantes morphologiques de carcinomes papillaires, *i.e.* les carcinomes papillaires encapsulés, solides et invasifs ont des profils immunohistochimiques et génomiques très similaires, suggérant qu'ils constituent la même maladie et sont à considérer comme des carcinomes invasifs de bas grade histologique.

D'autres études à haut débit (séquençage nouvelle génération [49, 50], études épigénétiques) permettront de déterminer si la morphologie particulière de ces cancers peut être expliquée par des mécanismes génétiques non détectables en CGH array (réarrangements structuraux de type translocations équilibrées, mutations somatiques) ou par des mécanismes de type épigénétique.

Ce travail de Recherche a été rédigé sous forme d'article, dans la perspective d'une soumission dans une revue de Pathologie.

Devant la négativité des résultats ici rapportés, nous avons décidé de compléter ce manuscrit avec les résultats d'analyses complémentaires de type séquençage nouvelle génération, actuellement réalisées sur cette série de carcinomes papillaires, au sein du Breakthrough Breast Cancer Research Center.

1. Tavassoli FA, Devilee P (eds). *Tumours of the Breast. International Agency for Research of Cancer (IARC)*: Lyon, 2003.
2. Geyer FC, Marchio C, and Reis-Filho JS. *The role of molecular analysis in breast cancer.* Pathology 2009; 41(1): 77-88.
3. Sorlie T, Perou CM, Tibshirani R, et al. *Gene expression patterns of breast carcinomas distinguish tumor subclasses with clinical implications.* Proc Natl Acad Sci U S A 2001; 98(19): 10869-74.
4. Perou CM, Sorlie T, Eisen MB, et al. *Molecular portraits of human breast tumours.* Nature 2000; 406(6797): 747-52.
5. Foulkes WD, Smith IE, and Reis-Filho JS. *Triple-negative breast cancer.* N Engl J Med 2010; 363(20): 1938-48.
6. Badve S, Dabbs DJ, Schnitt SJ, et al. *Basal-like and triple-negative breast cancers: a critical review with an emphasis on the implications for pathologists and oncologists.* Mod Pathol 2011; 24(2): 157-67.
7. May WA, Lessnick SL, Braun BS, et al. *The Ewing's sarcoma EWS/FLI-1 fusion gene encodes a more potent transcriptional activator and is a more powerful transforming gene than FLI-1.* Mol Cell Biol 1993; 13(12): 7393-8.
8. Burmeister T and Thiel E. *Molecular genetics in acute and chronic leukemias.* J Cancer Res Clin Oncol 2001; 127(2): 80-90.
9. Simpson PT, Reis-Filho JS, Gale T, et al. *Molecular evolution of breast cancer.* J Pathol 2005; 205(2): 248-54.
10. Weigelt B and Reis-Filho JS. *Histological and molecular types of breast cancer: is there a unifying taxonomy?* Nat Rev Clin Oncol 2009; 6(12): 718-30.
11. Weigelt B, Geyer FC, and Reis-Filho JS. *Histological types of breast cancer: how special are they?* Mol Oncol 2010; 4(3): 192-208.
12. Reis-Filho JS and Lakhani SR. *Breast cancer special types: why bother?* J Pathol 2008; 216(4): 394-8.
13. Weigelt B, Horlings HM, Kreike B, et al. *Refinement of breast cancer classification by molecular characterization of histological special types.* J Pathol 2008; 216(2): 141-50.
14. Tognon C, Knezevich SR, Huntsman D, et al. *Expression of the ETV6-NTRK3 gene fusion as a primary event in human secretory breast carcinoma.* Cancer Cell 2002; 2(5): 367-76.
15. Persson M, Andren Y, Mark J, et al. *Recurrent fusion of MYB and NFIB transcription factor genes in carcinomas of the breast and head and neck.* Proc Natl Acad Sci U S A 2009; 106(44): 18740-4.
16. Rakha EA, Patel A, Powe DG, et al. *Clinical and biological significance of E-cadherin protein expression in invasive lobular carcinoma of the breast.* Am J Surg Pathol 2010; 34(10): 1472-9.
17. Reis-Filho JS, Pinheiro C, Lambros MB, et al. *EGFR amplification and lack of activating mutations in metaplastic breast carcinomas.* J Pathol 2006; 209(4): 445-53.
18. Rakha EA, Aleskandarany M, El-Sayed ME, et al. *The prognostic significance of inflammation and medullary histological type in invasive carcinoma of the breast.* Eur J Cancer 2009; 45(10): 1780-7.
19. Lacroix-Triki M, Suarez PH, MacKay A, et al. *Mucinous carcinoma of the breast is genomically distinct from invasive ductal carcinomas of no special type.* J Pathol 2010; 222(3): 282-98.

20. Marchio C, Iravani M, Natrajan R, et al. *Genomic and immunophenotypical characterization of pure micropapillary carcinomas of the breast.* J Pathol 2008; 215(4): 398-410.
21. Reis-Filho JS, Simpson PT, Turner NC, et al. *FGFR1 emerges as a potential therapeutic target for lobular breast carcinomas.* Clin Cancer Res 2006; 12(22): 6652-62.
22. Pal SK, Lau SK, Kruper L, et al. *Papillary carcinoma of the breast: an overview.* Breast Cancer Res Treat 2010; 122(3): 637-45.
23. Lefkowitz M, Lefkowitz W, and Wargotz ES. *Intraductal (intracystic) papillary carcinoma of the breast and its variants: a clinicopathological study of 77 cases.* Hum Pathol 1994; 25(8): 802-9.
24. Solorzano CC, Middleton LP, Hunt KK, et al. *Treatment and outcome of patients with intracystic papillary carcinoma of the breast.* Am J Surg 2002; 184(4): 364-8.
25. Grabowski J, Salzstein SL, Sadler GR, et al. *Intracystic papillary carcinoma: a review of 917 cases.* Cancer 2008; 113(5): 916-20.
26. Wynveen CA, Nehhozina T, Akram M, et al. *Intracystic papillary carcinoma of the breast: An in situ or invasive tumor? Results of immunohistochemical analysis and clinical follow-up.* Am J Surg Pathol 2011; 35(1): 1-14.
27. Collins LC and Schnitt SJ. *Papillary lesions of the breast: selected diagnostic and management issues.* Histopathology 2008; 52(1): 20-9.
28. Lininger RA, Park WS, Man YG, et al. *LOH at 16p13 is a novel chromosomal alteration detected in benign and malignant microdissected papillary neoplasms of the breast.* Hum Pathol 1998; 29(10): 1113-8.
29. Esposito NN, Dabbs DJ, and Bhargava R. *Are encapsulated papillary carcinomas of the breast in situ or invasive? A basement membrane study of 27 cases.* Am J Clin Pathol 2009; 131(2): 228-42.
30. Collins LC, Carlo VP, Hwang H, et al. *Intracystic papillary carcinomas of the breast: a reevaluation using a panel of myoepithelial cell markers.* Am J Surg Pathol 2006; 30(8): 1002-7.
31. Marchio C, Iravani M, Natrajan R, et al. *Mixed micropapillary-ductal carcinomas of the breast: a genomic and immunohistochemical analysis of morphologically distinct components.* J Pathol 2009; 218(3): 301-15.
32. Jacquemier J, Ginestier C, Bertucci F, et al. *[Tissue microarrays a powerful tool in transfer and quality control in oncology].* Bull Cancer 2003; 90(1): 31-8.
33. Kononen J, Bubendorf L, Kallioniemi A, et al. *Tissue microarrays for high-throughput molecular profiling of tumor specimens.* Nat Med 1998; 4(7): 844-7.
34. Lambros MB, Natrajan R, and Reis-Filho JS. *Chromogenic and fluorescent in situ hybridization in breast cancer.* Hum Pathol 2007; 38(8): 1105-22.
35. Natrajan R, Lambros MB, Rodriguez-Pinilla SM, et al. *Tiling path genomic profiling of grade 3 invasive ductal breast cancers.* Clin Cancer Res 2009; 15(8): 2711-22.
36. Nocito A, Bubendorf L, Tinner EM, et al. *Microarrays of bladder cancer tissue are highly representative of proliferation index and histological grade.* J Pathol 2001; 194(3): 349-57.
37. Reis-Filho JS, Simpson PT, Gale T, et al. *The molecular genetics of breast cancer: the contribution of comparative genomic hybridization.* Pathol Res Pract 2005; 201(11): 713-25.
38. Coe BP, Ylstra B, Carvalho B, et al. *Resolving the resolution of array CGH.* Genomics 2007; 89(5): 647-53.

39. Tan DS, Lambros MB, Natrajan R, et al. *Getting it right: designing microarray (and not 'microawry') comparative genomic hybridization studies for cancer research.* Lab Invest 2007; 87(8): 737-54.
40. Gunnarsson R, Staaf J, Jansson M, et al. *Screening for copy-number alterations and loss of heterozygosity in chronic lymphocytic leukemia--a comparative study of four differently designed, high resolution microarray platforms.* Genes Chromosomes Cancer 2008; 47(8): 697-711.
41. Reis-Filho JS, Savage K, Lambros MB, et al. *Cyclin D1 protein overexpression and CCND1 amplification in breast carcinomas: an immunohistochemical and chromogenic in situ hybridisation analysis.* Mod Pathol 2006; 19(7): 999-1009.
42. Elsheikh S, Green AR, Aleskandarany MA, et al. *CCND1 amplification and cyclin D1 expression in breast cancer and their relation with proteomic subgroups and patient outcome.* Breast Cancer Res Treat 2008; 109(2): 325-35.
43. Vincent-Salomon A, Gruel N, Lucchesi C, et al. *Identification of typical medullary breast carcinoma as a genomic sub-group of basal-like carcinomas, a heterogeneous new molecular entity.* Breast Cancer Res 2007; 9(2): R24.
44. Roylance R, Gorman P, Papior T, et al. *A comprehensive study of chromosome 16q in invasive ductal and lobular breast carcinoma using array CGH.* Oncogene 2006; 25(49): 6544-53.
45. Natrajan R, Lambros MB, Geyer FC, et al. *Loss of 16q in high grade breast cancer is associated with estrogen receptor status: Evidence for progression in tumors with a luminal phenotype?* Genes Chromosomes Cancer 2009; 48(4): 351-65.
46. Roylance R, Gorman P, Hanby A, et al. *Allelic imbalance analysis of chromosome 16q shows that grade I and grade III invasive ductal breast cancers follow different genetic pathways.* J Pathol 2002; 196(1): 32-6.
47. Abdel-Fatah TM, Powe DG, Hodi Z, et al. *Morphologic and molecular evolutionary pathways of low nuclear grade invasive breast cancers and their putative precursor lesions: further evidence to support the concept of low nuclear grade breast neoplasia family.* Am J Surg Pathol 2008; 32(4): 513-23.
48. Rakha EA, El-Sayed ME, Green AR, et al. *Biologic and clinical characteristics of breast cancer with single hormone receptor positive phenotype.* J Clin Oncol 2007; 25(30): 4772-8.
49. Reis-Filho JS. *Next-generation sequencing.* Breast Cancer Res 2009; 11 Suppl 3: S12.
50. Shah SP, Morin RD, Khattra J, et al. *Mutational evolution in a lobular breast tumour profiled at single nucleotide resolution.* Nature 2009; 461(7265): 809-13.

SERMENT D'HIPPOCRATE

En présence des Maîtres de cette Faculté,
de mes chers condisciples
et selon la tradition d'Hippocrate,
je promets et je jure d'être fidèle aux lois de l'honneur
et de la probité dans l'exercice de la Médecine.

Je donnerai mes soins gratuits à l'indigent,
et n'exigerai jamais un salaire au-dessus de mon travail.

Admis à l'intérieur des maisons,
mes yeux ne verront pas ce qui s'y passe,
ma langue taira les secrets qui me seront confiés
et mon état ne servira pas à corrompre les mœurs
ni à favoriser le crime.

Respectueux et reconnaissant envers mes Maîtres,
je rendrai à leurs enfants
l'instruction que j'ai reçue de leurs pères.

Que les hommes m'accordent leur estime
si je suis fidèle à mes promesses.
Que je sois couvert d'opprobre
et méprisé de mes confrères
si j'y manque.

Académie d'Orléans – Tours
Université François-Rabelais
Faculté de Médecine de TOURS

DUPREZ Raphaëlle **Thèse n°**

CARACTÉRISATION MOLÉCULAIRE DES CARCINOMES PAPILLAIRES DU SEIN

96 pages – 13 tableaux – 12 figures

Résumé :
Le cancer du sein est une maladie très hétérogène, et la classification actuelle de l'OMS, basée sur des critères morphologiques, en décrit plus de 17 types. Or, il a été prouvé qu'une classification incluant des critères moléculaires aurait plus de valeurs pronostique et prédictive. Par ailleurs, les types particuliers de cancer du sein se sont avérés bien plus homogènes entre eux du point de vue moléculaire que les classiques carcinomes canalaires infiltrants dits « no special type » (CCI-NSTs), constituant ainsi de bons modèles d'étude des altérations moléculaires survenant dans les cancers du sein.
Pour cette raison, nous avons étudié une série multicentrique de 64 cas de carcinomes papillaires du sein, à la fois de variantes encapsulée, solide et invasive, par immunohistochimie sur tissu microarrays, hybridation génomique comparative (CGH array) et hybridations *in situ*. Nous les avons comparés à 64 cas de CCI-NSTs équivalents en termes de grade histologique et de statut hormonal.
Nos résultats montrent que les carcinomes papillaires du sein sont des tumeurs de bas grade histologique (91%), exprimant les récepteurs aux œstrogènes (100%) et sans surexpression d'*HER2* (100%), appartenant ainsi au phénotype moléculaire luminal. Ils présentent significativement moins d'invasions lympho-vasculaires et de métastases ganglionnaires que les CCI-NSTs équivalents, moins d'expression de la p53 et une plus fréquente expression de la CCND1.
Leur profil génomique en CGH array est simple, caractérisé par de rares amplifications géniques et quelques gains et pertes chromosomiques, dont la perte du bras long du chromosome 16, altération génomique caractéristique des CCI-NSTs de bas grade œstrogéno-dépendants. L'absence de différence significative en analyse non supervisée entre carcinomes papillaires et CCI-NSTs suggère que les deux types de tumeurs appartiendraient au même spectre lésionnel plutôt qu'à deux entités génomiquement distinctes.
D'autre part, les trois variantes de carcinomes papillaires ont des profils génomiques semblables, suggérant qu'ils représentent la même maladie.
D'autres analyses à haute résolution (*i.e.* séquençage nouvelle génération) détermineront si la morphologie papillaire de ces tumeurs peut être expliquée par des mécanismes moléculaires non détectables en CGH (translocations équilibrées, mutations somatiques).

Mots clés : carcinome papillaire, cancer du sein, hybridation génomique comparative, immunohistochimie, tissu microarray, hybridation *in situ*

Jury :
Président : **Monsieur le Professeur S. GUYÉTANT**
Membres : **Monsieur le Professeur P. BOUGNOUX**
Monsieur le Professeur J-C PAGÈS
Madame le Docteur F. ARBION
Monsieur le Docteur P. MICHENET
Madame le Docteur A. VINCENT-SALOMON
Date de la soutenance : 11 avril 2011